Calcium carbonate precipitation during subsurface injection of RO-brine

The effect on the hydraulic conductivity

Frans Willem Hamer

29th July 2016

TU Delft

Calcium carbonate precipitation during subsurface injection of RO-brine

The effect on the hydraulic conductivity

By:
Frans Willem Hamer

For the degree of:
Master of Science in Civil Engineering

Supervising committee:

Prof. Dr. Ir. Luuk Rietveld

Dr. Ir. Bas Heijman

Prof. Dr. Ir. Walter van der Meer

Dr. Ir. Mark Bakker

Sanitary Engineering Section, Department of Water Management
Faculty of Civil Engineering and Geosciences
Delft University of Technology, Delft

ABSTRACT

The increase in salinity of groundwater is a global problem (Van Weert et al. 2009). In the west of the Netherlands, seepage of saline and brackish groundwater into layers of freshwater increases the salinity in polders and around drinking water wells (Grakist et al. 2002, Olsthoorn 2008).

Systems like PURO and the Freshkeeper abstract brackish groundwater and turn it into drinking water. In both systems, the salty groundwater is desalinised with a reverse osmosis membrane and the leftover brine with a high salt content is injected in a deeper layer with saline groundwater.

A too high salt content will result in precipitation of crystals like calcium carbonate, which can clog the injection well. To prevent clogging, the production of freshwater should be balanced with the supersaturation of the brine. In addition, inhibitors can reduce or even completely hinder precipitation from supersaturated solutions.

This research looked at the effect of the degree of supersaturation of calcium carbonate on the precipitation and clogging in a porous medium with a series of column experiments. In addition, it looked at the inhibition of calcium carbonate precipitation by humic acids with batch experiments. A Literature research and modelling with Phreeqc in combination with Python supported the experiments.

Whenever the grains in the column were cemented together with calcium carbonate that has filled the pores, a clear decrease in the hydraulic conductivity could be observed. Both cementation and a decrease in hydraulic conductivity were found in the top of the column only. The presence of calcium carbonate crystals can trigger the precipitation of calcium carbonate from a metastable solution.

In the growth models of Plummer et al. (1978), Schagen et al. (2008) and Wolthers et al. (2012) the rate of precipitation is linearly related with the surface area of calcium carbonate crystals. Column simulations with those models hence show that with more calcium carbonate seed crystals present in the column, the location of precipitation shifts more to the very start of the bed.

Following the equation of Carman-Kozeney, precipitation focused on a short distance is much more disastrous for the hydraulic conductivity than when the same amount is distributed over a longer distance. Also, in radial flow, clogging close to the injection well will require a much higher pressure for injection than clogging further away from the well.

Both the results of the column experiments and the equation of Carman-Kozeney show that a clear exponential increase in hydraulic resistance can only be observed after a period where calcium carbonate has already been precipitating. It can make the effect of precipitating calcium carbonate on the hydraulic conductivity deceiving: this relationship between conductivity and decreasing porosity together with the precipitation rate and increase in surface area accelerating each other, make that during the initial period of precipitation clogging is unnoticed.

At relatively low $SI_{calcite}$'s – observed in column experiments with $SI_{calcite}$'s of 1.0 and 1.23 and calcium carbonate seeds – the presence of calcium carbonate seeds could trigger a metastable solution to become unstable. When there were no calcium carbonate crystals present, experiments with an $SI_{calcite}$ of 1.0, 1.14 and 1.23 remained metastable – yet, during one contradicting set of experiments without calcite seeds and an $SI_{calcite}$ of 1.14 precipitation and cementation did occur. Hence, the soil characteristics are crucial for the stability of a metastable solution. The dominant precipitation

processes at those $SI_{calcite}$'s are growth and 2D-nucleation. These processes both rely on the presence of calcium carbonate.

Nucleation becomes more dominant at higher values of $SI_{calcite}$, when the solution is no longer metastable. In the column experiments with an $SI_{calcite}$ of 1.5, the dominant processes were homogeneous and heterogeneous nucleation. In addition, crystals that were found prior to the sand bed, show that homogeneous nucleation had also taken place.

Consistent with the column experiments, the upper limit of metastability that was found in the batch experiments also lies somewhere between an $SI_{calcite}$ of 1.0 and 1.5. Humic acids can inhibit the precipitation of calcium carbonate at high enough concentrations. Homogeneous nucleation in solutions with an $SI_{calcite}$ of 1.5 was delayed, the rate was reduced and the final total precipitation was less in presence of 5.35mgC/l or more. 5.35 mgC/l Of humic acids also inhibited nucleation in solution with an $SI_{calcite}$ of 2.0. However, only a small reduction of the final total precipitation could be observed. At lower $SI_{calcite}$, no nucleation had taken place ($SI_{calctie}$ of 0.5) or no clear trend could be observed among different concentrations of humic acids ($SI_{calcite}$ of 1.0).

ACKNOWLEDGMENTS

First and foremost, I would like to thank my supervisors and committee members Prof. Dr. Ir. Luuk Rietveld, Dr. Ir. Bas Heijman, Prof. Dr. Ir. Walter van der Meer and Dr. Ir. Mark Bakker for their assistance and advice during the research, and also for their contribution to my education throughout my studies here at TU Delft.

When conducting the experiments I received a lot of direct assistance from Sherzad Anwari, Mohammed Jafar, Armand Middeldorp, Paul Vermeulen and Alexander Hendriks. Your helpful hands and brains in the laboratory show that it is always best to solve problems together.

In particular, I would like to thank Amir Haidari, Boris van Breukelen, Abel Heinsbroek, Peter de Moel and Mariëtte Wolthers for sharing their knowledge and therewith the enthusiasm for aquatic chemistry. Without your teachings it would be impossible to form a coherent structure of the matter of aquatic chemistry.

Last, I would like to thank my family, friends and fellow researchers who have supported me throughout my studies. Their presence during the process of this thesis have really motivated me to bring out my best and to keep enjoying what I am doing.

CONTENTS

1 INTRODUCTION

1.1 CHAPTER OVERVIEW

This thesis consists of the following chapters Introduction, Theory, Experimental methods, Experimental results, Discussion and Conclusion. The introduction is based on research of two pilot projects in the Netherlands and ends with the goals of this research. The chapter Theory goes deeper into the processes of calcium carbonate formation, inhibition and the effect of clogging on the flow through a porous medium. These chapters are followed by the chapters Experimental methods and Experimental results. The results are analysed in the chapter Experimental Results. Last, the main findings are presented in the chapter Discussion, Conclusion and Recommendations.

1.2 THE FRESHKEEPER AND THE PURO SYSTEM

Globally, many sources of fresh groundwater are affected by increasing salt concentrations. This reduces the availability of water for drinking, agriculture, households and industries. Natural drivers that affect groundwater salinity are seepage of fossil seawater, sea level variations, meteorological processes and changes in the hydrological cycle. Coastal protection, land reclamation, drainage, groundwater abstraction, irrigation and pollution are human drivers of the increase in groundwater salinity. (Van Weert et al. 2009)

The west of the Netherlands is a coastal delta with polders that lay below the sea level. The (ground) water level in the polders is maintained by continuous drainage. The drainage and the low water level result in seepage of saltwater and brackish water from deeper layers to the freshwater, polluting the freshwater. Figure 1-1 below shows a modelled example of the flow of brackish groundwater to the surface of a polder between two surface water reservoirs. (Olsthoorn 2008)

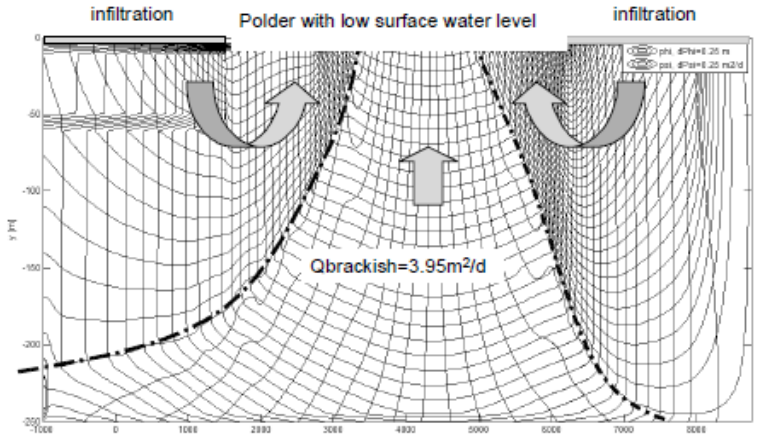

Figure 1-1 Cross section of upflowing brackish groundwater to a polder. The interface between freshwater and saltwater is indicated with the dotted-striped line. (From Olsthoorn 2008)

Before 2002, more than 100 groundwater pumping stations in the Netherlands had been closed because of exceeding salt concentrations and 20% of the then active pumping stations were expected to eventually experience salinization (Grakist et al. 2002). A well below the existing wells that abstracts the brackish water before it mixes with the freshwater around the wells and before it reaches the surface is a solution for the salinization of wells and polders.

Discharging the brackish groundwater in the natural environment causes pollution. A reverse osmosis (RO) system can produce freshwater (filtrate) from the brackish groundwater by pumping

the water through a RO membrane. Not all water can be converted into freshwater: the water that does not pass the membrane (the brine or concentrate) contains all the salts that are retained. Figure 1-2 shows the effect of a well that abstracts the brackish water on the situation shown previously in figure 1-1.

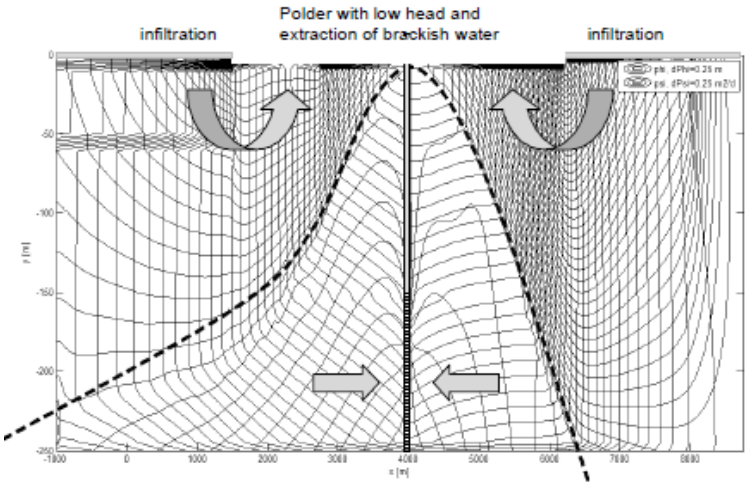

Figure 1-2 The effect of the installation of a well abstracting the brackish groundwater. The screens of the well are located between 150 and 200m below surface level. (From Olsthoorn 2008)

The remaining brine can be injected in a deeper aquifer with saltwater, which is separated from the brackish water with a clay layer. Examples of systems with brackish water abstraction, a RO-membrane and brine injection are the “zoethouder” (Freshkeeper) (Raat and Kooiman 2012) and PURO (Haidari 2015).

The Dutch drinking water companies Oasen, Vitens, Waternet and Brabant Water are investigating the application of these systems to keep their freshwater wells fresh. The Freshkeeper has been tested around wells in Noardburgum (Vitens) and Zevenbergen (Brabant Water). Waternet is considering to apply a similar system in the Horstermeer polder, which has a large flow of brackish water seeping into its surface water. Oasen has a pilot of the PURO system in their well field in Ridderkerk.

Schematic overviews of the Freshkeeper in Noardburgum and Zevenbergen are shown below in figure 1-3. Both systems use a RO-system that is placed above ground level. The brine in injected in a deeper saltwater aquifer.

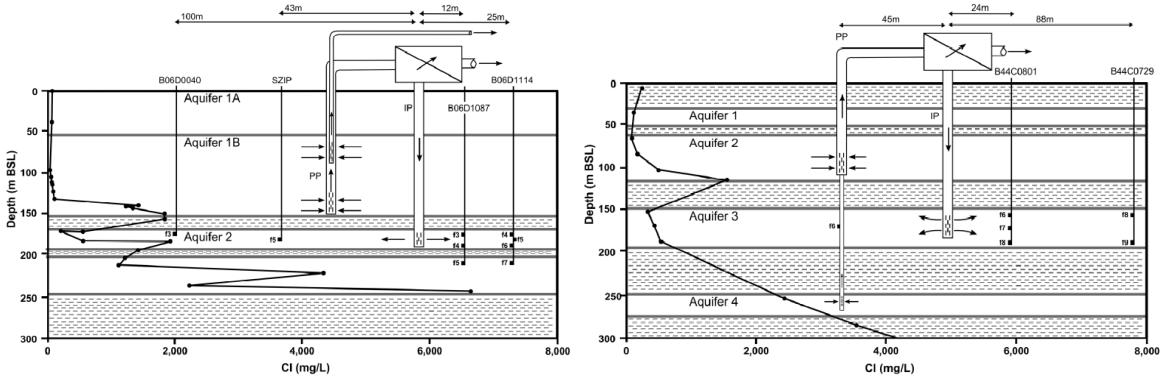

Figure 1-3 Schematic overviews of the Freshkeeper in Noardburgum (left) and in Zevenbergen (right) (from Raat and Kooiman 2012).

Oasen uses the PURO-system, which it has developed together with Waternet, Logisticon Water Treatment, Drilling Company Haitjema and Delft University of Technology. Where the Freshkeeper has two wells and its RO-membranes are above ground, PURO has a single borehole and the membranes are underground in the well itself, below the point where the brackish water is abstracted. Figure 1-4 below gives an overview and an impression of the PURO well.

Because of the position of the membranes, the pressure difference to push the permeate through the membrane can come for 80% from the hydrostatic pressure. The remaining 20% is provided by a feed pump. Since the permeate is produced underground, the brine does not have to be pumped to the surface and can be injected in the deeper layer of saltwater.

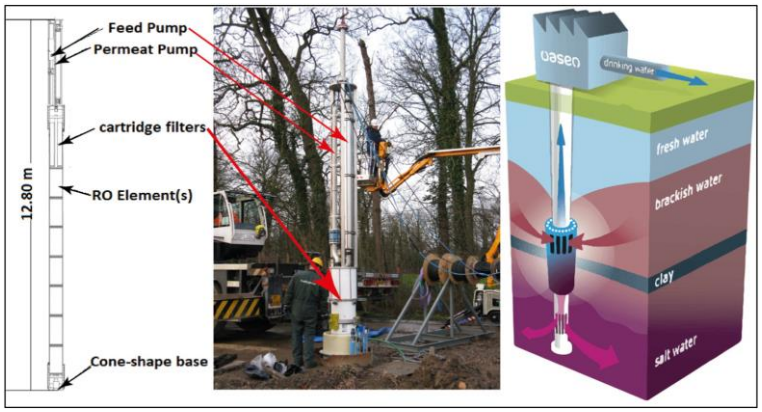

Figure 1-4 Left: Schematic overview of the PURO system with the RO membrane elements, the cartridge filter and pumps as installed in Ridderkerk. Middle: lowering of the membranes in the single well in Ridderkerk. Right: an impression of the processes inside PURO: brackish water is pumped into the well, goes down through the series of membranes. Only the produced freshwater (permeate) is pumped to the surface while the salty brine is injected in a deep layer of salt water. (From Haidari et al. 2015)

Antiscalants are dosed to the influent of an RO-system to prevent precipitation of salts from the concentrated water (scaling). Injecting these xenobiotic substances will pollute the groundwater. Lowering the recovery – the percentage of the influent that is filtered into freshwater – of the RO-system will reduce scaling of the brine. Therefore, both the Freshkeeper and PURO have a lower recovery than conventional RO-systems and do not dose antiscalants.

Precipitated material in the membranes can be removed by cleaning the membranes chemically or the membranes can be renewed. This is more convenient for the Freshkeeper than for PURO, since the RO-membranes are several meters below the surface in the well. When precipitation takes place in the sandy layer where the water is injected, it clogs the well and increases the resistance and therefore the energy needed to inject the water. Scaling can be prevented by lowering the recovery. However, a low recovery increases the energy demand per m^3 of freshwater that is produced. The Freshkeeper is operated most efficiently by balancing the production, scaling and clogging and energy requirements. Since PURO makes use of the hydrostatic pressure to produce the permeate, it uses most energy to pump the permeate to the surface. As a result, PURO's most efficient operation is less dependent on the recovery (Haidari et al. 2015).

1.3 The Freshkeeper in Zevenbergen and Noardburgum

Raat and Kooiman (2012) published a report on the operation of the two Freshkeeper pilots. In the fall of 2009, both the pilots in Zevenbergen and Noardburgum were started at a recovery of 50%. This gave a stable operation of the RO membranes for both Zevenbergen (during more than a year) and Noardburgum (during more than 250 days). However, as can be seen below in table 1-1, the

saturation indices of various salts are higher than 0.0 for both locations. Solutions with a saturation index higher than 0.0 have the potential to precipitate. Raat and Kooiman (2012) conclude that the saturation index would give a too conservative estimate of a safe recovery without precipitation.

However, while the membranes in Zevenbergen did not clog during the 50% recovery period, the concentrate contained relatively many particles larger than 10µm, the resistance to inject the water increased and measurements from an observation well (24m away from the injection point) show a decrease of iron, calcium and carbonate indicating the precipitation of calcium carbonate (calcite) and iron carbonate (siderite). Over the first 12 months with 50% recovery, about 35 tonnes or 13m^3 of calcium carbonate has precipitated between the injection point and the observation well and the resistance has increased by 7%. (Raat and Kooiman 2012)

When the recovery in Zevenbergen was increased to 65%, scaling took place on the membranes and the injection aquifer clogged quickly. The recovery of the pilot in Noardburgum could be increased to 70% without causing scaling in the RO membrane and in the injection aquifer. With a recovery of 75% the RO membrane had some precipitation of silica salts and sorption of PO_4, but no scaling of carbonates could be observed. Though the saturation indices are of similar order at both locations, the actual precipitation was different.

Raat and Kooiman (2012) expected the large amount of Fe^{+2} in the brine to have inhibited the precipitation and scaling of calcium carbonate in Noardburgum (Herzog et al. 1989). However, this does not explain why there was no precipitation of iron carbonate either. The higher concentrations of carbonate (CO_3^{-2}) in Zevenbergen contributed more to the oversaturation ($SI_{calcite}$) in Zevenbergen than in Noardburgum, where the cations calcium and iron are more present. Hence, the low availability of (bi)carbonate in Noardburgum might have inhibited precipitation and scaling. In addition, the injection aquifer in Zevenbergen contained more calcite than in Noardburgum, which promotes the precipitation of more calcium carbonate.

1.4 MODELLING THE ZEVENBERGEN INJECTION AQUIFER

Kaandorp (2014) used the computer program Phreeqc to simulate the precipitation of calcite ($CaCO_3$) and siderite ($FeCO_3$) in the injection aquifer of Zevenbergen. Along with cation exchange, the precipitation of these two carbonates causes the main changes in chemistry between the brine at the injection well and at the observation well. In Zevenbergen, as can be seen in table 1-1, the concentrations of calcium are more than a hundred times higher than the concentration of iron.

Figure 1-5 below shows graphs of the measurements and Phreeqc modelling of the observation well at 25 meters from the injection well. The different pumping regimes are separated by vertical lines. During period A and C, the 50% of the water was recovered. This resulted in a decrease of calcium and of the $SI_{calcite}$, indicated by the differences with the conservative transport. The resistance of the injection aquifer increases gradually over these periods.

During period B, the recovery was increased to 65%. This resulted in a higher supersaturation. These conditions resulted in a very strong increase of the required pumping head, caused by the precipitation of calcium carbonate. Between period B and C, the aquifer had to be rinsed with a HCl solution. CO_2 Was added during period D, E and F, what resulted in a lower $SI_{calcite}$. Though the $SI_{calcite}$ is still higher than zero, there was no precipitation of calcium carbonate.

Table 1-1 The water quality and the saturation indexes (SI) of the RO concentrate at the two locations during different recoveries. n.d.: not determined, n.a. does not apply (As of Raat and Kooiman 2012)

Locaton		Noardburgum			Zevenbergen	
RO recovery		50%	70%	75%	50%	65%
pH		6.97	7.12	7.18	7.52	7.54
EC	[mS/m]	473	670	845	256	350
CH4	[mg/l]	15.7	16.8	13.7	1.4	n.d.
Cl	[mg/l]	1409	2067	2700	583	771
Br	[mg/l]	5.54	8.06	9.59	1.82	2.7
F	[mg/l]	0.12	0.11	0.24	0.27	0.36
HCO3	[mg/l]	671	1100	1400	752	1140
SO4	[mgSO4/l]	<2.0	<2.0	<2.0	7.8	n.d.
tot-PO4	[mgP/l]	0.7	0.54	0.07	0.2	0.62
TOC	[mg/l]	9.6	15	20	7.8	12
Na	[mg/l]	174	222	250	328	465
K	[mg/l]	6.5	9.8	12.3	12.4	15.0
NH4	[mgN/l]	1.45	2.32	3.17	1.7	2.4
Ca	[mg/l]	754	1107	1423	259	365
Mg	[mg/l]	60.75	83.9	124.33	24.2	35.5
Sr	[µg/l]	2516	3730	4940	2106	3150
Ba	[µg/l]	533	740	1020	2.9	7
Fe	[mg/l]	78	116	146	3.4	5.2
Mn	[mg/l]	1.7	2.5	3.2	0.09	0.14
Si	[mgSi/l]	30	40.8	40.3	19.9	29.4
As	[µg/l]	<1.0	<1.0	n.d.	2	2.2
B	[µg/l]	n.d.	n.d.	n.d.	1239.1	n.d.
Ni	[µg/l]	<1.0	<1.0	n.d.	2.6	<d.l.
Saturation indexes (SI)						
Bariet ($BaSO_4$)		n.a.	n.a.	n.a.	-2.17	n.a.
Calcite ($CaCO_3$)		0.72	1.2	1.4	0.98	1.3
Dolomite ($CaMg(CO_3)_2$)		0.52	1.4	1.9	1.09	1.7
Fluorite (CaF_2)		-2.24	-2.1	-1.4	-1.67	-1.3
Gypsum ($CaSO_4$)		n.a.	n.a.	n.a.	-2.45	n.a.
Hydroxylapatite ($Ca_{10}(PO_4)_6(OH)_2$)		2.26	3.1	1.1	2.22	3.2
Quartz (SiO_2)		1.21	1.3	1.3	1.02	1.2
Rhodochrosite ($MnCO_3$)		0.44	0.8	1.0	-0.25	0.0
Siderite ($FeCO_3$)		1.83	2.2	2.4	1.12	1.4
SiO_2 (amorphous)		-0.14	0.0	0.0	-0.33	-0.2
Strontianite ($SrCO_3$)		-1.23	-0.8	-0.5	-0.59	-0.3
Talc ($H_2Mg_3(SiO_3)_4$)		-1.84	-0.1	0.6	-0.28	0.9
Vivianite ($Fe^{+2}Fe_2^{+2}(PO_4)_2.8H_2O$)		3.30	3.6	2.0	0.13	0.7
Witherite ($BaCO_3$)		-2.78	-2.3	-2.1	-4.11	-3.8

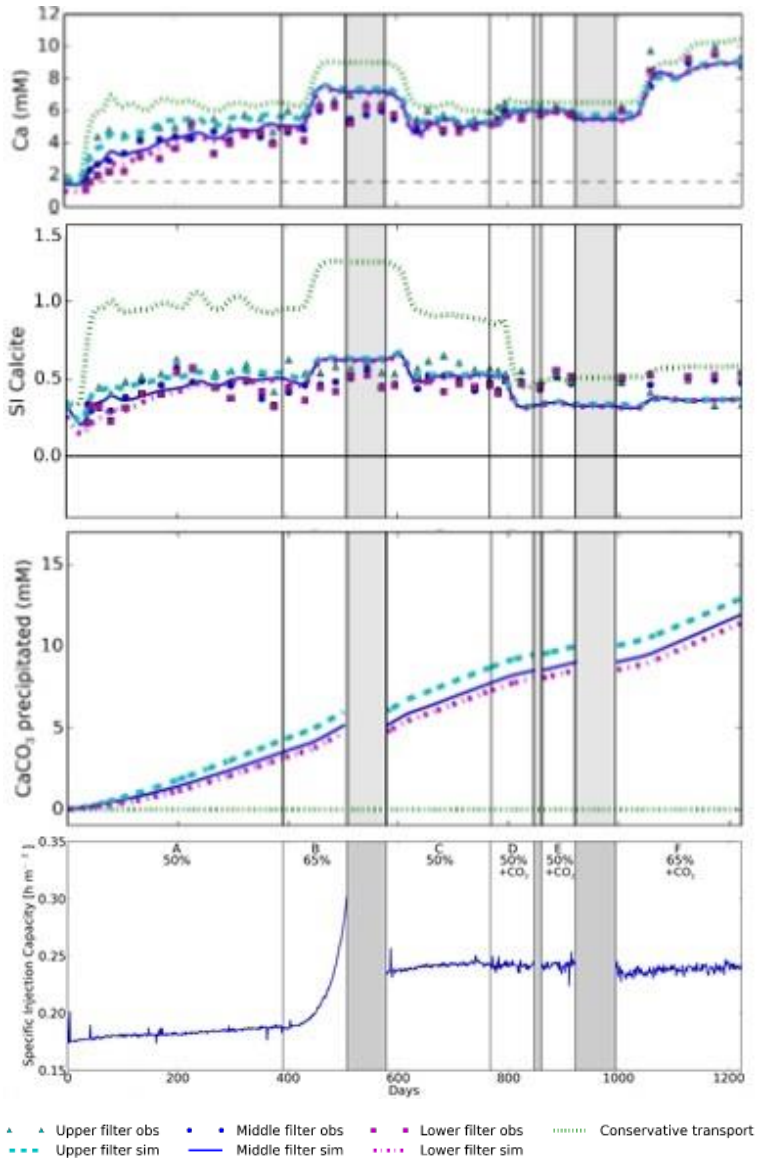

Figure 1-5 The observed and modelled calcium concentrations, $SI_{calcite}$ and precipitated calcium carbonate at the observation well in Zevenbergen during the operation period of 1200 days. A distinction is made between the hydrochemistry at different levels of the injection aquifer – upper, middle and lower. The line with the Conservative transport shows the concentrations and $SI_{calcite}$ without calcium carbonate precipitation. The vertical lines separate the periods with different operations – For example, during period F, the recovery was 65% and CO_2 was added to reduce the saturation index. The first grey zone indicates a period of regeneration with HCl. Pumping was interrupted in the other grey zones. The graph of the Specific Injection Capacity shows the hydraulic resistance (in $h.m^{-2}$) of the injection aquifer from the injection well. Individual graphs copied from Kaandorp (2014). The graph with Specific Injection Capacity is unpublished.

1.5 GOALS OF THIS RESEARCH

Clogging of the injection aquifer of calcium carbonate was for the largest part due to calcium carbonate precipitation. And where previous research was based on the precipitation of calcium carbonate in a pilot setup, this research looks at precipitation of calcium carbonate with laboratory experiments. The topics of this research are the hydraulic conductivity, the processes of calcium carbonate precipitation and inhibition by humic acids. The related research questions are written in italic in their sections below.

1.5.1 Hydraulic conductivity

One of the reasons for the pilot setups in Noardburgum, Zevenbergen and Ridderkerk is to assess if injection of RO-brine can be done without clogging of the injection aquifer. This research looks at the hydraulic resistance during the precipitation of calcium carbonate in a porous medium.

What are the effects of calcium carbonate precipitation on the hydraulic conductivity of the aquifer during injection of RO-brine?

The theory based on the Carman-Kozeny equation was tested by letting supersaturated water flow through a column with packed sand, while measuring the pressures increases over the column.

1.5.2 Processes of calcium carbonate precipitation

Calcium carbonate precipitation can be split into the processes of nucleation and growth, which take place under different circumstances. A good understanding of the precipitation processes of calcium carbonate is needed to be able to predict the precipitation potential of the RO-brine in the injection aquifer.

What are the relevant parameters and what are the conditions needed for the precipitation of calcium carbonate?

Parameters and conditions that are looked at experimentally were:

- Different degrees of supersaturation
- Presence of a calcium carbonate surface area
- Pore velocity of the super saturated water

The experiments were combined with a literature study and analysis, to give a good overview of calcium carbonate precipitation.

1.5.3 Inhibition by humic acids

Raat and Kooiman (2012) and Kaandorp (2014) both refer to the presence of inhibitors as the reason for super saturated brine from which calcium carbonate does not precipitate. According to Raat and Kooiman (2012), precipitation was inhibited because of the presence of high concentrations of Fe(II). Those high concentrations were not present in Zevenbergen. This research therefore looked at the inhibiting effects of humic acids:

What are the inhibiting effects of humic acids on the precipitation – nucleation and growth – of calcium carbonate?

The inhibition by humic acids was tested with batch experiments. The results were compared with literature.

2 THEORY

This chapter summarises the literature on calcium carbonate formation, its kinetics and flow through porous media. An introduction to aquatic chemistry is given first.

2.1 AQUATIC CHEMISTRY

Water can act as a solvent and as a chemical compound, as H_2O, in a liquid form, as a solid crystal, and as a gas. As a chemical compound it is part of the carbonic equilibrium by exchanging protons with carbonate, bicarbonate and carbonic acid, while as a solvent it allows these molecules to dissolve.

2.1.1 Concentrations and activities

A solute is a substance which is dissolved in another substance: the solvent. Concentrations of a solute in a solvent are either given as molality (m – moles of solute per kg of solvent), formality (F – moles of solute per kg of solution), molarity (M – number of moles of solute per litre of solution) and normality (N – number of equivalent weights of solute per litre of solution). Normality is sometimes used as an expression for the alkalinity: in terms of mg$CaCO_3$/l. The two most common used expressions are the molality and molarity. (Faure 1998)

To use the concentrations of ions and molecules dissolved in water (aqueous solutions) in calculations, they should be converted into activities: the concentration of "active" solutes. The activity (a) of a solute is equal to the concentration (c) times an activity coefficient (γ):

$$a = \gamma c$$

The activity coefficients of pure solids and of water (H_2O molecules) are equal to 1. The activity coefficient is related to the ionic strength. In very dilute concentrations, the activity coefficient is equal to 1. (Faure 1998)

In this thesis, activities are written as brackets [solute] while concentrations as parentheses (solute). However, there is no uniformity in literature in the use of these symbols where some use brackets and parentheses the other way round or use a_{solute} for activities.

Similarly, the units for activities aren't uniform in literature. The unit can be the same as for the concentration, which makes the activity coefficient dimensionless while the activity itself can be dimensionless as well. Then the activity coefficient has a dimension of $l.mol^{-1}$ or $kgw.mol^{-1}$ (kg of H_2O per mole of solute). In this thesis, the activities are dimensionless with the units of the activity coefficient in $l.mol^{-1}$ and otherwise it is mentioned for the size proportion.

2.1.2 Thermodynamics

Chemical reactions either consume or produce energy – they are endothermic or exothermic respectively. Thermodynamics are based on the balance between work (for example an increase in pressure, volume or temperature) and enthalpy (heat energy or heat of formation). The enthalpy is the sum of the internal energy and the pressure times the volume. Enthalpy can be changed by a flux of heat energy in or out of the system or by work done within the system. Not all enthalpy can be converted into work, since part will be used for an increase in entropy (best described by a value of randomness). (Faure 1998)

A form of energy that combines entropy (S) and enthalpy (H) is the Gibbs free energy (G):

$$G = H - TS$$

Where T is the absolute temperature in Kelvin, and the units for enthalpy and Gibbs free energy are generally kilocalories. The standard Gibbs free energy of a compound is the energy needed to form that compound from the elements in the standard state – the standard of oxygen is the O_2 molecule, for calcium the Ca-atom, for carbon the carbon atom etc. whose standard Gibbs free energies are all zero by definition. (Faure 1998)

The change in Gibbs free energy in a reaction ΔG_R° is equal to the sum of the standard Gibbs free energy of all the products minus the sum of the standard Gibbs free energy of all the reactants:

$$\Delta G_R^\circ = \sum n_i G_{fi}^\circ(products) - \sum n_i G_{fi}^\circ(reactants)$$

Where G_{fi} is the standard Gibbs free energy of a substance and n_i is the amount of that substance. $\Delta G = 0$ when the reactants and the products are in equilibrium. $\Delta G < 0$ when there are too few products and too many reactants in the system. Therefore, when $\Delta G < 0$ reactants will form a product and when $\Delta G > 0$ products will form a reactant – on condition that a reverse reaction is possible. This is where the chemical equations and balances follow from the thermodynamics. (Faure 1998)

2.1.3 Law of mass action

Following the laws of thermodynamics, pressure, energy, chemical reactions, concentrations and equilibria are all interrelated. Aquatic chemistry is basically a big balance of all substances in and in contact with water. The following chemical reaction:

$$A + B \leftrightarrow AB$$

Is in equilibrium when:

$$\frac{[AB]}{[A] + [B]} = K$$

With [AB], [A] and [B] the activities of the product AB and the reactants A and B respectively. The equilibrium constant K for aqueous solutions can be determined with the Van't Hoff equation, which is derived from the thermodynamic equations:

$$\ln(K_T) - \ln\left(K_{T^\circ}\right) = (-\frac{\Delta H_R^\circ}{R})(\frac{1}{T} - \frac{1}{T^\circ})$$

Where K_T is the equilibrium constant at temperature T in K, K_{T° is the equilibrium constant at the reference temperature T° (in K, generally 298.15K), ΔH_R° is the change in enthalpy during the reaction at the reference temperature – the change in enthalpy is negative for an exothermic reaction and positive for an endothermic reaction – in energy.mol^{-1} and R is the gas constant in energy.K^{-1}.mol^{-1}.

2.1.4 Calcium and carbonate equilibria

Calcium ions and the forms of carbonate ions form these equilibria when dissolved in water. Calcium ions Ca^{2+} and carbonate ions CO_3^{2-} in water are balanced with calcium carbonate:

$$Ca^{2+} + CO_3^{2-} \leftrightarrow CaCO_{3_{(s)}}$$

With:

$$[Ca^{2+}][CO_3^{2-}] = K_s$$

Calcium carbonate [$CaCO_{3(s)}$] is not part of the equation. Therefore, if the product of the activities of calcium and carbonate is larger than K_S, the solution is supersaturated and calcium carbonate will precipitate. The value of K_S depends on the type of crystal.

There are multiple parameters that describe super saturation. Two are most frequently used: the supersaturation ratio (Ω) and the saturation index (SI).

$$\Omega = \frac{\mathrm{IAP}}{K_s} = \frac{[Ca^{2+}][CO_3^{2-}]}{K_s} = e^{\frac{\Delta G}{RT}}$$

$$\mathrm{SI} = \log_{10} \Omega$$

Where the ion activity product (IAP) is the product of the activities of calcium and carbonate, ΔG the Gibbs free energy of the reaction (in joules generally), R the gas constant (8.31 $J.mol^{-1}.K^{-1}$) and T the temperature in K.

Carbonate ions balance with water H_2O, bicarbonate HCO_3^- and carbonic acid $CO_2(aq)$ in water. Carbonic acid is balanced with H_2CO_3 (an intermediate form) and with $CO_2(g)$ in the air. Since there is no exchange of H^+ between the two molecules and no change of phase, $CO_2(aq)$ and H_2CO_3 are generally put under one name as either $CO_2(aq)$, H_2CO_3 or $H_2CO_3^\circ$. In this thesis $CO_2(aq)$ is used for both forms since it is present 600x more at 25°C. (Stumm and Morgan 1996). That results in the following reactions of the carbonic equilibrium:

$$CO_{2_{(g)}} \leftrightarrow CO_{2_{(aq)}}$$

$$CO_{2_{(aq)}} + H_2O \leftrightarrow HCO_3^- + H_3O^+$$

$$HCO_3^- + H_2O \leftrightarrow CO_3^{2-} + H_3O^+$$

With equations:

$$\frac{[H_3O^+][HCO_3^-]}{\left[CO_{2_{(aq)}}\right]} = K_1$$

$$\frac{[H_3O^+][CO_3^{2-}]}{[HCO_3^-]} = K_2$$

With at 25°C $K_1 = 10^{-6.35}$ and $K_2 = 10^{-10.33}$. (Stumm and Morgan 1996) And for the gas water equilibrium:

$$\left[CO_{2_{(aq)}}\right] = K_H \, p_{CO_2}$$

Where p_{CO_2} is the partial pressure of CO_2 in the atmosphere – which is in the earth's atmosphere $10^{-3.5}$ atm. average. K_H is the gas equilibrium constant which is $10^{-1.5}$ atm. at 25°C. (Stumm and Morgan 1996)

Since H_3O^+ is either formed or used in the reactions above, the carbonic equilibrium is pH dependent:

$$H_3O^+ + OH^- \leftrightarrow H_2O$$

$$[H_3O^+][OH^-] = K_w$$

With at 25°C $K_w = 10^{-14}$. The pH is equal to:

$$pH = -log10([H_3O^+])$$

Or:

$$pH = -log10\left(\frac{K_w}{[OH^-]}\right)$$

Such balances in aquatic chemistry vary with concentration, ionic strength, pressure and temperature. Together with the reactions calcium and calcium carbonate, they form a balance with many substances – let alone the other substances that either calcium or the forms of carbonate react or balance with. All these substances dissolved or in contact with water together form one large balance. This will result in a long list of equations. Software like Phreeqc is a simulation tool for all these aquatic chemistry balances. More about Phreeqc can be read in section 2.4 Phreeqc.

2.2 FORMS OF CALCIUM CARBONATE

Calcium carbonate is a common material found in rock formations (limestone) and roughly all natural waters contain calcium and carbonate. In drinking water treatment processes, calcium carbonate is removed when the water is softened, to prevent scaling in pipes and boilers. Much is known about the formation and existence of calcium carbonate in these circumstances, which can help understanding the precipitation processes in the brine.

2.2.1 Forms and formation of calcium carbonate in geology

Oversaturated calcium ions and carbonate anions in aqueous solution precipitate and form calcium carbonate crystals. Pure calcium carbonate crystals can occur in three different forms: vaterite, aragonite and calcite. Vaterite crystals are very unstable. Therefore, occurrences in nature are exceptional. Vaterite is formed by organisms early in their life in shell structures alongside aragonite and calcite, which is later converted into calcite. (Tegethoff et al. 2001) The equilibrium constants K_S for calcite, aragonite and vaterite are $10^{-8.480}$, $10^{-8.336}$ and $10^{-7.913}$ (Plummer and Busenberg 1982). The lower equilibrium constant for calcite indicate a preference for the formation of calcite over the other species.

Aragonite is not stable on a geological timescale and gradually transform into calcite. Over many geological periods calcium is consumed by marine life and therefore the ratio between magnesium and calcium has shifted towards magnesium, which favours the precipitation of aragonite. Therefore, in marine environments it is more likely for aragonite to be formed than calcite. (Tegethoff et al. 2001) Since aragonite is unstable on a geological timescale, it is common in recent carbonate sediments while older limestone consists of calcite (Appelo and Postma 2005).

On a geological timescale, calcite is the stable form of calcium carbonate. In geology, when carbonate crystals precipitate, they are saturated with water and form an ooze: a muddy sludge. The precipitated calcite forms limestone rock by means of compression (compaction), recrystallization and cementing. During the cementing process oversaturated calcium carbonate from the surrounding water precipitates on the surface of the precipitates. It fills the pore space and bridges the previously formed precipitates with a dense structure. Most calcite rock formations are biogenic, from precipitated calcium carbonate made by marine organisms. Calcite rock formations often contain ooids, which are rounded precipitates, with layers of calcite or aragonite around a nucleus. Figure 2-1 below shows a picture of a cross section with two types of ooids. (Tegethoff et al. 2001).

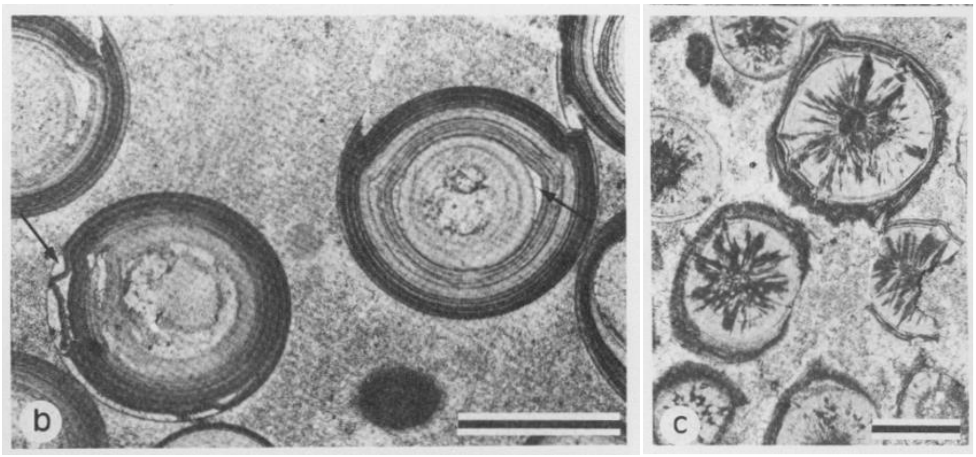

Figure 2-1: Calcite ooids with different structures caught in rock formations. Left: radial shaped ooids. Right: tangential shaped ooids. (Chow and James 1987)

Carbonate crystals have either a trigonal or orthorhombic structure. When a carbonate mineral is formed with a small cation, the crystal structure becomes trigonal and in case of a large cation, an orthorhombic crystal is formed. The calcium ion is of intermediate size and can either form calcite and aragonite, which are shaped trigonal and orthorhombic respectively. (Appelo and Postma 2005)

2.2.2 Softening in pellet reactors

In water treatment, pellet reactors are used to reduce the hardness of the water. In the reactor, water flows upwards through a fluidized bed of calcium carbonate pellets. A seeding material is added on which the calcium carbonate crystals are formed. The seeding material is often calcite grains, garnet sand – a silicate mineral with a divalent and a trivalent cation in the crystal – with a diameter of about 0.5mm (Schetters 2013) or pure silica sand with a diameter smaller than 0.1mm (Rankin and Sutcliffe 1999).

By injecting caustic soda (NaOH) or lime ($Ca(OH)_2$) at the bottom of the reactor the water becomes super saturated with calcium carbonate. As the super saturated calcium carbonate precipitates on the pellets, the pellets grow in size and move downward in the fluidised bed. At the bottom of the reactor, the saturation of calcium carbonate is the highest and decreases as the water flows upwards.

The structure of the pellets can be compared to the structures of the ooids described earlier: as the pellets grow larger over time, the precipitated calcite shifts from irregularly tangential shaped crystals around the centre to more organised radial shaped crystals on the outer layers. These patterns can be seen below in Figure 2-2.

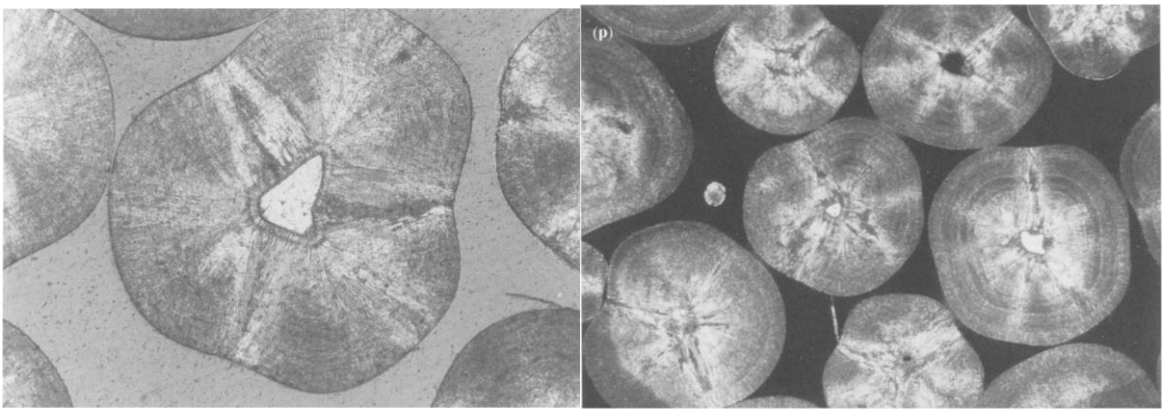

Figure 2-2 Left: The cross section of a pellet with calcite grown around a silica sand grain (field of view: 4mm). Right: difference between the irregular tangential crystals in the centre and the radial crystals on the outside (field of view: 1cm). (from Rankin and Sutcliffe 1999)

2.2.3 Stability of solutions and precipitates

Active precipitates have a disordered crystalline structure and are formed in the early stages of precipitation from strongly oversaturated solutions. A stable form of the precipitates is formed over a longer time when the active precipitate is in a metastable equilibrium with the solution. The only stable form of calcium carbonate is calcite, while aragonite and vaterite are active (or metastable) forms.

The metastable zone spans the concentrations within the threshold of oversaturation and undersaturation: the concentration at which an oversaturated solution has become undersaturated and all precipitates dissolve and the concentration at which an undersaturated solution has become oversaturated and precipitates are formed. As can be seen below in Figure 2-3, when an oversaturated solution becomes undersaturated the active precipitates will dissolve at a higher concentration of the dissolved compound than the stable precipitates. (Stumm and Morgan 1996)

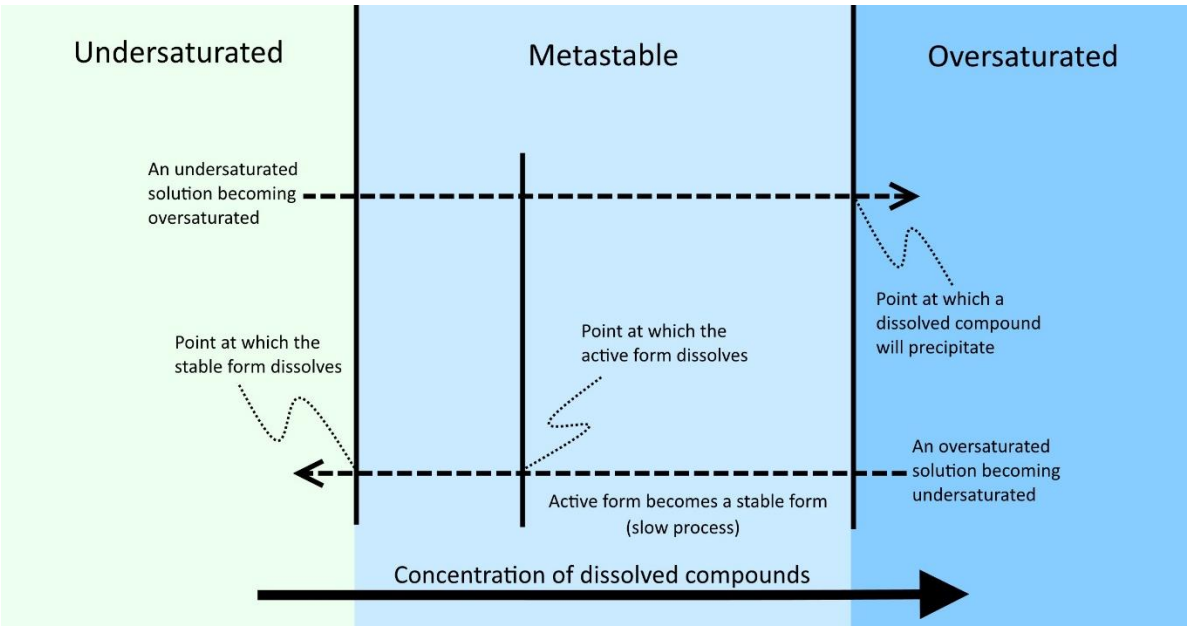

Figure 2-3 - Undersaturated, metastable and oversaturated solutions

2.3 PRECIPITATION

Calcium carbonate can precipitate by either forming nuclei or by growing on an existing calcite surface area. Nuclei formed by nucleation are either formed on surface media (heterogeneous nucleation) or in the solution (homogeneous nucleation).

Thermodynamics make that nucleation and growth are different. Because of the bonds within the crystal structure, the free energy of a molecule that lies within that structure is lower than when dissolved. The molecules on the crystal surface however, have less bonds within the crystal and therefore a higher free energy. The difference in free energy between a surface molecule and its ionic compounds in the solution is the interfacial free energy. The interfacial free energy is always positive, which makes the surface unstable. (De Yoreo and Vekilov 2003)

Therefore, when many (or all) of the molecules of a crystal lay on its surface, as in the case of a small nucleus, it is unstable. When, in case of a nucleus consisting of only one molecule, a second molecule is added, it even increases the free energy making it more unstable. After the nucleus has reached the critical size, adding more molecules to its crystal lowers the free energy – the Gibbs-Thompson effect. Only high enough concentrations can overcome the difference in free energy to form stable nuclei. (De Yoreo and Vekilov 2003)

These thermodynamics make that a calcite molecule more easily precipitates on the surface of a crystal larger than the critical size (growth) than by forming nuclei (nucleation). Therefore, at low super saturations, calcium carbonate does grow but does not form nuclei.

2.3.1 Homogeneous and heterogeneous nucleation

For heterogeneous nucleation the media properties are important: oversaturated calcium carbonate solutions in the metallic media stainless steel and chrome have a higher nucleation rate and begin forming nuclei sooner than in plastic media like PA (polyamide) and PVC (Ben Amor et al. 2004). In the experiments of Ben Amor et al. (2004), heterogeneous nucleation on the media surface took place at a water hardness of 2 mmol.l^{-1} Ca^{2+}. With a higher water hardness of 4 mmol.l^{-1} Ca^{2+} they observed that the media surface lost its effect on the total nucleation rate. However, at that concentration the nucleation didn't become solely homogeneous, but a combination of the two. The fraction of heterogeneous nucleation decreased with increasing supersaturation as more homogeneous nucleation took place. Table 2-1 below shows the results overview of the experiments by Ben Amor et al. (2004). Heterogeneous nucleation can also occur on the surfaces of suspended particles and even bacteria, which makes it hard to tell the difference between the two types (Lebron and Suarez 1998).

Table 2-1: Nucleation time T_n in minutes and heterogeneous precipitation percentage (HPP) at different concentrations and in different media. As of Ben Amor et al (2004).

Parameters	**Water hardness 2 mmol.l^{-1}**		**Water hardness 4 mmol.l^{-1}**	
	T_n	*HPP*	*T_n*	*HPP*
PA	90	99	9	86
PVC	45	98	10	61
Chrome	23	98	9	55
Stainless steel	12	97	10	44

2.3.2 The nucleation process

The nucleation rates for both heterogeneous and homogeneous nucleation are related to the number of nucleation sites or possibilities and the chance of a nucleus to grow larger than the critical size.

To pass the critical size, the nucleus must overcome the interfacial free energy barrier. The lower the interfacial free energy barrier, the larger the chance that a nucleus will grow to a stable size (Kalikmanov 2013). Figure 2-4 below shows the Gibbs free energy of the un-nucleated state A and the nucleated state B and the free energy barrier between the two states.

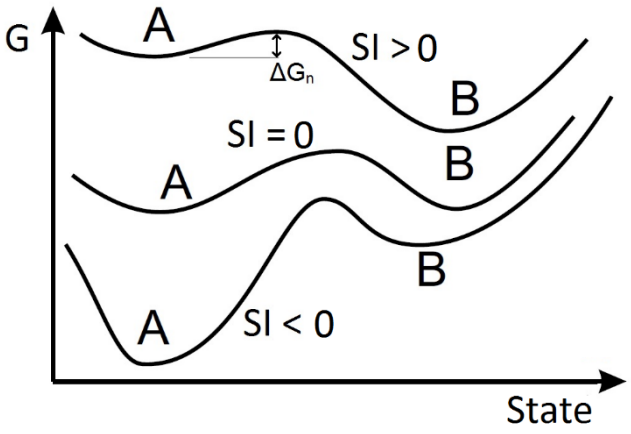

Figure 2-4 The Gibbs free energy (G) of two states A (dissolved) and B (stable nucleus) for different saturation indexes (SI). The height of the bulge relative to the local minimum A is the thermodynamic barrier for nucleation (ΔG_n, shown for SI>0), which should be overcome to for a system in state A to go to state B. In the case of SI > 0 the system is metastable at A and stable at B, for SI = 0 A and B are both stable and for SI < 0 A is the stable state and B is metastable (Modified from Vehkamaki 2013).

The equations used to calculate the nucleation rate of calcium carbonate are often very complex and comprehensive (Spanos and Koutsoukos 1998, Perez et al. 2007, Kawano et al. 2009). Yet they originate from the classical nucleation rate (Nielsen 1964, De Yoreo and Vekilov 2003, Hu et al. 2013):

$$J_n = A * \exp(-\frac{\Delta G_n}{k_b T})$$

Where J_n is the number of nuclei that are formed per unit of volume and time (e.g. $m^{-3}s^{-1}$), A is a kinetic factor with the same units as J_n and depends on the number of nucleation sites and nucleation possibilities, the level of super saturation and many other parameters – which is why models based on the classical nucleation rate are often complex – ΔG_n is the thermodynamic barrier in Joules, k_b is the Bolzmann's constant ($1.38*10^{-23}$ $J \cdot K^{-1}$) and T the Temperature in K (Hu et al. 2013).

The term $\exp(-\Delta G_n / k_b T)$ is the chance that a nucleus will pass the critical size and overcomes barrier ΔG_n (Kalikmanov 2013, Hu et al. 2013). The larger the barrier ΔG_n, the lower the chance that a nucleus will become stable. The height of the barrier varies with the level of supersaturation (see figure 2-5) and with the surface characteristics (for heterogeneous nucleation). The critical size reduces with increasing supersaturation. Before the critical size has been reached, the energy barrier increases as the nucleus grows. Past the critical size, the energy barrier goes down. This corresponds with the theories of the Gibbs-Thompson effect. Figure 2-5 below shows this variation of $\Delta G_n / k_b T$ at different sizes of the nucleus and for different supersaturations (left), and for homogeneous nucleation and heterogeneous nucleation with different surface characteristics (right).

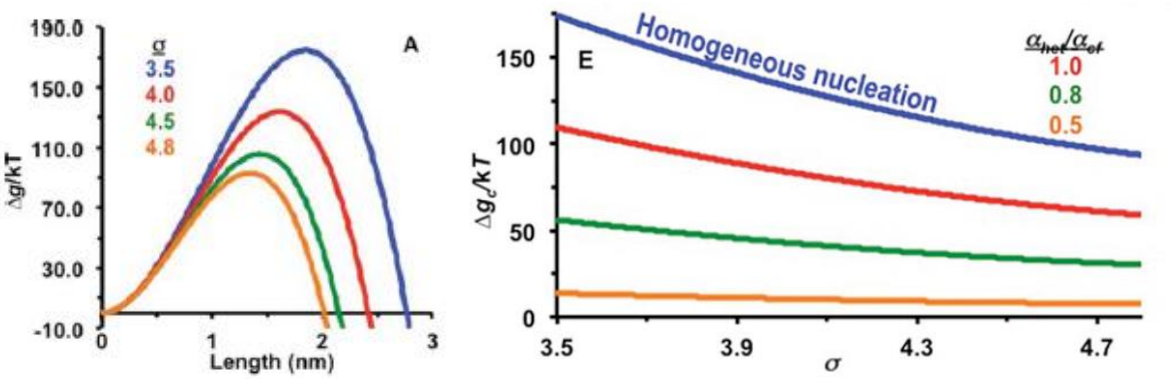

Figure 2-5 Left: The dependence of the energy barrier Δg/kT on the length of an equally shaped rhombohedron for homogeneous nucleation with different supersaturations σ = ln([Ca^{2+}][CO_3^{2-}]/K_s). Supersaturations 3.5, 4.0, 4.5 and 4.8 correspond with saturation indexes of 1.52, 1.74, 1.95 and 2.08 respectively. Equal moles of $CaCl_2$ and $NaHCO_3$ have been dosed. Right: The energy barriers for Homogeneous nucleation (blue) and for heterogeneous nucleation with improved surface characteristics – a lower α_{het}/α_{ef}. (From Hu et al 2013).

2.3.3 Amorphous and polymorphous nuclei

Ogino et al. (1987) analysed the mechanisms of the nucleation of calcium carbonate from super saturated solutions with an SI of 3.1. At those high supersaturations, amorphous calcium carbonate (ACC, calcium carbonate without the orderly structure of a crystal) precipitates initially and after several minutes the amorphous form is transformed into a polymorph – a combination of two or more crystal species. At low temperature (14 to 30°C), the polymorphs are vaterite and calcite, at high temperature (60 to 80°C) aragonite and calcite are formed and at intermediate temperature (40 to 50°C) all three combinations were formed. (Ogino et al. 1987)

Since aragonite and vaterite are unstable, they gradually stabilise and transform into calcite. At 25°C, the transformation of vaterite takes about 200 minutes. At 60-80°C, the transformation of aragonite takes 1000-1300 minutes. Ogino et al. distinguished the periods with ACC, polymorphs and calcite as the “unstable stage”, “metastable stage” and the “stable stage” respectively.

Gebauer et al. (2008) state that the intermediate state of ACC at the barrier is also metastable. In their experiments, they continuously dosed calcium chloride to water with carbonate and a pH between 9 and 10 while measuring the calcium concentration. Their results are shown below in figure 2-6.

Figure 2-6 shows that before nucleation takes place, the product of the activities of calcium and carbonate exceed the equilibrium concentrations of vaterite, aragonite and calcite. After nucleation takes place, the concentrations do not reduce to one of those equilibria, but to two different equilibria of ACC, depending on the pH. The solubility products K_S are $3.1*10^{-8}$ and $3.8*10^{-8}$ for ACC I and ACC II respectively.

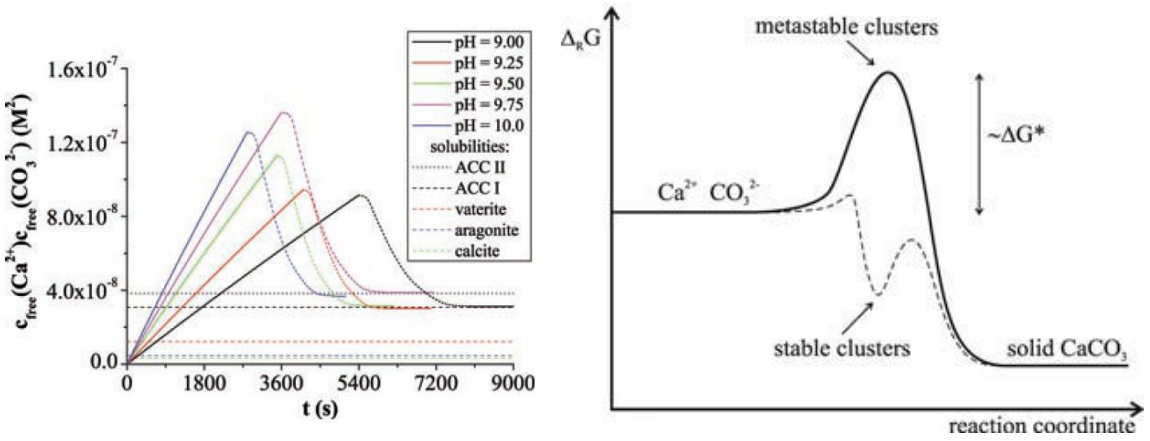

Figure 2-6 The concentration of free calcium and carbonate ions over time for different pH, and with the solubility products of ACC I, ACC II, Vaterite, Aragonite and Calcite (Gebauer et al. 2008).

Gebauer et al. (2008) propose an alternative mechanism of $CaCO_3$ nucleation, for which they add other processes to the original concept of solely single ion attachment. Originally, the nuclei are seen as unstable clusters to which individual ions attach before they have reached the critical size. In the alternative mechanism, (meta)stable clusters of calcium carbonate are formed in equilibrium with the dissolved calcium carbonate ions, even at undersaturated conditions. A schematic overview can be seen below in figure 2-7. At high enough supersaturations, the clusters form nuclei of ACC which over time convert into a crystalline form which can grow in size. Gebauer et al. (2008) found that nuclei not only formed by attachment of single molecules, but more significantly by cluster aggregation. (Gebauer et al. 2008, Gebauer and Cölfen 2011)

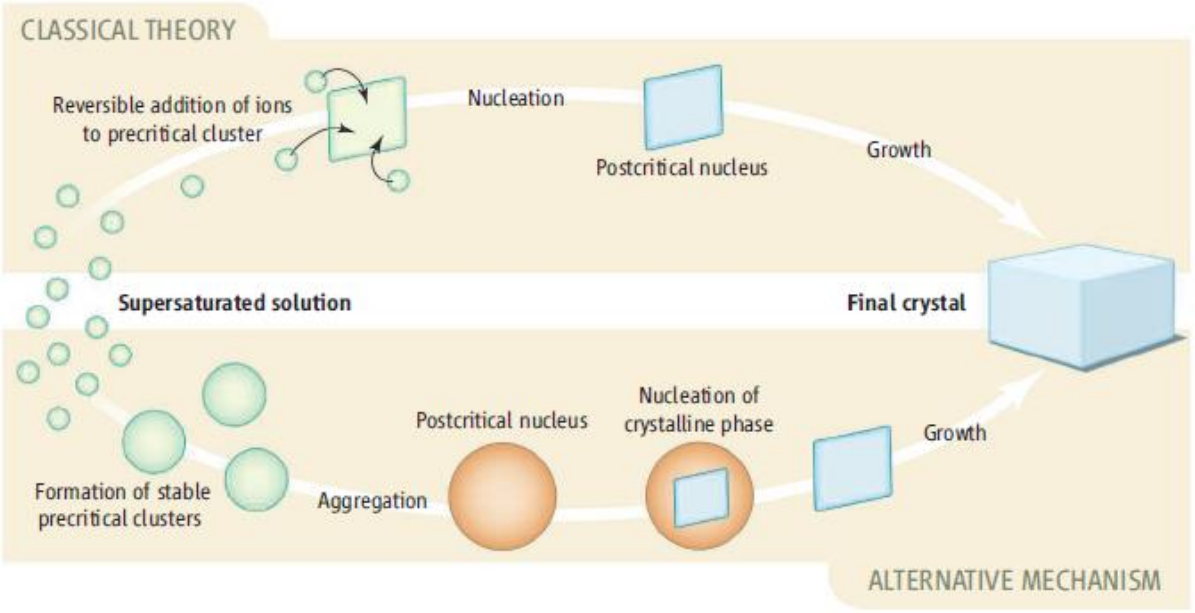

Figure 2-7 The classical theory for nucleation and the alternative mechanism proposed by Gebauer et al. (2008). From Meldrum and Sear (2008).

2.3.4 Crystal growth

Three models for crystal growth are evaluated in this section: the model of Plummer, Wigley and Parkhurst (1978) (the PWP model), the model of Wolthers et al. (2012) and the model of Schagen et al. (2006).

2.3.4.1 *The PWP model*

Plummer et al. (1978) developed a model for calcium dissolution. There are three chemical reactions or mechanisms that occur simultaneously during the dissolution of $CaCO_3$ (in the absence of inhibition):

$$CaCO_3 + H^+ \leftrightarrow Ca^{2+} + HCO_3^-$$

$$CaCO_3 + CO_{2\,(aq)} \leftrightarrow Ca^{2+} + 2HCO_3^-$$

$$CaCO_3 + H_2O \leftrightarrow Ca^{2+} + HCO_3^- + OH^-$$

With these formulas and with their experimental results Plummer et al. (1978) formed the following relation of calcite dissolution:

$$r_{cal} = k_1[H^+] + k_2\left[CO_{2\,(aq)}\right] + k_3[H_2O] - k_4[Ca^{2+}][HCO_3^-]$$

Where r_{cal} is the rate of calcite dissolution [mmol/cm^2/s] which can be split into a forward rate (in front of the minus sign) and a backward rate (after the minus sign) (Appelo and Postma 2005). The forward rate or the calcite dissolution component is equal to:

$$r_{diss} = k_1[H^+] + k_2\left[CO_{2\,(aq)}\right] + k_3[H_2O]$$

The backward rate or the calcite precipitation component is then equal to:

$$r_{prec} = k_4[Ca^{2+}][HCO_3^-]$$

The rate constants of the forward rate are temperature dependent:

$$logk_1 = 0.198 - \frac{444}{T}$$

$$logk_2 = 2.84 - \frac{2177}{T}$$

$$logk_3 = -5.86 - \frac{317}{T}\ for\ T \leq 298K$$

$$logk_3 = -1.1 - \frac{1737}{T}\ for\ T > 298K$$

Where T is the temperature [K].

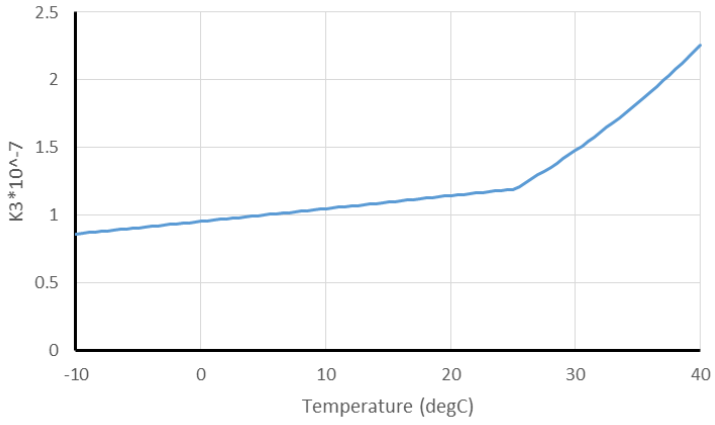

Figure 2-8 - k3 related to the temperature

The rate constant of the backward rate [mmol/cm^2/s] is given by (Plummer et al. 1978):

$$k_4 = \frac{K_2}{K_c}\left\{k_1' + \frac{1}{[H^+]_s}\left(k_2\left[CO_{2\,(aq)}\right]_s + k_3[H_2O]_s\right)\right\}$$

With K_2 and K_C as equilibrium constants:

$$K_2 = [H^+]_s[CO_3^{2-}]_S/[HCO_3^-]_S$$

$$K_C = [Ca^{2+}][CO_3^{2-}]$$

Where $[H^+]_s$, $\left[CO_{2\,(aq)}\right]_s$ and $[H_2O]_s$ are the activities of the surface layer – between the bulk liquid and crystal surface. The reaction with H^+ is transport limited, and therefore the activity of H^+ in the surface layer differs from the activity in the bulk fluid and is in equilibrium with calcite. For $CO_{2\,(aq)}$ and H_2O the activities in the surface layer are essentially equal to the activities in the bulk layer. (Plummer et al. 1978)

Combining these equations, Appelo et al. (1998) give the more simplified equations based on SI. For unaerated systems, where there is no exchange of CO_2 gas, the rate can be approximated by (Appelo et al. 1998):

$$r_{cal} = r_{diss} * (1 - 10^{SI})$$

And for aerated systems, where the rate can be approximated by (Appelo et al. 1998):

$$r_{cal} = r_{diss} * (1 - 10^{\frac{2}{3}*SI})$$

So that for both rate equations with SI > 0, $r_{cal} < 0$ and calcite precipitates (grows) and with SI < 0, $r_{cal} > 0$ and calcite dissolves.

Crystal growth is generally self-catalysing: a larger surface area per volume gives a faster dissolution of calcium carbonate from that volume. This is also seen in many models related to calcite growth. The standard calcite dissolution/growth model in Phreeqc – if the phreeqc.dat database is used – is based on the relation of Plummer et al. (1978), but adds an existing surface area of calcite:

$$R_{cal} = (k_1[H^+] + k_2[CO_2] + k_3[H_2O])\left(\frac{A_{calcite}}{V}\right)\left(\frac{m}{m_0}\right)_{cal}^{0.67}(1 - 10^{\frac{2}{3}SI_{calcite}})$$

Where R_{cal} is the rate of calcite dissolution or growth [mmol/s] if larger than zero or lower than zero respectively. This is since the calcite concentration in Phreeqc is the amount of calcite in the solution without the precipitated calcium concentration. $A_{calcite}$ is the surface area of calcite [cm^2] in the volume V [liter], m/m_0 is the ratio between the concentration of calcite m and the initial concentration of calcite m_0. The factor $(1 - 10^{\frac{2}{3}SI_{calcite}})$ can be replaced with $(1 - 10^{SI_{calcite}})$ for unaerated systems like a confined aquifer.

Chou et al. (1989) proposed a different model with the same dissolution but with different precipitation reactions (based on the product of calcium and carbonate activities instead of calcium and bicarbonate activities) from his experiments on a fluidised bed reactor with calcite pellets. The model was fitted to four different carbonate minerals: Calcite ($CaCO_3$), Aragonite ($CaCO_3$), Witherite ($BaCO_3$) and Magnesite ($MgCO_3$). The net calcite dissolution rate is modelled as:

$$r_{cal} = k_1[H^+] + k_2\left[H_2CO_2^\circ\right] + k_3[H_2O] - k_{-3}[Ca^{2+}][CO_3^{2-}]$$

With at 25°C $logk_1 = -4.05$, $logk_2 = -7.30$, $logk_3 = -10.19$ and $logk_{-3} = -1.73$.

2.3.4.2 The growth model of Wolthers et al. (2012)

Solutions in most aqueous environments are non-stoichiometric, especially regarding calcium carbonate. The calcite precipitation and dissolution rate is highly affected by anion and cation concentration ratios (Wolthers et al. 2012).

Wolthers et al. (2012) made a model for calcite growth kinetics by adding the surface complexation model of Wolthers et al. (2008) to the growth model of binary symmetrical electrolyte crystals of Zhang and Nancollas (1998). Their model approaches the formation of calcite on molecular level, incorporating the effects of kink sites, step edges, corner sites and surfaces of the crystal and their difference in surface chemistry. The model zooms in on the processes of calcite growth, in which dissolved calcium carbonate attaches to crystalline calcium carbonate – calcite is formed on calcite.

Wolthers et al. (2012) have proposed two empirical models for calcite growth. One model was fitted to results of different experiments with background electrolyte solutions – dissolved KCl or NaCl – ionic strength 0.001-0.7M) and one was fitted to experiments in diluted and undiluted artificial seawater of Zhong and Mucci (1989) containing inhibitors such as magnesium, sulphate and phosphate.

Calcite growth (precipitation) rate in electrolyte solutions is modelled as:

$$R_{p\,BE} = I^{-0.004} pH^{-10.71} r_{aq}^{-0.35} (S-1)^2$$

Calcite growth (precipitation) rate in diluted and undiluted artificial seawater is modelled as:

$$R_{p\,SW} = I^{-0.36} pH^{-10.99} r_{aq}^{-0.71} (S-2)^2$$

Where $R_{p\,BE}$ and $R_{p\,SW}$ are the rates in m/s, which can be converted to mmol/cm^2.s by multiplying it with the density of calcite, 2.71*10^4 mol/m^3 = 2.71*10^3 mmol/cm^2.m. I is the ionic strength in mol/l, $r_{aq} = [Ca^{2+}]/[CO_3^{2-}]$ is the activity ratio and $S = \Omega^{1/2} = ([Ca^{2+}][CO_3^{2-}]/K_c)^{1/2}$ is the saturation ratio. The growth rate is highest at an activity ratio $r_{aq} = 1$, though it varies with the pH (Wolthers et al. 2011).

The increase of ionic strength in seawater has a stronger reducing effect than the increase in ionic strength of an electrolyte solution: higher ionic strength means less diluted artificial seawater which has higher inhibitor concentrations.

According to Wolthers et al. (2011), a solution with equal activities of calcium and carbonate ions (a stoichiometric solution) has a higher growth rate than a solution with unequal activities (a non-stoichiometric solution). A crystal grows by first forming a kink (a single molecule of calcium carbonate or calcium bicarbonate sticking out of the crystal surface) and then by propagation of this kink where a row of calcium and carbonate or bicarbonate molecules attaches consecutively to the primary kink. The growth mechanisms of calcite are shown below in figure 2.9.

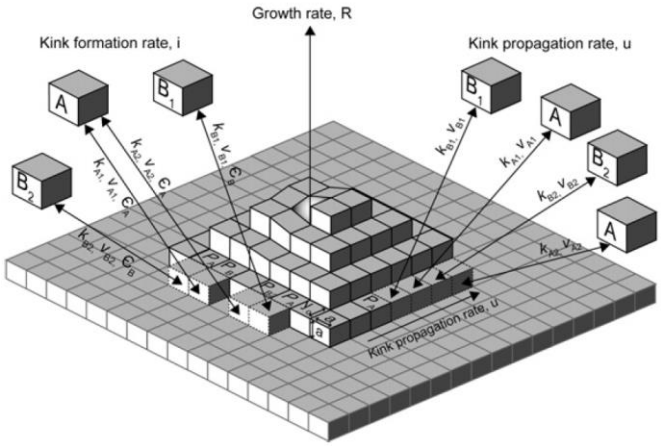

Figure 2-9 The growth mechanisms of calcite. Kink sites are formed and then propagated. Calcium ions (A) and carbonate ions (B1) or bicarbonate ions (B2) attach to the kink consecutively (from Wolthers et al. 2011).

Because of the attachment of both calcium and carbonate or bicarbonate ions, the rate depends on the ratio between the carbonate and calcium activities. The dependency of the rate on the ratio is shown below in figure 2-10. The position of the maximum growth and the shape of the graph depend on the pH. At low pH, the growth relies more on the attachment of bicarbonate ions since less carbonate ions are present than at high pH. This effect is larger at lower supersaturation ratios.

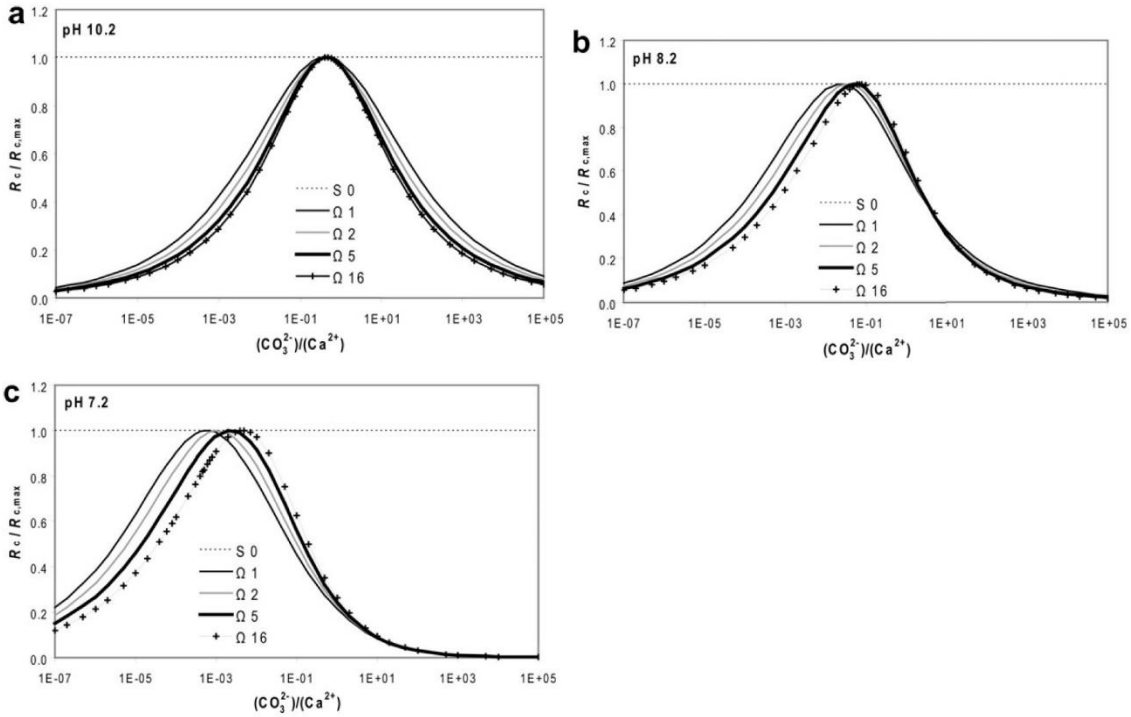

Figure 2-10 The effect of the ratio of carbonate and calcium activities ($[CO_3^{2-}]/[Ca^{2+}]$) on the rate of calcium carbonate growth at different pH for each figure and with different supersaturations in each figure. The rates are plotted normalised to the maximum rate found at that pH and supersaturation. Supersaturation ratios correspond to SI values of 0.0, 0.30, 0.70 and 1.2. The rates are model results based on experimental results (From Wolthers et al. 2011).

2.3.4.3 The growth model of Schagen et al. (2008)

The previous models are based on batch experiments with high Reynolds numbers (Plummer et al. 1978). The transport of H^+ between the surface layer and the bulk solution – which largely

determines the calcite dissolution rate by reaction with H^+ – as in the PWP model is affected by the stirring speed. Velocities around the grains might therefore affect the calcite growth rate.

Van Schagen et al. (2008) made a calcium precipitation model for pellet softening. The formula for calculating the precipitation rate (in mmol/cm^2.s) is:

$$r_{cal} = K\left((Ca^{2+})(CO_3^{2-}) - \frac{K_s}{f^8}\right) * 10^{-1}$$

Where K is the crystallisation kinetics factor (l.m/s.mmol), K_s is the solubility product (mmol^2/l^2) and f is the activity factor (-). The crystallisation kinetics factor (K) depends on the temperature and on the Reynolds number via the Sherwood number:

$$K = \frac{\kappa_T \kappa_f}{\kappa_T + \kappa_f}$$

κ_T is a temperature dependent crystallisation constant (l.m.s^{-1}.mmol^{-1}):

$$\kappa_T = 1.53 * 1.053^{(T-20)}$$

The constant κ_f depends on the transportation of ions to the crystal surface, based on the Reynolds (Re), Schmidt (Sc) and Sherwood (Sh) number. For ions to move from the solution to the crystal surface they have to pass a boundary layer. The movement of ions depends on the diffusion and on the thickness of this layer. The layer becomes thinner at higher velocities (thus higher Reynolds number) and with higher temperatures (lower viscosity results in a higher Schmidt number and Reynolds number).

$$\kappa_f = \frac{Sh \cdot D_f}{d}$$

$$Sc = \frac{D_f}{\upsilon}$$

$$Sh = 0.66 Re_h^{0.5} Sc^{0.33}$$

Where D_f is the diffusivity coefficient (m^2.s^{-1}), d is the average diameter (m) and υ is the viscosity (m^2.s^{-1}). The Reynolds number for flow in porous media is:

$$Re = \frac{q \cdot d}{\upsilon}$$

Where q is the flow through the bed (m.s^{-1}), d is the characteristic length (m) and υ is the viscosity (m^2.s^{-1}). The characteristic length should represent the channel between the grains. Often, from a grain size distribution graph, the diameter of which 10% of the grains are smaller (d_{10}) is taken as the characteristic length d (Bear and Verruijt 2012).

2.3.4.4 Comparison of the growth models

Wolthers et al. (2012) have shown that the precipitation of calcium carbonate depends on the ratio of carbonate and calcium activities: $[CO_3^{-2}]/[Ca^{+2}]$. The three models are compared for different ratios of carbonate and calcium. The PWP model is evaluated for both the closed and the open variant: using $(1\text{-}10^{SIcalcite})$ and $(1\text{-}10^{2/3*SIcalcite})$ respectively. The results are shown below in figure 2-11. While $[CO_3^{-2}]/[Ca^{+2}]$ varies, the $SI_{calcite}$ and pH are kept constant at 1.0 and 7.5 respectively.

Though the model of Wolthers et al. (2012) is directly related to the ratio of carbonate and calcium, the effect of increasing growth rates at with increasing $[CO_3^{-2}]/[Ca^{+2}]$ can also be found in both PWP

models. The highest growth rate calculated with the model of Schagen et al. (2008) was obtained at $[CO_3^{-2}]/[Ca^{+2}] \approx 0.2$.

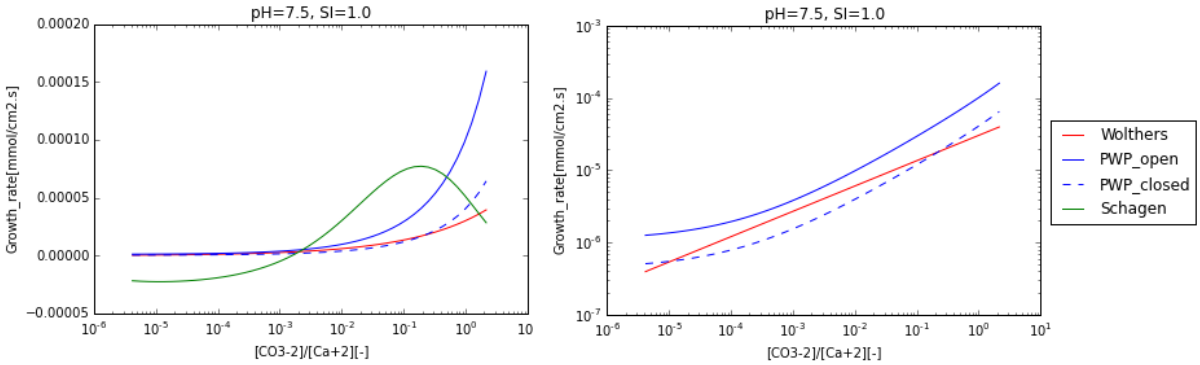

Figure 2-11: Comparison of the PWP growth model (both the open and the closed version), the model of Wolthers et al. (2012) and the Schagen et al. (2008) model. Left: the values on the vertical axis are linear. Right: the values on the vertical axis are logarithmic. The value used for the variable K in the Schagen model is 10^{-3} l.m.s^{-1}.mmol^{-1}, to give it the best fit compared to the other models.

The model of Schagen et al. (2008) uses the product of the concentrations of calcium and carbonate to calculate the precipitation rate, where the other models use the product of the activities. Figure 2-12 below shows the concentration product of calcium and carbonate under the same conditions as the growth rate simulations. While the activity product is constant – a result of the constant $SI_{calcite}$ – the graph of the concentration product shows the same shape as the graph of Schagen et al. (2008). Hence, this different shape of Schagen et al. (2008) compared to the PWP model and the model of Wolthers et al. (2012) is a result of using the concentrations instead of the activities. There is no consensus whether activities or concentrations should be used in these rate models (Lasaga 1998).

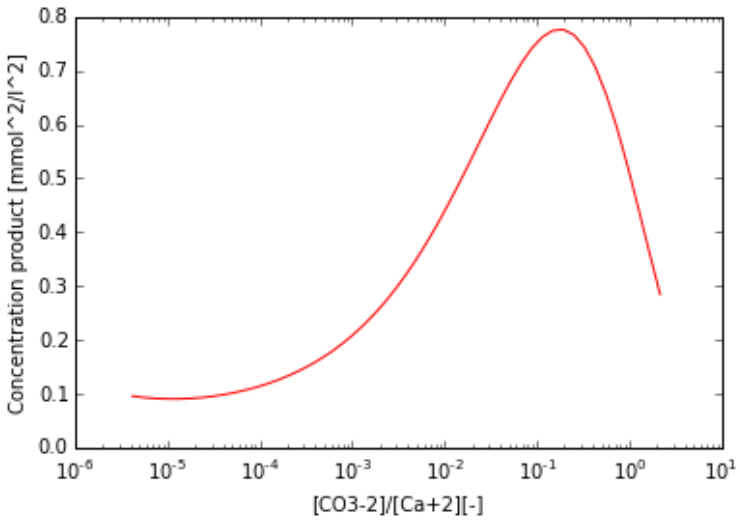

Figure 2-12 The concentration product (Ca+2)(CO3-2) under the same conditions as the comparison of the growth models. Note: the activity product [Ca+2]*[CO3-2] is constant, since the SI is 1 for all [CO3-2]/[Ca+2]*

2.3.5 2D-nucleation

As discussed earlier, Wolthers et al. (2012) modelled the kink formation and kink propagation of a growing calcite crystal. Calcite has relatively few kinks, and therefore kink formation is the rate limiting process and not kink propagation (Stack and Grantham 2010). The precipitation of a single molecule of calcium carbonate on a perfectly smooth and flat calcite surface without any kinks and edges is least favourable, since it is only linked to the crystal on a single point. This process is called

(homogeneous) two-dimensional nucleation. The 2D-nucleus is the base to which more calcium carbonate molecules can attach and form a new surface. Because of the energy barrier that has to be overcome for a 2D-nucleus to form, crystals grow predominantly by kink propagation at low supersaturations (Liu et al. 1997). During their experiments, Lin and Singer (2006) observed that at an $SI_{calcite}$ of 0.3 or less, calcite growth occurs step by step but at and $SI_{calcite}$ of more than 0.3, 2D-nucleation becomes more important.

In practice, natural waters contain many small particles like dust, gas bubbles, macro molecules, polymers and small crystals in suspension. These particles are unavoidable in any water, and can be a good base for heterogeneous nucleation. When a particle is attached to a crystal surface, it forms a good base for a 2D-nucleus to grow (heterogeneous 2D-nucleation). In addition, a particle on the crystal surface can block the movement of kinks and step edges. At low supersaturations, heterogeneous 2D-nucleation is the favourable process. At high supersaturations however, homogeneous nucleation becomes more favourable. (Liu et al. 1997)

2.3.6 Inhibitors

There are several inhibitors delaying or preventing the precipitation of calcium carbonate. The relevant substances are listed below in table 2-2. Calcium carbonate growth can either be inhibited when precipitation sites on the crystal are blocked by the inhibiting substance or by the formation of complexes with the inhibitor and calcium or carbonate ions. The incorporation of ions in complexes results in a reduction of the activity of either calcium or carbonate in the solution.

Natural organic matter (NOM) reduces the precipitation of calcite by forming a layer of calcium-organo compounds on the crystal surface (which can also incorporate a phosphate component) and by forming complexes with the NOM (Suess 1969). NOM has a greater effect on the growth of calcite than on nucleation: in water with a dissolved organic carbon content higher than 0.05mmolC/l growth can be neglected and calcium carbonate solely nucleates (Lebron and Suarez 1996). According to Lebron and Suarez (1996), calcite growth is not the dominant mechanism of precipitation in earth surface systems, where DOC > 0.05mmol/l. A DOC concentration of 0.3mmolC/l completely inhibits nucleation and a concentration of 0.15mmolC/l limits the growth of the nuclei (Lebron and Suarez 1996). Since the NOM coats the surface of the existing crystal, the limiting concentration for growth depends on the surface area. In the experiments of Lebron and Suarez (1996) this was $2m^2/l$.

Iron can either be present as Fe^{+3} and Fe^{+2} in aerobic and anaerobic conditions. Both have different effects on the precipitation of calcium carbonate. In the presence of oxygen, the present Fe^{+2} attaches OH^- ions and form colloids on which the super saturated calcium carbonate can nucleate. Similar to Ca^{+2}, Fe^{+2} reacts with CO_3^{-2} and forms $FeCO_3$. Single $FeCO_3$ molecules precipitate onto the surface of a calcium carbonate crystal, and hence block the growth sites (Herzog et al. 1989).

Phosphorous dissolved in water is present in the form of PO_4^{-3}. It can react with many other substances in water. In the experiments of Lin and Singer (2006), phosphorous occurs as H_3PO_4, $H_2PO_4^-$, HPO_4^{-2}, PO_4^{-3}, $CaH_2PO_4^+$, $CaHPO_4$, $CaPO_4^-$, $NaHPO_4^-$ and $KHPO_4^-$. The species $CaHPO_4$ was found to be blocking the growth sites on the crystal surface and disrupting the crystal growth. Lin and Singer observed two effects of phosphorous on calcium carbonate: when phosphorous was present, the nuclei formed by 2D-nucleation ($SI_{calcite}$ > 0.3) have amorphous instead of structured shapes and during layered growth ($SI_{calcite}$ < 0.3) the steps in nucleation are more jagged than straight. (Lin and Singer 2006)

Magnesium and calcium can replace each other in their carbonate crystals – a solid solution. If incorporated at about the same quantities, magnesium and calcium form together with carbonate a mineral called dolomite ($CaMg(CO_3)_2$). At low concentrations, growing calcium carbonate incorporates magnesium cations as a solid solution. This increases the solubility of calcium carbonate: dolomite has a higher solubility than calcite. At high concentrations, magnesium cations occupy the calcium growth sites on the crystal. Because of the competition with calcium, the activity of calcium increases the activity at which magnesium inhibits the growth. (Zang and Dawe 2000, Nielsen et al. 2013)

*Table 2-2 – Calcium carbonate precipitation inhibitors (adjusted from Kaandorp 2014) and their occurence in the Zevenbergen study of Kaandorp (2014) and around the PURO well in Ridderkerk. TOC concentrations are given in mmoles of carbon per litre. *The concentrate in Ridderkerk is double the concentrations in the abstraction aquifer.*

Inhibitor	References	Relevant above (mM):	Zevenbergen		Ridderkerk	
			Concentrate with 50% recovery (mM):	Injection aquifer (mM):	Concentrate with 50% recovery* (mM):	Injection aquifer (mM):
Mg2+	Astilleros et al. (2010), Nielsen et al. (2013), Reddy (2012), Zhang and Dawe (2000)	0.25	1.000	1.687	3.492	2.030
SO42-	Flaathen et al. (2011)	20	0.078	0.035	<detection	<detection
Sr2+	Bracco et al. (2012), Nielsen et al (2013)	0.03-0.8	0.023	0.045	0.029	0.013
PO43-	Lin and Singer (2006)	0.001	0.006 (P)	0.003 (P)	0.016	0.011
Fe2+	Herzog et al. (1989)	0.1	0.0605 (Fe)	0.031 (Fe)	0.178 (Fe)	0.061 (Fe)
Fe3+	Takasaki et al. (1994)	0.001-0.005	0.0605 (Fe)	0.031 (Fe)	0.178 (Fe)	0.061 (Fe)
Cu2+	Parsiegla and Katz (1999,2000)	0.1-1	-	-	Negligible	Negligible
Organics (DOC)	Lebron and Suarez (1996), Reddy (2012)	0.1 (complete inhibition at 0.3)	0.648	0.272	0.677	0.338

2.4 PHREEQC

Phreeqc is a computer program for geochemical calculations. It can simulate equilibrium reactions, ion exchangers, surface complexes, solid solutions, gases and kinetics. It has various libraries which contain a set of the parameters of the most frequently occurring substances and reactions, which can be used to model the aquatic chemistry in different circumstances. In the written code, extra substances and processes with parameters can be added, or the parameters from the library can be adjusted. (Parkhurst and Appelo 2013).

For this research, the equilibrium reactions and constants are used for the calculations. Phreeqc is used alone as Phreeqc interactive and as a COM-module in Excel (De Moel et al 2012) and in Python (Charlton and Parkhurst 2011).

2.4.1 Differences in thermodynamics

Phreeqc can call on various databases, each with different parameters and variables. The database used in this research is the Phreeqc.dat database. As explained earlier in section 2.1.3 Law of mass action, the Van 't Hoff equation is used to calculate the equilibrium constants (K) and this equation is used in Phreeqc as well. However, the phreeqc.dat database uses an analytical expression to calculate the equilibrium constant K, which overrules the Van 't Hoff equation.

$$K = A_1 + A_2 T + \frac{A_3}{T} + A_4 \log_{10} T + \frac{{A_5}^2}{T} + {A_6}^2 T$$

With the coefficients A_x that vary for every equilibrium reaction and the temperature T in Kelvin. The coefficients in Phreeqc for calcite and aragonite are based on those of Plummer and Busenberg (1982).

2.4.2 Kinetics

Phreeqc does not automatically let the substances from supersaturated waters precipitate or dissolve. It can either be modelled as a reaction where a specific amount of moles is added or removed from the solution; it can be modelled as a reaction to reach another saturation index – optionally with other substances like acids and bases that only change the pH; or with kinetics.

Phreeqc has some equations in its database to compute the kinetics of precipitation and dissolving matter and equations can be added or replaced. The standard Phreeqc kinetics reaction in the phreeqc.dat database is the aerated PWP model. One can change the kinetics by adding one of the models described in section 2.3.4 Crystal growth or any other model in the Phreeqc code.

2.5 FLOW THROUGH POROUS MEDIA

Water flows between two points when there is a difference in potential between them and the flow is not restricted. In geohydrology, the Darcy equation describes the flow through a saturated porous medium as a function of the change in head. Darcy for one-dimensional flow:

$$q = -K \frac{dH}{dx}$$

Where q is the flux in m/d, K is the Darcy constant in m/d and $\frac{dH}{dx}$ is the gradient of the head H over distance x in m/m.

2.5.1 Carman-Kozeny

The pore space between the grains of the sandy aquifer determines for a large part the hydraulic conductivity of the soil. As more and more calcite is formed on the sand grains, the porosity slowly decreases and that decreases the conductivity. The calcite growth models mentioned above refer to the growth on existing crystals, not the growth in a stretch of soil.

Hubbert (1957) derived the equation of Darcy's law from the Navier-Stokes equations, and gave the following expression of Darcy's law:

$$q = -(Nd^2)\left(\frac{\rho}{\mu}\right) g * \nabla h$$

Where q is the velocity (m/s), N is a grain-shape factor (-), d is the diameter of randomly packed uniform spheres (m), ρ is the density of the liquid (kg/m^3), μ is the viscosity of the liquid (Pa.s) and ∇h the gradient in head. This equation is similar to the one of Carman-Kozeny:

$$q = -\frac{1}{180}\frac{p^3}{(1-p)^2}d^2\left(\frac{\rho}{\mu}\right)g * \nabla h$$

Where the grain-shape factor is replaced by a factor based on the porosity p (-). Precipitating calcite can have two effects: a reduction of the porosity and an increase in grain size. If calcite precipitates and fills and clogs the pores, it decreases the porosity. If calcite precipitates in layers around grains as in a pellet reactor, it would result in an increase in grain size diameter and decrease in porosity. In both equations, an increasing diameter results in an increase in hydraulic conductivity. This means that the grain shape factor N is not constant during calcite precipitation.

Packed sand with larger grains will have fewer grains and pores per volume than sand with smaller grains. If both have the same porosity, the individual pore sizes between the large grains will be larger than between the small grains. The hydraulic resistance of sand with large grains is therefore lower.

The size of the grain with a layer of calcium carbonate can be calculated with (Schagen et al 2008):

$$d(V_{CaCO_3}) = d_0(1 + \frac{V_{CaCO_3}}{V_o})^{\frac{1}{3}}$$

With d_0 the initial diameter of the grains (m) and V_0 the volume of grains without calcium carbonate (m^3). V_{CaCO_3} is the volume of calcium carbonate that has precipitated (m^3). If a volume of sand is well packed and confined, there is no room for the grains to expand. Clogging of an aquifer is therefore most likely to be caused by a reduction of the porosity. Figure 2-13 below shows the effect of precipitating calcium carbonate that reduces the pore size on the pressure gradient (dH/dL). The pressure gradient (dH/dL) increases exponentially as more calcium carbonate precipitates and the porosity decreases. In the initial stages of precipitation the increase in resistance will be hardly noticeable, compared to a later stage when the resistance increases faster as more calcium carbonate has precipitated.

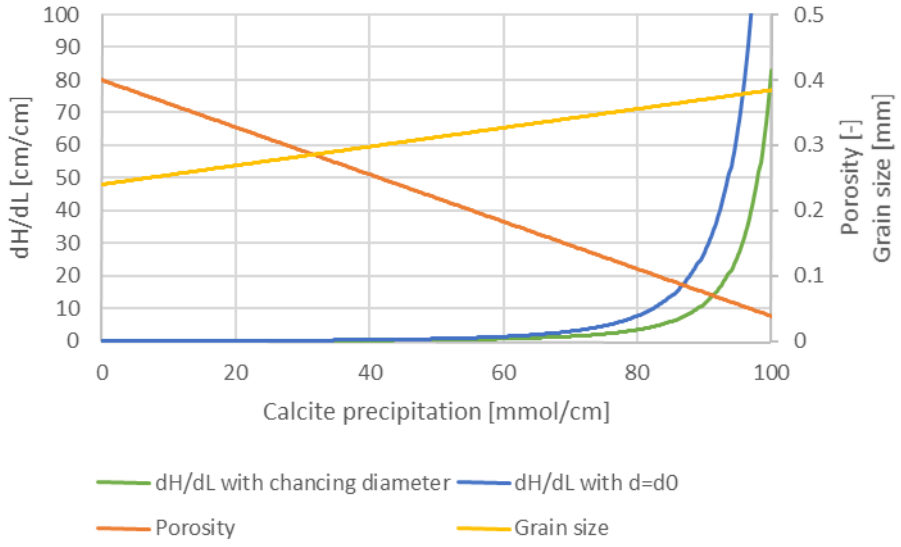

Figure 2-13 The effect of calcite precipitation on the porosity and the pressure gradient (dH/dL) calculated with Carman-Kozeny, either with or without the increase in grain size taken into account. The values used are the values of the column setup: Grain size is 240µm. Porosity without precipitated calcite is 0.4. The flux is 3.7l/d though a column with a diameter of 10.22cm². The molar density of the precipitated calcite is 27.1 mmol/cm³.

2.5.2 Radial flow

For both the Freshkeeper and PURO, the injection aquifer is always confined. For a single well, the hydraulics can be modelled as radial flow, where the velocity decreases as the distance from the well increases. As what follows from the formulas of Darcy and Carman-Kozeny, the pressure gradient increases linearly with the flow. For a confined aquifer, the head around the well can be calculated with:

$$H(x) = H_0 - \frac{Q}{2\pi hK}\ln(\frac{x}{x_0})$$

Where H(x) is the head (in m) at a distance x (in m) from the well. H_0 is the head at x_0, Q is the discharge through the well (in m^3/d), h is the thickness of the aquifer (in m) and K is the Darcy constant (in m/d). The head decreases exponentially over the distance from the well. The effect of a reduction in permeability K close to the well on the required pumping head is therefore much larger than further from the well.

Taking into account both the effect of decreasing porosity with Carman-Kozeny and the effect of distance from radial flow, precipitation of calcium carbonate at a larger distance from the well has much less effect on the required pumping head than precipitation close to the well. Also, precipitation of the same amount of calcium carbonate over a larger distance compared to a short distance results in a slower reduction in porosity and therefore a slower increase in required pumping head. Precipitation over a long distance far away from the well is therefore favourable.

2.5.3 Therzaghi's criteria

Oversaturated RO-brine can also contain homogeneously formed nuclei. Those nuclei can be caught by the aquifer sand as a filter if they are large enough. Therzaghi established the classical criteria that are used for the granular filter clogging. The criteria are based on a granular filter layer below a layer of soil that prevents the washout of the smaller soil grains.

$$d_{15F} \geq 4 \; or \; 5 \; d_{15S}$$

$$d_{15F} \leq 4 \; or \; 5 \; d_{85S}$$

Where d_{15F} is the diameter for which 15% of the filter grains is smaller. d_{15S} and d_{85S} are the diameters of the covering soil grains for which 15% and 85% are smaller respectively. The aquifer sand can be seen as the filter grains and the covering soil as the nuclei. If the first criterion is not met the permeability of the filter is too small. If the second criterion is not met the filter will not retain the particles. The opening size of a filter is the diameter of the largest sphere that can pass through a filter: (Giroud 2010)

$$Opening\ size \approx \frac{d_{F15}}{5}$$

The sand in Zevenbergen has a diameter of 240µm, and it will filter out all the particles that are larger than 48µm. There is no diameter defined for which 100% of the particles that are smaller will pass the filter.

3 EXPERIMENTAL METHODS

Two types of experimental setups have been used. The experimental methods are discussed per type of setup: column experiments and batch experiments. The column experiments are designed to simulate the injection of brine in a sandy aquifer. Each column is filled with fine sand. Two influent streams – one contains sodium bicarbonate and the other calcium chloride – are mixed and pumped through the column. The mixed water is supersaturated with calcium carbonate. Pressures along the column and the pH of the effluent are measured continuously. Samples are taken from the influent and the effluent to test the alkalinity and the calcium and (bi)carbonate concentrations.

The batch experiments are used to test the kinetics of calcium carbonate precipitation. Sand is added as seed material. The batch bottles are closed and placed in a shaker to ensure complete mixing. Various amounts of humic acids are dosed to test their inhibiting effect.

3.1 COLUMN EXPERIMENTS

Two columns with packed sand are used for the column experiment. They are of similar length and diameter. One will be referred to as the blue column and one as the green column. Water flows through the column from the top to the bottom to prevent fluidisation of the sand.

3.1.1 Column setup

Both columns are just under 90cm long – the Green and the Blue column are 87.7 cm and 87.5 cm long respectively – and have a connection for a pressure sensor at about every 12cm. The diameter is 3.60cm – the surface area of the cross section is 10.22 cm^2. The sand is packed between two PVC filter plates with 250µm holes. A schematic overview of the setup is shown below in figure 3-1.

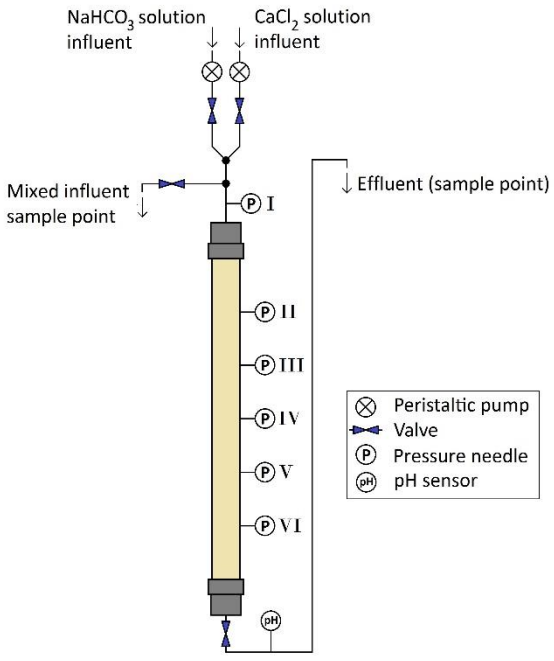

Figure 3-1 Overview of the column setup with the locations of the pressure needles I – VI and the locations of the sample points for the effluent and the influent.

The influent consists of two solutions: a $NaHCO_3$ solution and a $CaCl_2$ solution. The solutions are connected to the same peristaltic pump and are therefore mixed 1:1. Only the mixed solution is supersaturated with calcium carbonate ($SI_{calcite} > 0$). The $SI_{calcite}$, pH and concentrations of calcium

and carbonate species of both influent solutions and the resulting mixed solution are calculated with Phreeqc. The concentrations are chosen such that the mixed solution has a $SI_{calcite}$, a pH and calcium and carbonate concentrations similar to the injected brine in Zevenbergen and a recovery of 50%.

3.1.2 Pressure sensors

Eight pressure sensors (Honeywell 24PC01SMT) that are numbered 1-8 can be used to measure the pressure in the column at different heights. Every column has five locations to which a pressure sensor can be connected. An extra point is added to measure the pressure at the top of the column. The locations in the column consist of a needle of which the tip reaches the centre of the column. The needle is connected to the sensor with a flexible tube (Saint Gobain Tygon S3™, 1/16 x 1/8", 36.0 psi). When testing the setup, it appeared that the connection between the sensor and the tube was leaking. Therefore, some high vacuum grease (DOW CORNING®) was applied in the tube with a small brush which sealed the leak.

The height at which the two effluent tubes of both columns end is the level at which the hydrostatic pressure in the column equals zero. Figure 3-2 below shows a picture with the tubes and the hydrostatic pressure line. The hydrostatic pressure in both columns is higher than zero, to prevent air from entering the column via small leaks during the experiment. Since the range of the pressure sensors is only 0-70cm of water column, the pressure tubes were only connected to the sensors after the water level in the tubes was at this hydrostatic pressure line. The pressure tubes were filled by letting the influent pump pump demiwater at the slowest rate through the column. The tubes were held at the same height and kept straight by two screw terminals.

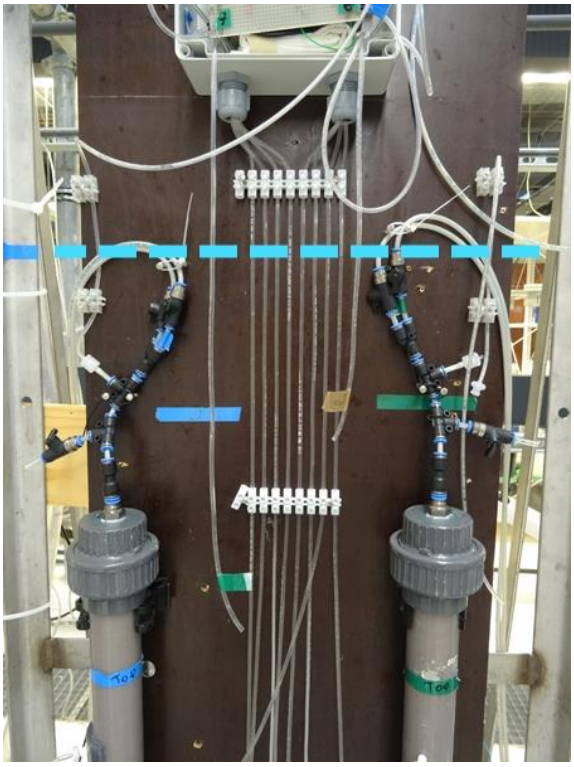

Figure 3-2 The tubes connecting the needles in the column to the pressure sensors (in the box on top of the picture). The hydrostatic pressure is zero at the height of the dashed blue line.

The pressure sensors give out a voltage signal (0-100mV) that is recorded by a Dataq Instruments data logger (DI-710) which is send and stored on the computer with Windaq software. Since the pressure is recorded for every 10 seconds, the number of datapoints are reduced by replacing them with an average over a longer time span (generally one hour). The 95% limits over each time span

are calculated as well. Also, the data of every day was written in a separate file. Reducing the amount of data and combining the files was done with Python.

3.1.3 Calibration of the pressure sensors

For calibrating the pressure sensors, an extension is attached to the top of the column. The pressure tubes are attached to the lowest four pressure needles of each column. A ruler has been put on the column and the extension to measure the water level. Water was added till the water level set point. When the water level in the tubes was at the same height, the tubes could be attached to the sensors. Water was added in steps of 5-10 centimetre each. The output was recorded during one hour per step with the data logger and the water level was read out and calculated with the diameter of the column and the volume of water added per step. The linear relationship between voltage and meters of water column (mwc) gives the calibration constants that are used to convert the signal to pressure. The results of the calibration can be found in attachment C Calibration of the pressure sensors.

3.1.4 pH sensor

A pH sensor and an electro conductivity (EC) sensor from *Hanna Instruments* are used to continuously measure the effluent of each column. The pH sensor (HI1001) and the EC sensor (HI3001) are connected to a pH & EC Transmitter (HI 98143-22) which converts the signals to a 4-20mA signal. The signal is measured over a 500Ω resistance by a Dataq Instruments data logger (DI-710) in Volts. The data logger stores the data on a SD-card which is removed after the experiment is finished. As with the data of the pressure measurements, the data was reduced and combined with Python. The pH sensor is calibrated in three buffer solutions with a pH of 4.0, 7.0 and 10.0. Calibration is done with the pH & EC Transmitter by tuning the signal output. Unfortunately, the EC meters had stopped working and could not be used during the experiments.

3.1.5 Temperature sensor

During the column experiments, it became clear that a pattern of daily temperature fluctuations in the lab was affecting the pressures. Therefore, a temperature sensor (LM60) was placed at the setup to measure the ambient temperature. The influent flowed through small tubes (4mmø) of more than 4 meters with a maximum velocity of about 12.5m/h. The water is assumed to have the same temperature as the lab.

3.1.6 Solution storage and preparation

The carbonate species in the solution will eventually be in equilibrium with the CO_2 in the surrounding air. Under average atmospheric conditions, CO_2 will escape from the $NaHCO_3$ solution and CO_2 will get into the $CaCl_2$ solution. In most other experiments, the carbonate concentrations are kept constant by having a gas with a constant CO_2 concentration flow through the solution. For these experiments, “bag in box” containers from *Bark-verpakkingen* have been used that generally are utilized for storing beverages and keeping them fresh. The solutions are stored inside plastic storage bags that do not allow for gas exchange and shrink with the volume as the solutions are pumped into the bag and out of the bag.

Every storage bag can store 20 litres of liquid. For every bag, 24 litre of solution is prepared in 25 litre vessels. The vessel is placed on a scale and 24kg of demiwater is added. Then, either $NaHCO_3$ or $CaCl_2$ salts are dissolved. The pH of the $NaHCO_3$ solution is lowered to the desired pH measured with a pH meter (WTW pH Elektrode SenTix® 940) by slowly adding drops of 37%HCl solution under constant mixing. Only the $NaHCO_3$ is adjusted for the pH since the carbonate species act as a buffer.

The $CaCl_2$ solution is not buffered for pH and has therefore little effect on the pH of the mixed solution.

An overview of the setup for filling the storage bags is shown below in figure 3-3. The vessels and the storage bag are then connected to a large peristaltic pump. First, the bags are emptied of both liquid and gas with the vacuum system, where the liquid is caught in the intercept bottle. About 1 litre of solution is pumped from the vessel to the storage bag, to rinse and flush the tubes and the bag. The rinsing solution is then sucked to the intercept bottle. Finally, 20 litres of the solution is pumped from the vessel to the storage bag. Following this procedure, the storage bag will only contain the solution and no air.

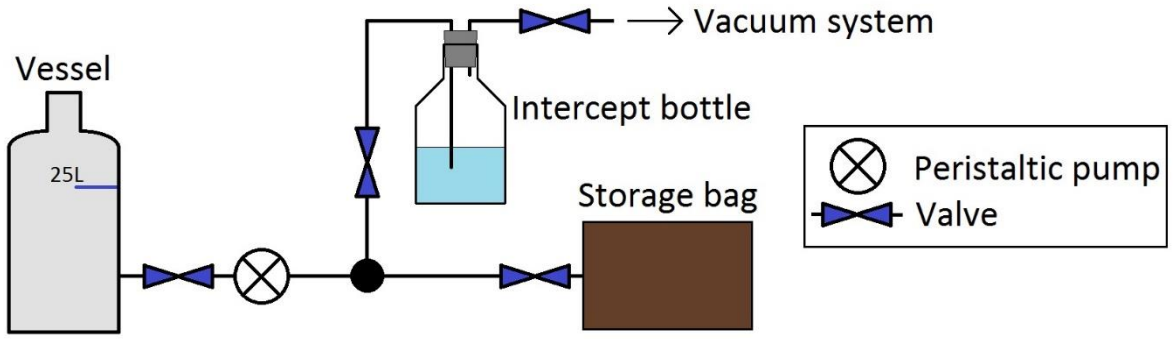

Figure 3-3 Schematic overview of the setup for filling the storage bags

Every bag is used multiple times, but is only filled with either a $NaHCO_3$ solution or a $CaCl_2$ solution. After use, the bags are flushed with demiwater twice, and then vacuumed and closed.

3.1.7 Sampling procedure

Samples can be taken from either the mixed influent and from the effluent. The sample of the mixed influent is taken by closing the valve at the bottom of the column and by opening the valve to the mixed influent sample point (Figure 3-1) so that no water from the column will flow up to the sampling point. Samples from the effluent are taken directly from the effluent tube.

The same sampling time is used throughout every experiment and ranges between 2 and 4 minutes, depending on the pumping speed used during the experiment. With the sampling time and by measuring the mass of the sample the discharge is calculated.

The samples are supersaturated with calcium carbonate, and have to be diluted till they are undersaturated before they can be analysed. The dilution is done by mixing ultrapure water with the sample with a pipette on a balance to obtain the highest possible accuracy.

To check if any large nuclei have been formed before the influent has reached the sand bed, half of the volume of the influent samples was filtered, analysed and compared to the unfiltered half. The size of the filter mesh was either 0.45µm and 0.20µm. This was only done during later experiments.

3.1.8 IC analysis

The ionic concentrations of both bicarbonate and carbonate anions (the sum of HCO_3^- and CO_3^{-2}) and calcium cations (Ca^{+2}) can be measured with the Metrohm 883 Basic IC plus (with ICSep ICE-COREGEL-64H Column) and the Metrohm 881 Compact IC pro (with Metrosep C 4- 150/4.0) respectively. The maximum concentration of calcium is 50ppm (mg/l) and the maximum concentration of (bi)carbonate is 100ppm ($mgCO_3$/l).

The samples have to be diluted with ultrapure water, since the samples are oversaturated and concentrations of the samples exceed the maximum concentrations. Calcium concentrations simply reduce with the factor of dilution. For carbonate however, the balance shifts when the samples are diluted. The results of the IC measurements for carbonate therefore have to be converted to the concentrations in the actual sample with Phreeqc. For this conversion, the pH of the sample should also be known. For the effluent samples the pH is measured continuously in the setup. The pH of the influent is constant: the pH of the storage bag with $NaHCO_3$ is checked after disconnecting but did never vary.

3.1.9 Determination of $SI_{calcite}$

With the measurements of pH, temperature, alkalinity and calcium and (bi)carbonate concentrations, the $SI_{calcite}$ of every sample is calculated with Phreeqc in combination with Python. Python loads a Phreeqc script into the Phreeqc COM module and let it run. With Python, the Phreeqc script can be run multiple times while changing the parameters.

The Phreeqc script works as follows: a solution is made with the variables temperature, pH, Ca (calcium concentration) and C(4) (all carbonate species) or alk (alkalinity). For the $SI_{calcite}$ calculations with alkalinity, the alkalinity and calcium concentrations can simply be adjusted with their respective dilution factors. The $SI_{calcite}$ can then be calculated with those adjusted parameters.

As mentioned before, (bi)carbonate concentrations obtained from the IC cannot be adjusted simply with the dilution factor. Also, in Phreeqc there are no input parameters for carbonate (CO_3^{-2}) and bicarbonate ($HCO3^-$), only for a combination of all carbonate species (C(4)). Each Phreeqc run consists of two parts: the undiluted sample is calculated first which is then diluted. The results of the undiluted and diluted samples are then coupled. Python is then used to do a maximum of a 1000 Phreeqc runs. In those 1000 runs, the undiluted C(4) concentration is increased from 0.95 to 1.4 times the measured (bi)carbonate concentration times the dilution factor. The other variables are the same for every run. The best fit between the modelled and measured (bi)carbonate concentration of the diluted sample then gives the $SI_{calcite}$.

3.1.10 Alkalinity measurements

Alkalinity is usually measured with titration of a strong acid till a pH of 4.3 is reached. However, the size of the samples is too small for this method. Instead, a cuvette test kit from *Merck Millipore* was used: *1.01758.0001 Acid Capacity Cell Test to pH 4.3 (total alkalinity)*. Only 1ml of sample is needed per cuvette. All alkalinity measurements are done as triplicate.

The test kit can measure the alkalinity between 0.40 – 8.00 meq/l or 20 – 400 $mgCaCO_3$/l. Other than (bi)carbonate concentrations, the alkalinity of a diluted sample can simply be converted to the actual concentration by multiplying it with the dilution factor.

The cuvette test kits were compared to the standard titration alkalinity test with six different solutions with $NaHCO_3$. The test with the test kits were done as triplicate and the titration tests were done once per solution. The alkalinity of the titration with 0.01 M HCl is equal to:

$$Alkalinity\ [meq/l]\ = \frac{V_{titrant} \cdot M_{titrant}}{V_{sample}}$$

Where $V_{titrant}$ is the volume of HCl solution added to obtain a pH of 4.3 (in ml), $M_{titrant}$ is the molarity of the HCl solution (10 mmol/l) and V_{sample} is the volume of the sample (in ml). The test kits are analysed in a photo spectrometer (Merck Millipore Spectroquant® NOVA 60), which returns the

alkalinity in $mgCaCO_3/l$. Alkalinity in units of meq/l can be easily converted to $mgCaCO_3/l$ by multiplying it with 50.04.

As can be seen below in figure 3-4, the alkalinities measured with the titration test correspond well with the Phreeqc calculations. The alkalinity measured with the cell test deviates from the two. The results from the cell tests therefore have to be converted by applying the following formula:

$$Alkalinity\ [\mathrm{mgCaCO_3/l}] = 1.0847 \cdot Result\ cell\ test\ [\mathrm{mgCaCO_3/l}] + 11.509$$

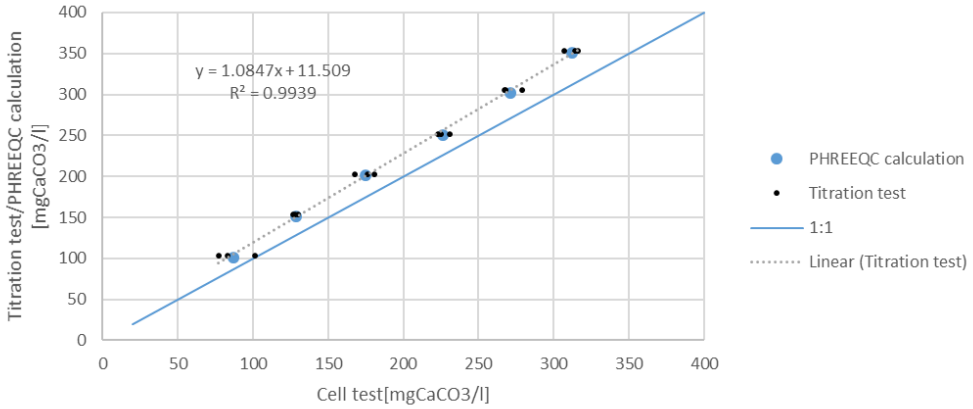

Figure 3-4 The comparison of the alkalinity measured with the cell test with the Phreeqc calculation and the titration test. The formula of the trend between the cell test and the titration test is used for the conversion of the alkalinity measured with the cell test. The line 1:1 indicates the trend if there would be no deviation of the cell test from the titration test and the Phreeqc calculation.

3.1.11 Emptying and washing the column

The sand was removed from the column by placing it in the same shaker with frame used for filling the column. Under continuous vibration, the sand slowly left the bottom of the column so that samples could be taken from the bottom, middle and top layers of the bed. The sampling locations are rough indications, and therefore not comparable. Any hard bits of sand and calcium carbonate was carefully removed with a hammer and chisel and kept as a sample. Any excess of water was removed before the samples were placed in an oven at 100°C to prepare them for analysis under the microscope and of precipitated calcium carbonate.

Before the columns were used for these experiments, possible impurities caused by previous experiments had to be removed. To remove possible organic material, crystals and other impurities, the columns were soaked in an HCl solution and subsequently in a NaOH solution for several days and then washed with demiwater.

After removing the sand from the column in the shaker, the remaining grains were removed by flushing the column and the caps with demiwater. Then, the column was reattached to the setup and a dilute HCl solution (about 1%) was pumped through the setup, cleaning all the tubes, valves and the column from precipitated calcium carbonate. The filters were cleaned with detergent to remove the high vacuum grease and placed in a dilute HCl solution (about 1% HCl) to remove calcium carbonate precipitates.

The column was taken out to remove sand that clogs the needles. Demiwater under high pressure (8bar) was pushed through the needles till they were clean. The column and tubes were washed with demiwater to remove the remaining HCl.

3.1.12 The sand bed

The used sand has a similar grain size as in the injection aquifer of the PURO well in Ridderkerk: d_{50} = 240µm. The sand is a 100% natural silica sand (SiO_2) from *Aqua-techniek B.V.*, which has been cleaned of contaminations like clay, dust, organic matter and other impurities – it meets the requirements of EN 12904 Type 1. Figure 3-5 below shows the grain size distribution of the sand used in the experiments as the amount of sand that has passed a sieve with a specific mesh size.

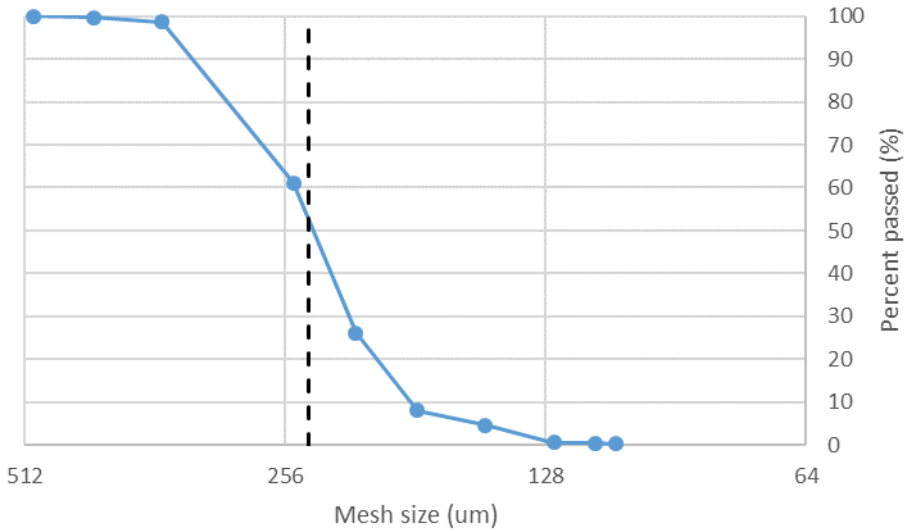

Figure 3-5 The grain size distribution of the sand used during the experiments (blue line) and the average grain size found in the injection aquifer in Ridderkerk (dashed black line at 240µm)

To be able to compare different experiments, the bed in every column should be similar, with similar pore space and uniformity of the pore spaces. Therefore, the columns are filled with demiwater and sand is added layer by layer (of about 2cm) under constant vibration of the column. The bottom of the column was closed with a filter and cap and sealed with high vacuum grease. Adding the sand slowly in small layers prevented a distribution of grain sizes over a large distance which would cause a varying permeability over the column. Adding the sand slowly under constant vibration minimised the number of large voids in the bed. If there were large voids visible from the outside, the sand was discarded and filled again. The vibration was induced by a shaker normally used for sieving sand for a grain size distribution. A framework was made for the shaker to attach the columns on vertically.

Air bubbles in the sand bed are very hard to remove, and should be avoided. Therefore, the columns were filled with demiwater before the sand was added. To remove the air below the bottom filter, the bottom tap was opened to flush the first air out with water. Then, the bottom tap was closed, the top of the column was sealed and connected to the vacuum system and by vibrating the column the last bubbles of air were removed from below the filter.

A picture of during the filling process is shown below in figure 3-6. The extension was placed on top of the column to have the bed submerged continuously during the filling process. About 10cm of the extension was filled with sand as well, to make sure the sand on top of the column was well packed. The extension was removed by sliding it away sideways, the top was “skimmed” with a ruler so that the remaining sand in the column was at level with the top of the column. If there would be too much sand, the filter would not seal the bed. If there would be not enough sand, there would be room for movement of the grains and expansion of the pores during the experiments. The cap with the top filter was placed on top of the column and sealed with the high vacuum grease. Both the

bottom and top cap were tightened with a pipe spanner. Before the influent tubes were attached to the top of the column, it was made sure that both the tubes and the void in the top cap were filled with water to avoid any flow of air in the column.

Figure 3-6 The columns with extensions placed on the shaker during filling.

3.1.13 Porosity

The value for the porosity was obtained by weighing the column filled with water, and then weighing the column filled with sand and water. The density of the sand is 2550kg/m^3 and the density of water is 1000kg/m^3. The volume of the column can be calculated with the diameter of the column and the distance between the two filters. Then, the porosity can be calculated with:

$$p = 1 - \frac{V_{sand}}{V_{total}}$$

With:

$$V_{sand} = \frac{m_{c,w,s} - m_{c,w}}{\rho_{sand} - \rho_{water}}$$

Where p is the porosity (-), V_{total} is the volume between the two filters (liter), V_{sand} is the volume of the sand (liter), $m_{c,w,s}$ is the combined mass of the column filled with water and sand (g), $m_{c,w}$ is the combined mass of the column filled with water (g), ρ_{sand} is the density of the sand (kg/m^3) and ρ_{water} is the density of water (kg/m^3). The average porosity of aquifers in the Netherlands is 0.34 (Olsthoorn 1977), the porosity obtained with this filling process is around 0.4.

3.2 BATCH TEST EXPERIMENTS

The batch test experiments were designed to test the inhibiting effect of humic acids on the precipitation of calcium carbonate. The analysis of the ionic concentrations is done as described previously under the column experiment.

3.2.1 Preparation of the batches

Every single batch test was done in a closed one litre bottle. Experiments were done for a range of $SI_{calcite}$ and for a range of different concentrations of total organic carbon (TOC). Six batches were prepared without TOC and with $SI_{calcite}$ values of -99 (no carbonate dissolved), 0.5, 1.0, 1.5, 2.0 and

2.5. The effect of humic acids was tested in batches with $SI_{calcite}$ values of 0.5, 1.0, 1.5 and 2.0. For each $SI_{calcite}$, six batches were prepared with TOC concentrations of 0.0535, 0.160, 0.535, 1.60, 5.35 and 16.0 mgC/l. A logarithmic distribution was chosen to test the effect of low concentrations and compare the results with those of Lebron and Suarez (1996).

The humic acids were obtained from the Dutch drinking water company Vitens, who separates humic acids from groundwater during their drinking water production from groundwater. These humic acids are purified to be sold as a fertilizer. The stock solution from Vitens contains 117.6gC/l. Three dilutions were prepared: 10x, 100x and 1000x and analysed for TOC as described by Olariu (2015).

The bottles were washed with a dilute HCl solution (about 1%) first and then in the dishwasher. The bottles for the batches with humic acids were filled with 1100 ml ultrapure water. Then, from each of the three solutions 0.5 and 1.5 ml was added to the six batches. Three samples of 30ml were taken for the analysis of TOC, and 10ml was abstracted so that every batch contained 1000ml. The TOC concentrations turned out to be too low for a proper analysis. The bottles for the batches without humic acids were filled with 1000ml of ultrapure water.

25.0g Sand was dosed to every batch as seed material to stimulate heterogeneous nucleation – the same sand as used in the column experiments. This was done to compare the precipitation of calcium carbonate in the batch to the column. Every bottle was equipped with a thermometer, a tube with a valve to take samples and a cap to dose the $CaCl_2$ solution. The batch was closed off from the environment to reduce exchange of CO_2.

The correct $SI_{calcite}$ was obtained by mixing a solution with $CaCl_2$ and a solution with $NaHCO_3$. $NaHCO_3$ salt was added to the 1l bottles and the pH was adjusted by adding HCl (0.1M and 37% solutions) so that directly after adding the $CaCl_2$ solution the pH would become 7.5. A $CaCl_2$ stock solution was made with 3.37mol/l – the concentration was analysed with the Metrohm IC analyser. A high concentration was used so that the change in volume is minimised when adding the solution to the batch and therewith the change in carbonate concentrations is minimised as well. As with the column experiments, the ratio $NaHCO_3$ / $CaCl_2$ is about 2. The calculations were done with Phreeqc. The dosages of $NaHCO_3$ and $CaCl_2$ with the corrected pH to obtain the different values of $SI_{calcite}$ are given below in table 3-1.

Table 3-1 The concentrations of $NaHCO_3$ and $CaCl_2$ and the pH_0 (pH of the $NaHCO_3$ solution before the 3.37mol/l $CaCl_2$ solution is dosed) and the resulting $SI_{calcite}$ and pH used for the batch experiments. Temperature is 25°C.

$NaHCO_3$ [mmol/l]	**pH_0**	**3.37 mol/l $CaCl_2$ dose [ml/1000ml]**	**$CaCl_2$ [mmol/l]**	**pH_{mix}**	**$SI_{calcite}$**
6	7.55	0.75	2.53	7.5	0.5
12	7.60	1.5	5.06	7.5	1.0
24	7.65	3.0	10.1	7.5	1.5
48	7.70	6.0	20.2	7.5	2.0
96	7.75	12.0	40.4	7.5	2.5
0	-	3.0	10.1	7.5	-99

3.2.2 Starting the batch experiments

The batches were placed in a shaker spinning at 200 rpm while keeping the temperature constant at 25°C. The batches were held in place on a moving tray, which could be taken out. At the start of the experiment – the moment when the calcium chloride solution was added – the tray with the batches was taken out of the shaker. The batches were closed immediately after the calcium chloride was dosed. The tray was placed in the shaker and the spinning was started.

3.2.3 Taking samples

The spinning had to be stopped during the sample taking process. To gather enough data for the kinetics, the time interval between two samples was initially small (15minutes) and was gradually increased (two samples per day). Samples were taken with a 5ml syringe and had a volume of 4ml. A tube was inserted in every batch with a valve to close it off from the environment.

When taking a sample, the syringe was connected to the valve and 4ml of air was inserted into the bottle, then 5ml of the solution was taken up and pushed out – both to flush the tube – and then the 4ml sample was taken. The sample was directly pushed through a 0.45µm filter into a vial. When the series of samples was taken, the samples were diluted with ultrapure water. This was done with a pipette and on a balance to ensure the correct and a very accurate mixing proportion. Proper mixing proportions were chosen to ensure that the mixed solution was not supersaturated and that the concentrations were within the range of the IC spectrometer. The mixing proportions are given in table 3-2 below.

Table 3-2 The volume of the sample and the volume of ultrapure water used to mix the samples.

$SI_{calcite}$	-99	0.5	1.0	1.5	2.0	2.5
Ultrapure water (ml)	10.0	10.0	10.0	10.0	10.0	10.0
Sample (ml)	0.600	2.00	1.0	0.600	0.300	0.100

3.2.4 Phreeqc calculations

As with the samples of the column experiments, the (bi)carbonate concentrations of the samples of the batch experiments had to be corrected for the dilution. Other than during the column test, the pH during the batch experiment is not measured. During the experiment, only the temperature is constant (25 °C).

Yet, all the initial conditions are known: (bi)carbonate concentration, pH and the $CaCl_2$ solution dosage. These initial conditions are also used for the Phreeqc calculation of the pH and $SI_{calcite}$ once the $CaCl_2$ solution is dosed. The Phreeqc script basically simulates one litre of demiwater to which in order $NaHCO_3$ is added, the pH is adjusted, and $CaCl_2$ is added. This gives the initial situation at t=0 in the batch. Then, in 1000 steps $CaCO_3$ is removed from the solution, which simulates precipitation. The precipitation sequence form the dataset with the values of calcium and (bi)carbonate concentrations, pH and $SI_{calcite}$. To widen the range of the dataset, some $CaCO_3$ is dissolved first, which is removed during the first 300 steps of the 1000 steps in which $CaCO_3$ is removed.

The measurements of calcium and (bi)carbonate are of the diluted samples. To fit the model, the corresponding concentrations of the diluted concentrations have to be modelled as well. To get the diluted dataset, the initial situation in the Phreeqc script is diluted by adding water. Then, the same amount of moles is added and then removed in those 1000 steps from the diluted simulated solution – only the volume differs. Each of the 1000 steps then corresponds with same step of the undiluted dataset.

With Python, the best fit between the results of (bi)carbonate and calcium is chosen from the diluted dataset as the values with the lowest sum of the differences in % between the modelled and measured concentrations. The corresponding values with the same step number of the undiluted dataset are then used to present the modelled values of the calcium and (bi)carbonate concentrations and the pH and $SI_{calcite}$ in the graphs. Graphs of the pH and $SI_{calcite}$ only consist of modelled values while the graphs of calcium and (bi)carbonate concentrations present both the measured and the modelled values. The graphs of the modelled and measured calcium and

(bi)carbonate concentrations are used to validate the model. The method of obtaining the actual values of calcium, (bi)carbonate, $SI_{calcite}$ and pH from the measured values with the IC is shown below in figure 3-7.

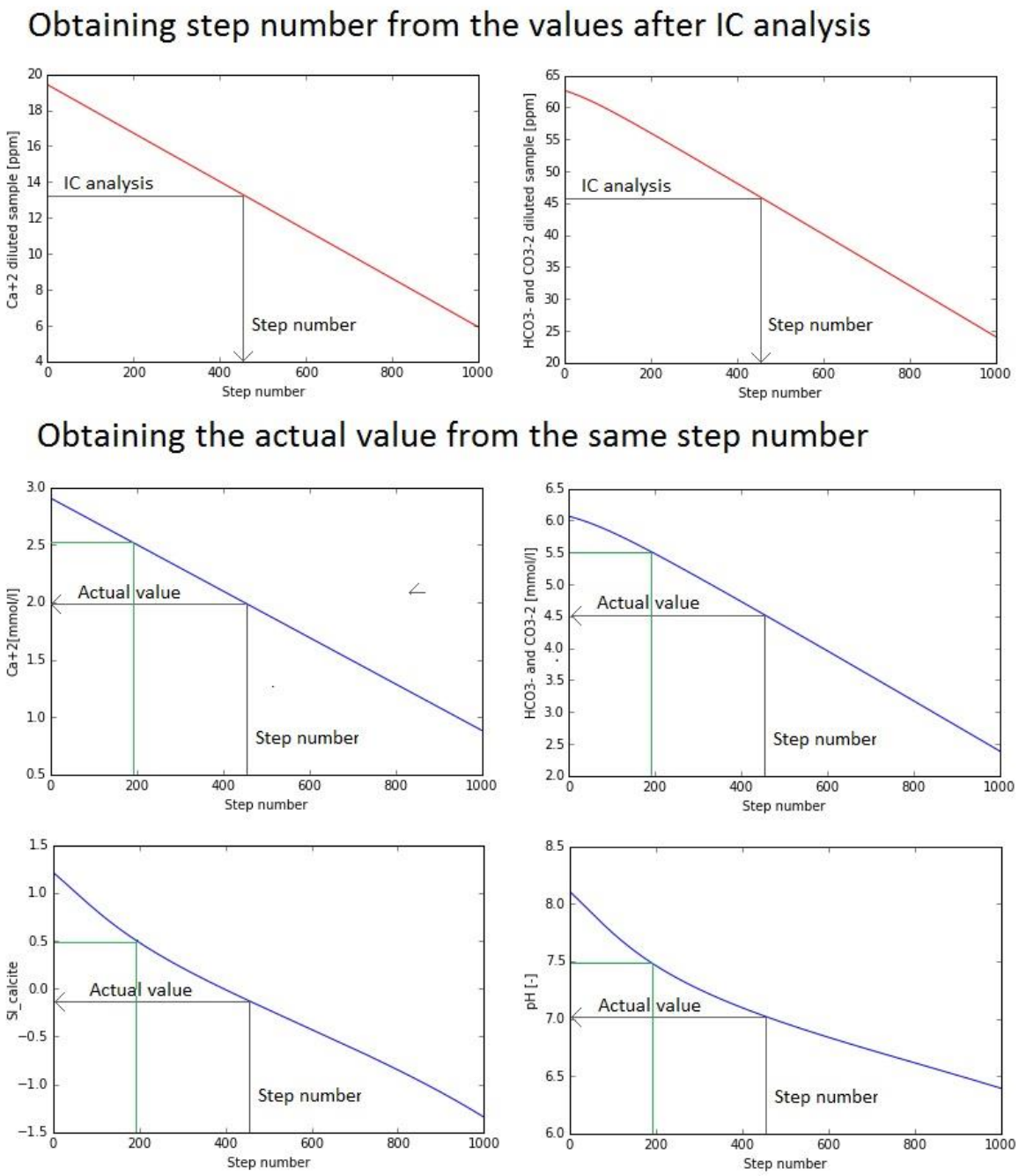

Figure 3-7 Modelling the precipitation of calcium carbonate in a batch. In the top two graphs, the best fitting step number is obtained from both the measured calcium and (bi)carbonate concentrations. This step number is then used to determine the actual (undiluted) values of calcium, (bi)carbonate, $SI_{calcite}$ and pH. The green line represents starting situation of the batch, which is used to model each line.

4 EXPERIMENTAL RESULTS

The results of all experiments are shown in attachment A Results of column experiments and attachment B Results of batch experiments. In this chapter, the most relevant results are shown and discussed, sometimes with references to the attachment. The experimental procedures are discussed previously in chapter 3 Experimental methods. The results of the column experiments are discussed first, followed by the batch experiments.

4.1 OVERVIEW COLUMN EXPERIMENTS

Six experiments with two columns have been conducted. The experiments differ in influent concentrations, flow, column characteristics and connections of the pressure sensors. An overview of the six experiments in each of the two columns (green and blue) is shown below in table 4-1. Experiments 1-3 have the same influent characteristics for the two columns, while the influent characteristics of the green and blue column experiments 4-6 are different.

*Table 4-1 Overview of the column experiments. The concentrations, pH and resulting SI are given after the two concentrations are mixed. The flow is set with the pump and is measured by weighing the samples. The locations to which the pressure sensors are connected are marked with an X – location I is connected to the influent tubes and locations II-VI are in the column from top to bottom. The samples are measured with the IC for calcium and carbonate, with the test kit for the alkalinity. Samples can be filtered with different mesh size. *1% of the grains is calcite as seed material.*

Experiment		Influent (mixed)					Hydraulics			Pressure sensor positions						Samples			
Number	Column	$CaCl_2$ [mmol/l]	$NaHCO_3$ [mmol/l]	pH	$SI_{calcite}$	Temperature [°C]	Pump [rpm]	Flow [cm/h]	porosity [-]	I (top)	II (16cm)	III (28cm)	IV (41cm)	V (53cm)	VI (66cm)	Filtration	Alkalinity	Carbonate	Calcium
1	Green	6.40	13.30	7.5	1.14	25	20.0	39.2	0.41		x	x	x		x	none	x		X
1	Blue	6.40	13.30	7.5	1.14	25	20.0	36.9	0.40		x	x	x		x	none	x		X
2	Green	6.40	13.30	7.5	1.14	25	10.0	20.4	0.42	x	x	x			x	none	x		X
2	Blue	6.40	13.30	7.5	1.14	25	10.0	19.8	0.42	x	x	x			x	none	x		X
3	Green	11.52	24.30	7.5	1.51	21	10.0	13.7	0.41	x	x	x			x	none	x	x	X
3	Blue	11.52	24.30	7.5	1.51	21	10.0	12.3	0.40	x	x	x			x	none	x	x	X
4	Green	8.23	16.45	7.5	1.23	20	10.0	16.7	0.40	x	x	x			x	0.45µm		x	X
4	Blue	5.78	11.55	7.5	1.01	20	10.0	14.9	0.40	x	x	x			x	0.45µm		x	X
5	Green	8.23	16.45	7.5	1.23	19	20.0	33.7	0.40	x	x	x			x	0.45µm		x	X
5	Blue	5.78	11.55	7.5	1.01	19	20.0	31.8	0.40	x	x	x			x	0.45µm		x	X
6	Green	8.23	16.45	7.5	1.22	19	10.0	18.6	0.39*	x	x	x			x	0.20µm		x	X
6	Blue	5.78	11.55	7.5	1.01	19	10.0	20.2	0.38*	x	x	x			x	0.20µm		x	X

4.2 RESULTS OF THE COLUMN EXPERIMENTS

Each paragraph below states whether precipitation of calcium carbonate was noticed during different observations. Whether calcium carbonate precipitation was seen after opening the column is shown under cementation. This is followed by the interpretation of the measurements from the pressure sensors and from the pH sensor, alkalinity and calcium and (bi)carbonate concentrations.

4.2.1 Cementation

Apart from the measurements of pressure, pH and concentrations, precipitation and clogging was well noticeable as calcium carbonate cemented the grains. Cementation is the process where a mineral precipitates between the grains and binds them together. The cemented sand and calcium carbonate in the column formed a solid but brittle mass. Whenever cementation occurred, it caused a clear increase in pressure. When emptying the column, those parts of the sand that had cemented

together had to be removed with a chisel. Those pieces were kept for analysis under the microscope and for analysing the calcium carbonate concentration. Table 4-2 below gives an overview of the columns where calcium carbonate had formed. More pictures can be found in attachment A Results of column experiments.

Table 4-2 The presence of cemented sand and calcium carbonate in the column after opening the column.

Experiment series	**1** no seeds, SI = 1.14		**2** no seeds, SI = 1.14		**3** no seeds, SI = 1.51		**4-5** no seeds, SI_{green} = 1.23 SI_{blue} = 1.01		**6** with seeds, SI_{green} = 1.23 SI_{blue} = 1.01	
Column	Green	Blue	Green	Blue	Green	Blue	Green	Blue	Green	Blue
Cementation	Yes	Yes	No	No	Yes	Yes	No	No	Yes	No

If cementation did take place in the column, it was always at the top right below the filter. It resulted in a solid circle over the full cross section of the column directly under the filter. Beneath this circle, the cementation was less uniform over the profile, but it was all attached to this top part. Preferential flow patch between the cemented grains allowed for the water to pass the cemented zone.

To measure the increase in pressure over the first 15 centimetres, the extra connection (location I) was added to the influent of the columns after experiment 1. The columns during experiment 2, 4-5 did not show any cementation. In those columns however, calcium carbonate had precipitated on the tip of the metal pressure needles. Pictures of the cemented top of the columns are shown below in figure 4-1.

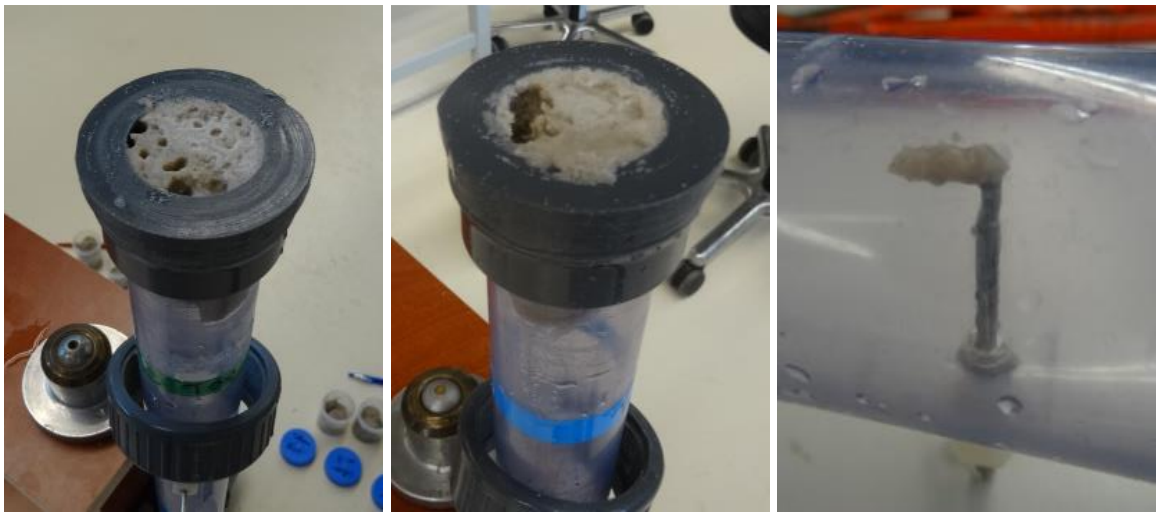

Figure 4-1 From left to right: Cementation at the top of the green column after experiment 1. Cementation at the top of the blue column after experiment 1. Cementation on one of the pressure needles of the green column after experiment 2.

4.2.2 Pressure sensors

Since the calcium carbonate only cemented in the top layer of the column, there was only a clear increase in pressure recorded by the sensors at locations I and II – an increase in pressure at location I relative to location II shows that there is an increase in resistance between the two locations. Figure 4-2 below shows two graphs: one with and one without an observed increase in pressure.

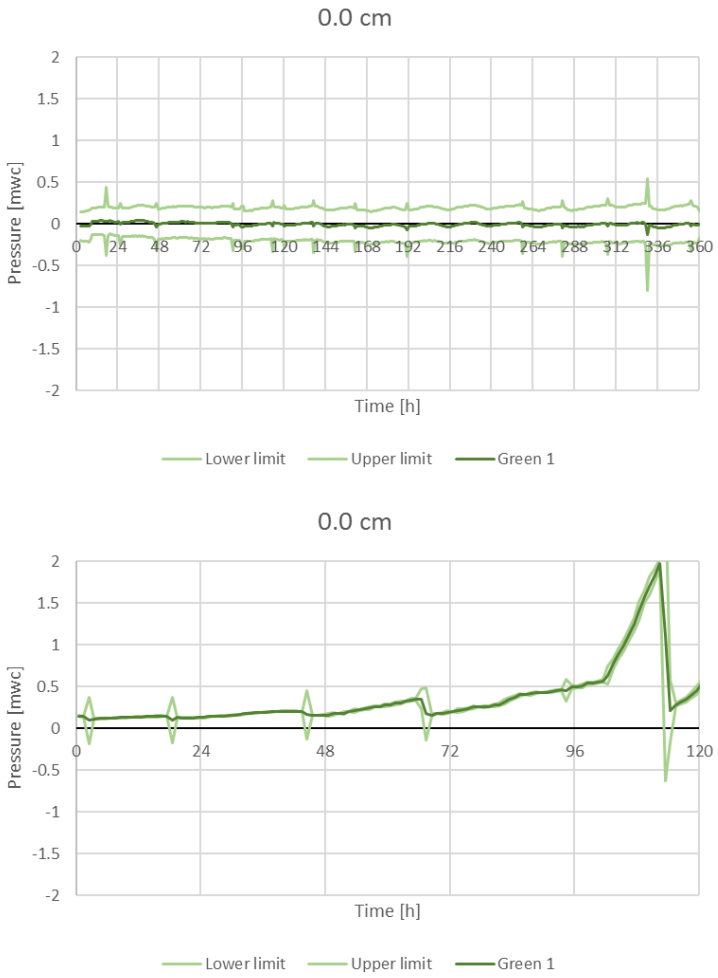

Figure 4-2 The pressures recorded by the top sensor in the green column during experiments 2 (top) and 3 (bottom). The graph of experiment 2 shows no increase in pressure where the graph of experiment 3 does show a clear increase.

Graphs showing the increase in pressure can be found in attachment A Results of column experiments. Table 4-3 below lists the experiments during which the pressure increased between two locations. Only if the pressure sensors show a clear increase in pressure – that is, when the pressure data either shows a continuous strongly increasing trend relative to the pressure data of the lower location – it is listed as "pressure increase" in the table. Because of the uncertainty in the values recorded by the pressure sensors and the temperature induced variations, small increases are hard to relate to an actual decrease in hydraulic conductivity.

*Table 4-3 Increases in pressure observed with pressure sensors between two subsequent locations. Only clear increases are considered as an increase in pressure. *The pattern of the data obtained during these experiments was too irregular to make a statement.*

Experiment series		**1** no seeds, SI = 1.14		**2** no seeds, SI = 1.14		**3** no seeds, SI = 1.51		**4** no seeds, SI_{green} = 1.23 SI_{blue} = 1.01		**5** no seeds, SI_{green} = 1.23 SI_{blue} = 1.01		**6** with seeds, SI_{green} = 1.23 SI_{blue} = 1.01	
Column		Green	Blue	Green	Blue	Green	Green	Green	Blue	Green	Blue	Green	Blue
	Locations												
Pressure increase	I-II	-	-	No	No	Yes	Yes	-*	-*	-*	-*	Yes	No
	II-III	No	No	No	No	No	No	No	No	No	No	No	No
	III-IV	No	No	No	No	No	No	No	No	No	No	No	No
	III-VI	-	-	No	No	No	No	No	No	No	No	No	No
	IV-VI	No	No	-	-	-	-	-	-	-	-	-	-

A daily fluctuation of the pressures was observed during all experiments and in all sensors. During the day the pressures decreased, while at night the pressure increased. This corresponds with the daily pattern of the temperatures in the lab. A higher temperature during the day results in a lower viscosity of the water and therewith a lower pressure gradient to push the water though the column. At night the temperature would go down and as a result the pressures increase. The maximum daily fluctuation is about 2 °C. Graphs of the ambient temperature during experiment 2-6 can be found in attachment A Results of column experiments.

4.2.3 pH, alkalinity and calcium and (bi)carbonate concentrations.

A lower pH, alkalinity and calcium and (bi)carbonate concentrations of the effluent compared to the influent indicates that calcium carbonate has precipitated in the column. The pH of the influent of all experiments is 7.5. The alkalinity and the concentrations vary per experiment. Table 4-4 below lists whether these parameters have decreased after the passage through the column.

Table 4-4: The occurrence of a decrease in pH, alkalinity and calcium and (bi)carbonate concentrations over the column.

Experiment series	**1** no seeds, SI = 1.14		**2** no seeds, SI = 1.14		**3** no seeds, SI = 1.51		**4** no seeds, SI_{green} = 1.23 SI_{blue} = 1.01		**5** no seeds, SI_{green} = 1.23 SI_{blue} = 1.01		**6** with seeds, SI_{green} = 1.23 SI_{blue} = 1.01	
Column	Green	Blue	Green	Blue	Green	Green	Green	Blue	Green	Blue	Green	Blue
pH decreases	Yes	Yes	Yes	Yes	Yes	Yes	No	No	No	No	Yes	Yes
Calcium decreases	Yes	Yes	No	No	Yes	Yes	No	No	No	No	Yes	Yes
Alkalinity decreases	Yes	Yes	No	No	Yes	Yes	-	-	-	-	-	-
(bi)carbonate decreases	-	-	-	-	Yes	Yes	No	No	No	No	Yes	No

Precipitation of calcium carbonate was observed from the decreases in alkalinity, pH and calcium and (bi) carbonate concentrations. Of all the concentration measurements, calcium appeared to be the most reliable, though alkalinity and (bi)carbonate are also good indicators. The continuous measurements of the pH were suitable for observing the precipitation of calcium carbonate. Measuring the concentrations with samples could be replaced by a combined measurement of the conductivity and the pH of both the influent and the effluent.

4.2.4 Formation of nuclei

The top of the top filter of experiment 3 was littered with small calcium carbonate crystals. The filters were therefore analysed under the microscope. A picture of the filter of the Green column is shown below in figure 4-3. The various calcium carbonate crystals were either shaped like a rhombohedron or like a star. Rhombohedron shaped crystals are typically calcite while the star shaped structures are generally aragonite, though aragonite is usually formed in the presence of magnesium (Tegethoff et al. 2001) or at higher temperatures (Ogino et al. 1987). No crystals were observed on the filters of experiments 4-6.

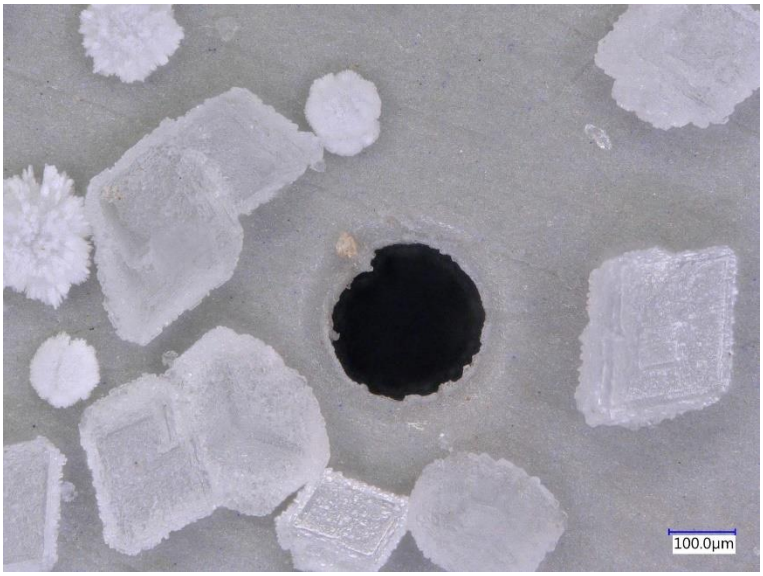

Figure 4-3 Microscope image of the top of the top filter of the green column, with calcium carbonate crystals around one of the filter holes.

In Zevenbergen, Raat and Kooiman (2012) observed calcium carbonate precipitation and clogging in both the RO-filter and in the injection aquifer at a recovery of 65% and with an $SI_{calcite}$ of 1.3. It could be possible, that nuclei were formed in the RO-filter and then caught between the sand in the injection aquifer. Those nuclei would be caught close to the point of injection, where clogging causes a larger increase in pumping head. The caught nuclei will then act as seed material on which calcium carbonate will grow.

To test this theory, the influent and effluent during series 4, 5 and 6 were filtered either with a 0.20µm filter or a 0.45µm filter. From experiment 4 onwards, the effluent and influent were filtered to check for the presence of small nuclei. Table 4-5 below shows if there are any differences between the concentrations in calcium and (bi)carbonate of the filtered and the non-filtered sample.

*Table 4-5 The comparison of the concentrations of the sample when filtered to the non-filtered sample. *a 0.20µm filter was used instead of a 0.45µm filter.*

Experiment series	**1** no seeds, SI = 1.14		**2** no seeds, SI = 1.14		**3** no seeds, SI = 1.51		**4** no seeds, SI_{green} = 1.23 SI_{blue} = 1.01		**5** no seeds, SI_{green} = 1.23 SI_{blue} = 1.01		**6** with seeds, SI_{green} = 1.23 SI_{blue} = 1.01	
Column	Green	Blue	Green	Blue	Green	Green	Green	Blue	Green	Blue	Green	Blue
Influent carbonate	-	-	-	-	-	-	None	None	None	None	None[1]	None[1]
Influent calcium	-	-	-	-	-	-	None	None	None	None	None[1]	None[1]
Effluent carbonate	-	-	-	-	-	-	None	None	None	None	None[1]	None[1]
Effluent calcium	-	-	-	-	-	-	None	None	None	None	None[1]	None[1]

The $SI_{calcite}$ of those experiments was lower, with values of 1.01 and 1.23. There was no difference observed between the filtered and unfiltered samples. Hence, no nuclei larger than 0.20µm are formed in waters with an $SI_{calcite}$ of 1.01 and 1.23. It is therefore unlikely that the aquifer in Zevenbergen was clogged by the intercepted nuclei. Whether nuclei were formed prior to the filter bed with an $SI_{calcite}$ of 1.51 cannot be denied or confirmed.

All sand samples after the experiment were analysed under the microscope. Figure 4-4 below shows a picture of the cemented parts of experiments 1 and 3. Calcium carbonate was not formed in layers around each grain, covering the whole surface like a softening pellet or an ooid. Calcium carbonate

precipitates were shaped as a rombohedron. The crystals are all attached to other crystals. It is therefore likely that 2D nucleation has been a dominant process: a new calcium carbonate nucleus is formed on an existing calcium carbonate surface. This nucleus then grows to be a rombohedron crystal, on which new nuclei can be formed. This process progresses through the pores, filling the pores spaces and blocking the flow of water. In the cemented top layer of experiment 3, the same crystal shapes as seen on top of the top filter and some plates. All the crystals in the other cemented layers of the other experiments have rombohedron shapes. The crystals of experiment 3 are not connected as in the other experiments. 2D nucleation becomes less dominant at high concentrations where homogeneous nucleation and heterogeneous nucleation become more favourable.

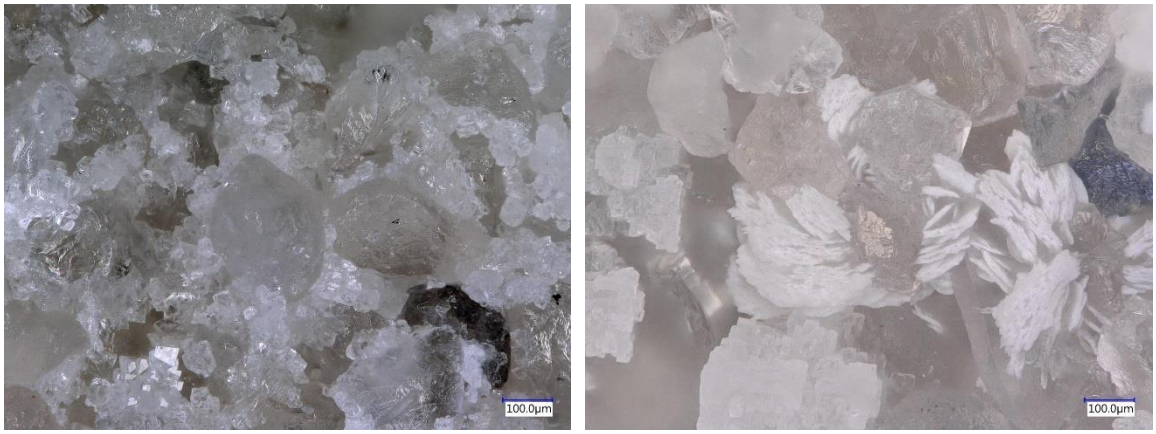

Figure 4-4 The precipitates between the grains in the green column after experiment 1 (left) and in the green column after experiment 3 (right).

4.3 DISCUSSION OF THE COLUMN EXPERIMENTS

For the discussion of the column experiments, a distinction is made between precipitation of calcium carbonate and clogging. The symptoms for precipitation are a decrease in pH, a decrease in alkalinity and decreases in the concentrations of calcium and (bi)carbonate. The symptoms of clogging are cementation and an increase in the pressure gradient. The results are summarised and an overall evaluation on precipitation and clogging is given in table 4.6 below.

For all experiments, an increase in pressure gradient was only observed in the first top centimetres of the column, where cementation had taken place. During experiment 1, there was no pressure sensor connected to the influent. Therefore, no increase in pressure was observed over these first centimetres while cementation did occur. Therefore, it was concluded that clogging has occurred during experiment 1. For the other experiments (2-6), an increase in pressure did go hand in hand with the observation of cementation.

Table 4-6 A combined overview of the tables from the results. The symptoms of precipitation of calcium carbonate are distinguished from the symptoms of clogging. Whether calcium carbonate precipitates is based on a decrease of the concentrations and a decrease of the pH. Whether the sand bed gets clogged is based on the observation of cementation and the increase in pressure. [1]Carbonate did not clearly decrease, but there were irregularities in the data. [2]Both the pH sensor for the Green and the Blue column show a gradual, minor decrease in pH – from 7.5 to 7.4. [3]No pressure sensors measured the gradient over the first section of the column. [4]The data from the pressure sensors was too irregular to make a statement.

Experiment series	1		2		3		4		5		6	
Column	Green	Blue	Green	Blue	Green	Blue	Green	Blue	Green	Blue	Green	Blue
Temp. (°C)	25	25	25	25	21	21	20	20	19	19	19	19
$SI_{calcite}$	1.14	1.14	1.14	1.14	1.51	1.51	1.23	1.01	1.22	1.00	1.22	1.00
$[Ca^{+2}]/[CO_3^{-2}]$	209	209	209	209	196	196	238	239	243	244	243	244
Flow [cm/h]	39.2	36.9	20.4	19.8	13.7	12.3	16.7	14.9	33.7	31.8	18.6	20.2
Seed crystals	No	No	No	No	No	No	No	No	No	No	Yes	Yes
Precipitation of calcium carbonate												
Concentrations	Yes	Yes	No	No	Yes	Yes	No	No	No	No	Yes	Yes[2]
pH	Yes	Yes	No[2]	No[2]	Yes	Yes	No	No	No	No	Yes	Yes
Precipitation	**Yes**	**Yes**	**No**	**No**	**Yes**	**Yes**	**No**	**No**	**No**	**No**	**Yes**	**Yes**
Clogging of the sand bed												
Cementation	Yes	Yes	No	No	Yes	Yes	No	No	No	No	Yes	No
Pressure	No[3]	No[3]	No	No	Yes	Yes	–[4]	–[4]	–[4]	–[4]	Yes	No
Clogging	**Yes**	**Yes**	**No**	**No**	**Yes**	**Yes**	**No**	**No**	**No**	**No**	**Yes**	**No**

4.3.1 Moment of clogging and precipitation

Both clogging and precipitation was observed during experiment 1, 3 and the Green column of experiment 6. Although in the Blue column of experiment 6 no cementation was observed, the calcium concentrations and the pH clearly indicate the precipitation of calcium carbonate. It is likely that at the relatively low $SI_{calcite}$ of 1.00, calcium carbonate did grow on the calcite seed crystals but did not (yet) form cementation.

In every experiment where clogging occurred, the precipitation of calcium carbonate was observed before the increase in pressure. This is in agreement with the effect of a decreasing porosity on the pressure gradient in the Carman-Kozeney equation. As stated in section 2.5.1 Carman-Kozeney, a decreasing porosity has little initial effect, as the pressure gradient increases exponentially. A good example of this behaviour is the green column of experiment 6, in which the pressure increases exponentially long after precipitation is observed. In figure 4-5 below, the pressures and calcium concentrations during experiment 1 and experiment 2 shown.

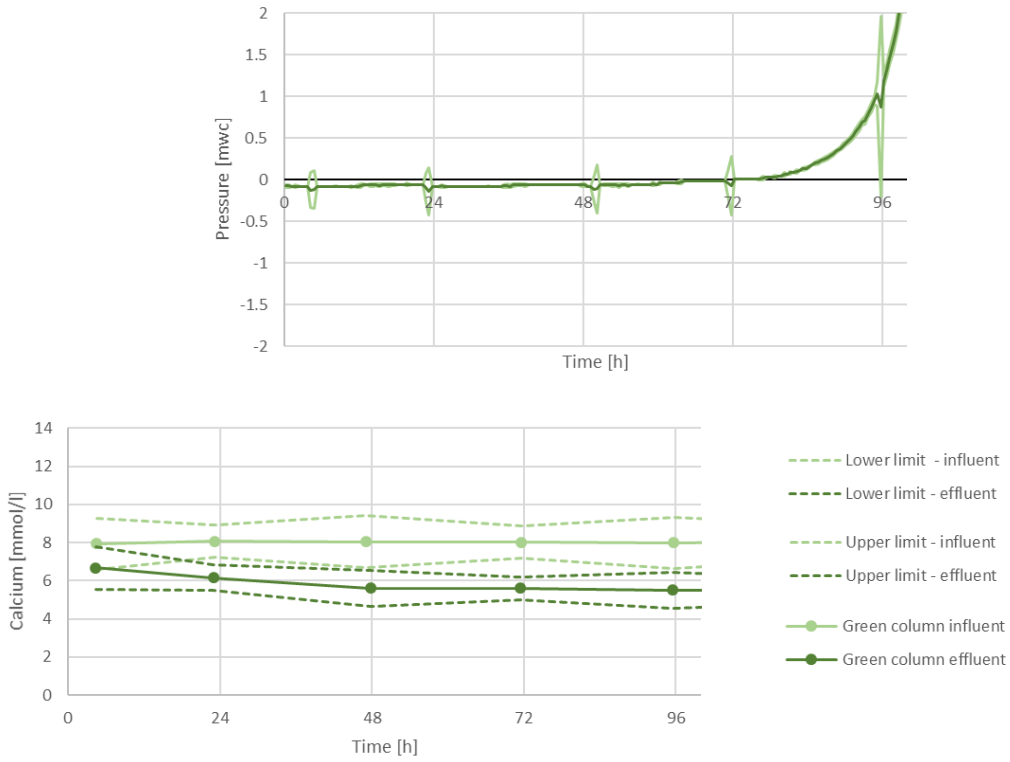

Figure 4-5 Results of the green column of experiment 6. Top: the pressures at location I (influent/top). Bottom: The concentrations of calcium of the influent and effluent. Precipitation is observed from the reduction in calcium before the increase in pressure.

4.3.2 The effect of calcite seeds

For experiment 4, 5 and 6, the $SI_{calcite}$ of the influent of the green and blue columns was 1.23 and 1.01 respectively. During experiment 4 and 5, no calcium carbonate had precipitated – neither did the column clog. 1 Gram of calcite seeds with a diameter of 2.5mm was added to every 100 grams of sand in both columns during experiment 6. The presence of these seeds resulted in a rapid clogging of the Green filter with the higher $SI_{calcite}$. As discussed before, the lower $SI_{calcite}$ in the blue column did not result in clogging, but in growth on the calcite grains of the Green column.

The presence of seed material can trigger the precipitation of calcium carbonate from a solution that would otherwise be metastable. If nuclei are formed from the metastable solution and are caught in the bed, it will act as a surface area for growth. For all experiments without calcite seeds where precipitation was observed, there is a period of delay before the pH, alkalinity and (bi)carbonate and calcium concentrations decrease. In the presence of the calcite seeds, there is no period of delay before precipitation will start. As can be seen in figure 4-6 below, with calcite seeds, the pH of the effluent is initially far below the value of the influent of 7.5. Without calcite seeds, there is an initial delay. This delay much shorter for higher supersaturations (experiment 3 with $SI_{calcite}$ = 1.55) than for lower supersaturations (experiment 1 with $SI_{calcite}$ = 1.14).

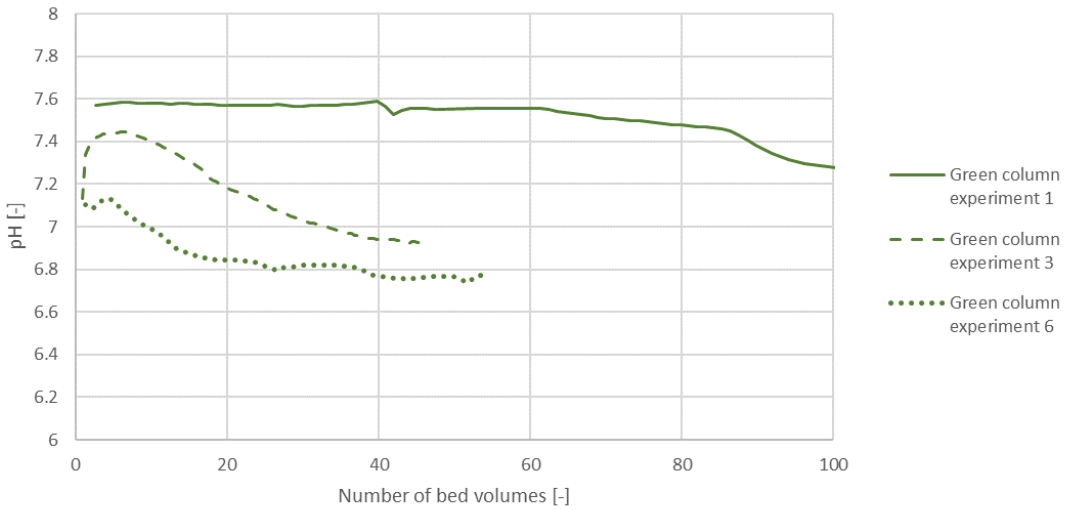

Figure 4-6 The difference in pH of the effluent without and in the presence of calcite seeds. The green columns of experiment 1 and 3 did not contain calcite seeds and the influent had an $SI_{calcite}$ of 1.14 and 1.55 respectively. The green column of experiment 6 did contain calcite seeds and the influent had an $SI_{calcite}$ of 1.22. The influent of all columns had a pH of 7.5.

The size of the calcium carbonate surface area increases as more and more calcium carbonate precipitates on the nuclei. The growth of the surface area accelerates the precipitation of more calcium carbonate. Initially, the surface area of calcium carbonate is very small which causes the delay. Eventually, when the pH has reached equilibrium, calcium carbonate precipitates with the highest rate. It is supported by the three models of calcium carbonate growth that were discussed in section 2.3.4 Crystal Growth (Parkhurst et al. 1978, Schagen et al. 2008 and Wolthers et al. 2012): a larger calcium carbonate surface area increases the rate at which calcium carbonate precipitates linearly for all three models.

This becomes obvious when plotting the total precipitated calcium carbonate over time. Figure 4-7 below shows the precipitated calcium carbonate as the difference of the calcium concentrations between the influent and the effluent for the column experiments where precipitation was observed, divided by the flow through the column. The amount of precipitated calcium carbonate during experiment 1 increases exponentially. Initially there is no calcium carbonate present. As more and more calcium carbonate precipitates, the surface area increases which results in a higher precipitation rate. This exponential increase of precipitated calcium carbonate is less obvious during experiment 3 and 6. Only when the concentrations of the effluent have been constant over time, the surface area has had no influence on the rate of precipitation. For all experiments, also 3 and 6, the effluent has decreased towards this equilibrium during the first days.

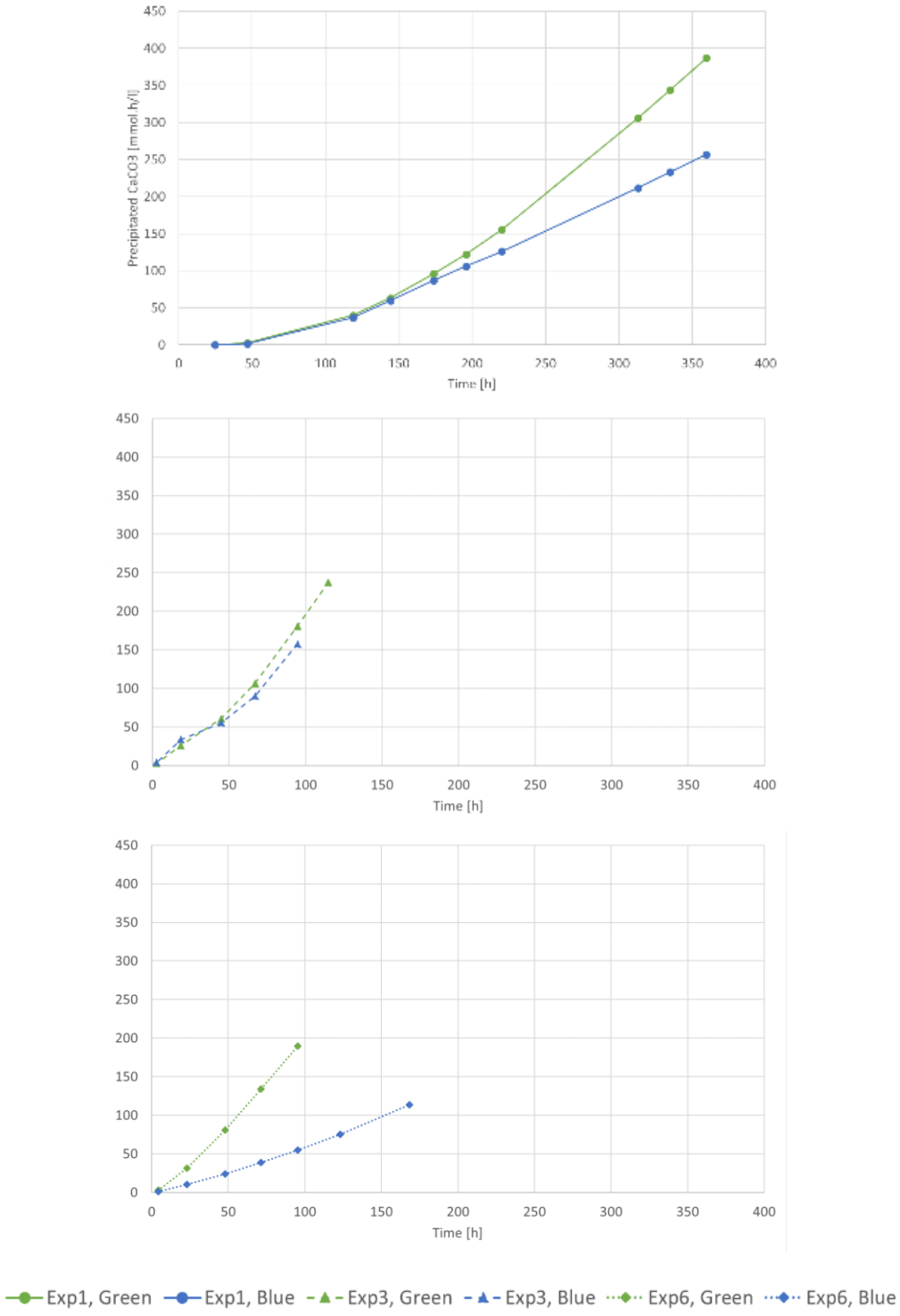

Figure 4-7 The amount of precipitated calcium carbonate divided by the discharge through the column for column experiment 1 ($SI_{calcite}$ = 1.14), 3 ($SI_{calcite}$ = 1.5) and 6 (green: $SI_{calcite}$ = 1.23, blue $SI_{calcite}$ 1.0 both with calcite seeds).

There were no calcite seeds used for experiment 1 and experiment 3. Yet, the exponential increase of precipitated calcium carbonate during experiment 3 is less obvious. Of course, the $SI_{calcite}$ of experiment 3 is higher, which increases the rate of precipitation. In addition, homogeneous nucleation could be more dominant at an $SI_{calcite}$ of 1.5, while at a lower $SI_{calcite}$ of 1.0 and 1.23 heterogeneous nucleation, 2D nucleation and growth are more important – all these processes depend on surface characteristics. Hence, when seed crystals were present, as during experiment 6,

calcium carbonate precipitates from an otherwise metastable solution. The rate of precipitation was also lower during the initial stages of experiment 6. The presence of seeds however, did significantly reduce the period before the effluent has become stable.

4.4 OVERVIEW OF THE BATCH EXPERIMENTS

In total, 30 batches were prepared to analyse the kinetics of calcium carbonate precipitation in the presence of sand and humic acids. A list of all batches is given below in table 4-7. The batch with an $SI_{calcite}$ of -99 did not receive any $NaHCO_3$, and therefore has a very low negative $SI_{calcite}$.

*Table 4-7 Overview of batch tests, ordered per $SI_{calcite}$ and the dosage of humic acids. Each batch is indicated by an X. *The batches with humic acid received too much $CaCl_2$: 6.74mmol/l instead of the planned 5.06mmol/l.*

$SI_{calcite}$	$CaCl_2$ dose [mmol/l]	$NaHCO_3$ dose [mmol/l]	pH	Humic acid concentration [mgC/l]						
				0.0	0.0535	0.160	0.535	1.60	5.35	16.0
				Humic acid concentration [µmolC/l]						
				0.0	4.46	13.3	44.6	133	446	$1.33 \cdot 10^3$
-99	10.1	0.0	7.5	X						
0.5	2.53	6.0	7.5	X	X	X	X	X	X	X
1.0	5.06/6.74*	12.0	7.5	X	X*	X*	X*	X*	X*	X*
1.5	10.1	24.0	7.5	X	X	X	X	X	X	X
2.0	20.2	48.0	7.5	X	X	X	X	X	X	X
2.5	40.4	96.0	7.5	X						

After every experiment, a sample of the sand was taken, dried and analysed under the microscope. The pictures show calcium carbonate crystals both on the grains scattered around the grains. It is hard to indicate whether the crystals were attached to those grains in the batch or became attached after drying. In general, it was very easy to remove the crystals from the grains: moving the sand around on the object glass was enough to remove some crystals. In a batch that is shaken, the sand swirls around on the bottom of the bottle and causes many collisions. It is therefore unlikely that nuclei formed on the sand could remain attached to the grains in the batch. This not does exclude the process of heterogeneous nucleation of calcium carbonate on the sand. Nuclei can initially be formed on the grains and then be eroded off. Whether the main precipitation process was heterogeneous or homogeneous nucleation remains unsure.

4.5 RESULTS OF THE BATCH EXPERIMENTS

The concentrations of calcium and (bi)carbonate were measured by taking samples at regular intervals. Unlike the column experiments, the pH was not measured continuously – the pH was measured and adjusted after the dose of $NaHCO_3$ and after the experiment (equilibrium pH), when the batches were opened. The pH and the $SI_{calcite}$ in the graphs below were modelled after the reduction in calcium and (bi)carbonate with Phreeqc.

All graphs are shown in attachment B Results of batch experiments. Here, only the graphs of the $SI_{calcite}$ and the calcium concentrations are shown. The graphs are ordered per series with the same $SI_{calcite}$. In the graphs of the calcium and (bi)carbonate concentrations, the measured concentrations of calcium are shown as dots while the corresponding modelled concentrations are shown as a line in the same colour. The lines in the graphs of the pH and the $SI_{calcite}$ only show the modelled results. An exception are the measurements of the carbonate concentrations of the batches without humic acids, that are not used for the calculation of the $SI_{calcite}$ and the pH. Those measurements deviated

too much from the equilibrium concentrations, most likely due to a measurement error with the IC spectrometer. Therefore, only the calcium concentrations are presented in this chapter.

4.5.1 Batches with $SI_{calcite}$ = 0.5

The dosage of calcium chloride to the batches with an $SI_{calcite}$ of 0.5 was 2.53 mmol/l. Figure 4-8 below shows the modelled and measured calcium concentrations and figure 4-9 shows the modelled $SI_{calcite}$ values.

During the entire experiment, the concentrations did not decrease for this $SI_{calcite}$, irrespective of the humic acid concentration. The modelled $SI_{calcite}$ of the experiment did not decrease either, but the modelled results of the different batches are between 0.25 and 0.8, while the $SI_{calcite}$ was aimed at 0.5. This is very likely due to the low dosages of calcium and carbonate: a small deviation has a relative large effect on the concentration.

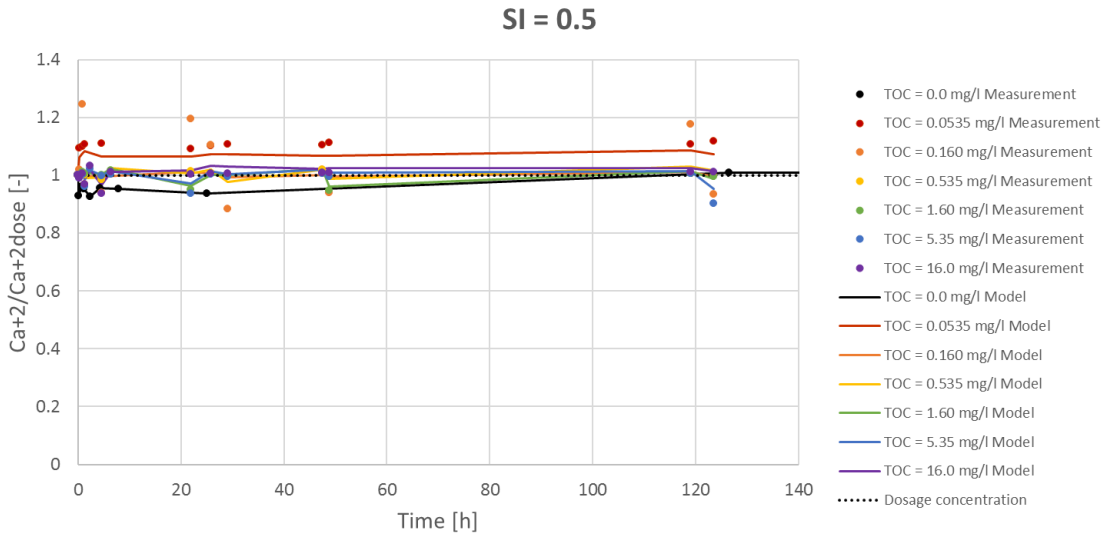

Figure 4-8 The calcium concentrations relative to the amount of calcium dosed (2.53mmol/l) of the batches with an $SI_{calcite}$ of 0.5. The different amounts of humic acids dosed in mgC/l in each batch are indicated by different colours. The dots represent measured concentrations while the lines represent the modelled concentrations.

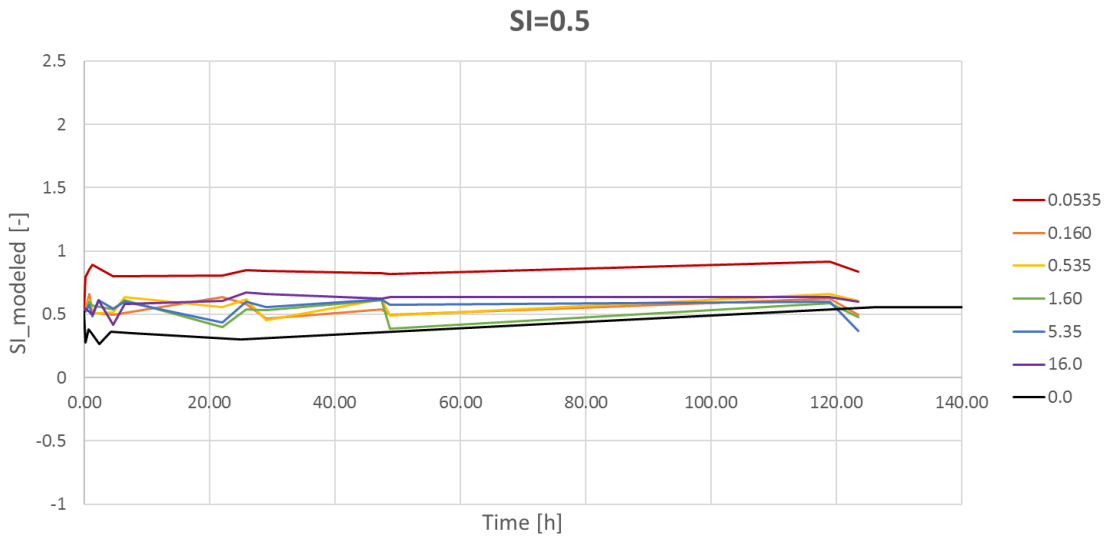

Figure 4-9 The modelled $SI_{calcite}$ values of the batches that at t=0 had an $SI_{calcite}$ of 0.5. The different amounts of humic acids dosed in mgC/l in each batch are indicated by different colours.

The pH of the equilibrium situation was both modelled with the calcium and carbonate concentrations and measured after the experiment was finished. The results are shown below in table 4-8. Both the measured pH and the modelled pH have not been reduced and do not differ from each other. From the concentrations and the measured pH, it can be concluded that no calcium carbonate has precipitated in any batch with an $SI_{calcite}$ of 0.5.

Table 4-8 The measured and modelled pH of the steady state situation of the batches with an $SI_{calcite}$ of 1.5.

	Humic acid concentration (mgC/l)						
SI = 0.5	0.0	0.0535	0.160	0.535	1.60	5.35	16.0
Measured	7.53	7.51	7.55	7.61	7.70	7.85	7.67
Modelled	7.52	7.77	7.51	7.56	7.49	7.51	7.58

4.5.2 Batches with $SI_{calcite}$ = 1.0

The batches with an $SI_{calcite}$ of 1.0 and with humic acids were dosed with a wrong volume of the calcium chloride solution. Therefore, the concentrations of those batches was 6.74mmol/l of calcium while the aim was to dose 5.06mmol/l. This resulted in a $SI_{calcite}$ of 1.1 for the bottles containing humic acids, while the $SI_{calcite}$ of the bottle without is 1.0.

The figures 4-10 and 4-11 below show the graphs of the calcium concentrations and the $SI_{calcite}$ respectively. The calcium concentrations of all bottles have reduced during the experiment. The $SI_{calcite}$ ranges from 1.1-0.5. All lines except for 5.35mgC/l show a decreasing calcium concentration and decreasing $SI_{calcite}$, indicating calcium carbonate precipitation. However, there is no clear trend visible related to the different concentrations of humic acids. Yet, calcium carbonate can precipitate at an $SI_{calcite}$ of 1.0.

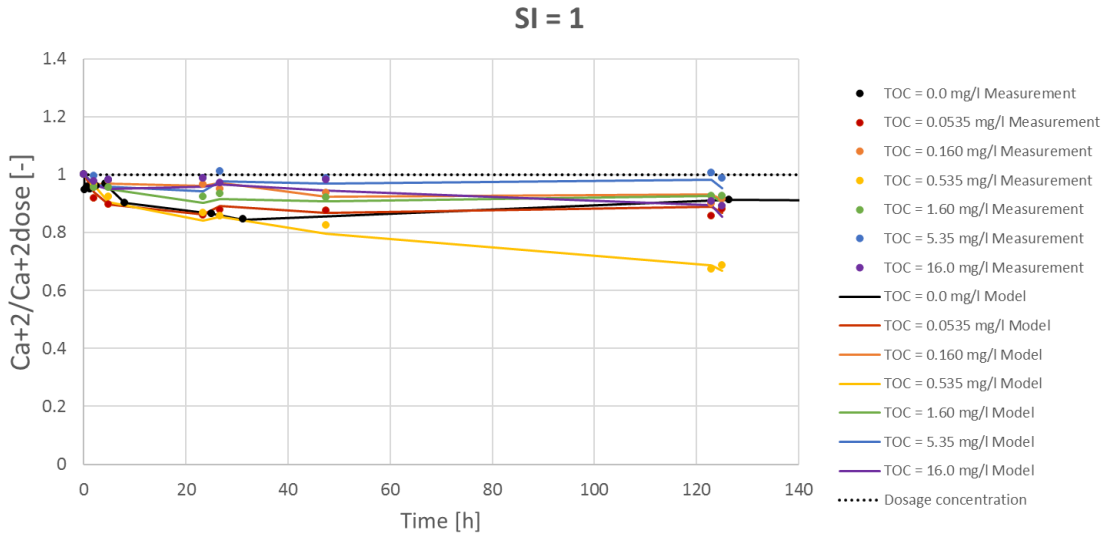

Figure 4-10 The calcium concentrations relative to the amount of calcium dosed (5.06/6.74) of the batches with an $SI_{calcite}$ of 1.0. The different amounts of humic acids dosed in mgC/l in each batch are indicated by different colours. The dots represent measured concentrations while the lines represent the modelled concentrations. Note: the dosage concentrations of calcium chloride for the batch without humic acids (solid black line and black markers) was 5.06mmol/l while for the batches with humic acids (solid coloured lines and coloured markers) 6.74mmol/l of calcium chloride was added.

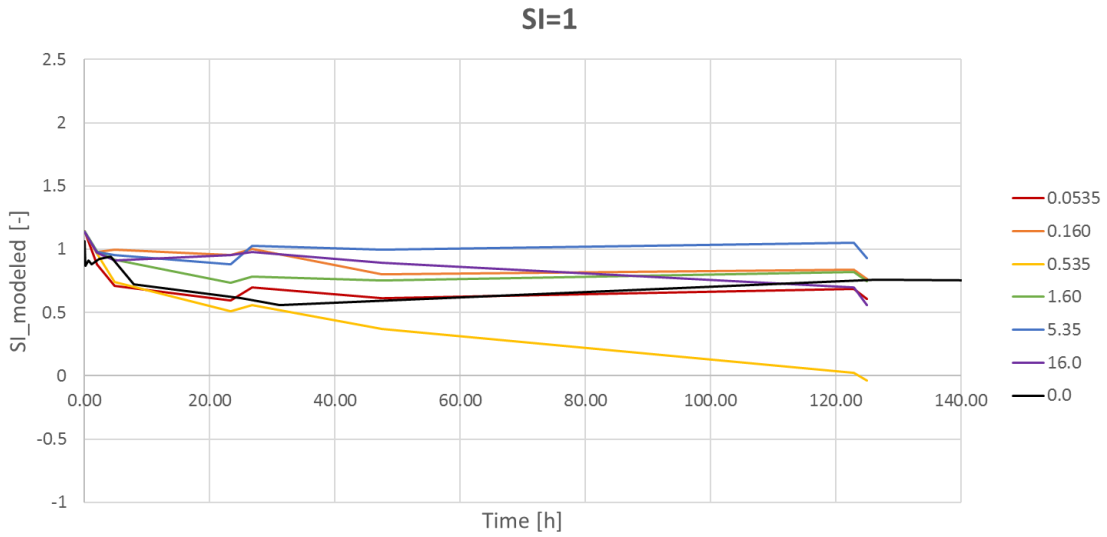

Figure 4-11 The modelled $SI_{calcite}$ values of the batches that at t=0 had an $SI_{calcite}$ of 1.0. The different amounts of humic acids dosed in mgC/l in each batch are indicated by different colours. Note: the dosage concentrations of calcium chloride for the batch without humic acids (solid black line and black dots) was 5.06mmol/l while for the batches with humic acids (solid coloured lines and coloured dots) 6.74mmol/l of calcium chloride was added.

The measured and modelled pH's are shown below in table 4-9. There is no trend related to the humic acid concentrations for both the modelled as well as the measured pH. The modelled pH is lower than the measured pH for all batches.

Table 4-9 The measured and modelled pH's of the steady state situation of the batches with an $SI_{calcite}$ of 1.5.

	Humic acid concentration (mgC/l)						
SI = 1.0	0.0	0.0535	0.160	0.535	1.60	5.35	16.0
Measured	7.38	7.23	7.37	7.46	7.47	7.61	7.71
Modelled	7.20	7.11	7.29	6.87	7.21	7.37	7.24

4.5.3 Batches with $SI_{calcite}$ = 1.5

The dosage of calcium chloride to the batches with an $SI_{calcite}$ of 1.5 was 10.1 mmol/l. The graphic results of the calcium concentrations and the $SI_{calcite}$ values can be found below in figure 4-12 and figure 4-13.

In all batches, the calcium concentrations have reduced over time and have reached equilibrium. The batches with humic acid concentrations of 0.0-1.60mgC/l approach the same equilibrium concentration, while the higher concentrations of humic acids have a higher equilibrium concentration of calcium carbonate.

The batches with no and a low concentration of humic acids, eventually reach an equilibrium state with a $SI_{calcite}$ of 0.30-0.40. The equilibrium states of the batches with 5.35mgC/l and 16.0mgC/l have an $SI_{calcite}$ of 0.75 and 1.1 respectively. Precipitation in those two batches is delayed initially, and their rate of precipitation is reduced as well. The delay is longer and the precipitation is slower in the batch with 16.0mgC/l of humic acids than in the batch with 5.35mgC/l.

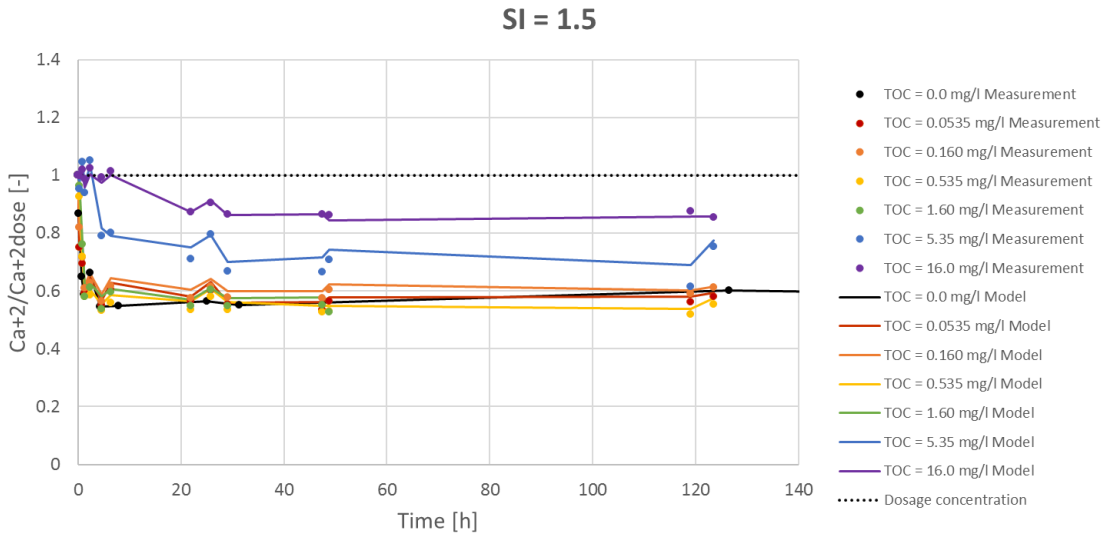

Figure 4-12 The calcium concentrations relative to the amount of calcium dosed (10.1 mmol/l) of the batches with an $SI_{calcite}$ of 1.5. The different amounts of humic acids dosed in mgC/l in each batch are indicated by different colours. The dots represent measured concentrations while the lines represent the modelled concentrations.

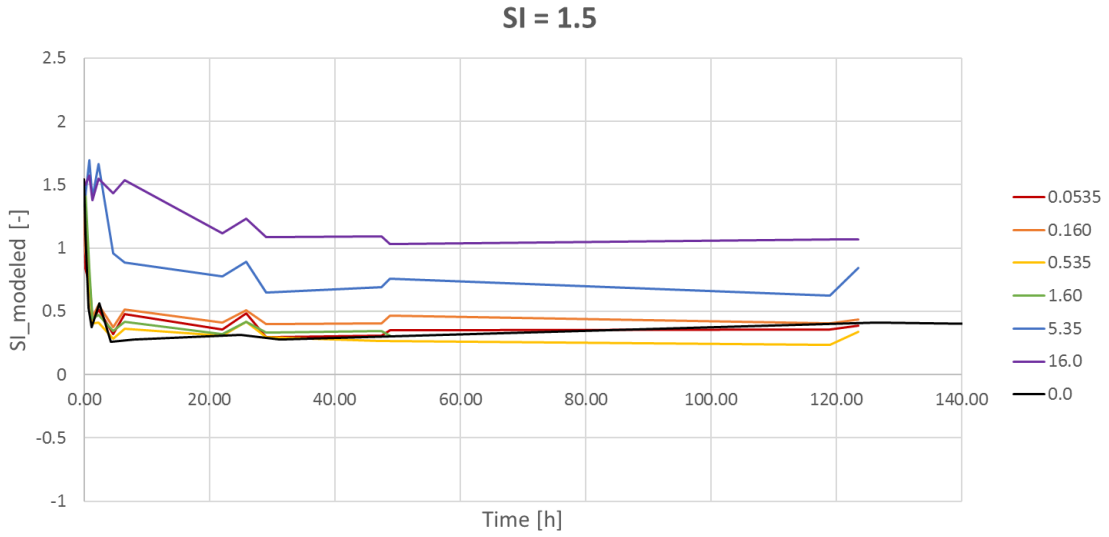

Figure 4-13 The modelled $SI_{calcite}$ values of the batches that at t=0 had an $SI_{calcite}$ of 1.5. The different amounts of humic acids dosed in mgC/l in each batch are indicated by different colours.

The measured and modelled pH's can be found below in table 4-10. The modelled pH's naturally follow the trend of the calcium concentrations, with a high equilibrium pH's for the batches with a high concentration of humic acid. The measured results however, do not follow this trend.

*Table 4-10 The measured and modelled pH's of the steady state situation of the batches with an $SI_{calcite}$ of 1.5. *bottle broken at the end of the experiment*

	Humic acid concentration (mgC/l)						
SI = 1.5	0.0	0.0535	0.160	0.535	1.60	5.35	16.0
Measured	7.24	6.84	7.19	6.88	-*	7.05	7.29
Modelled	6.67	6.71	6.75	6.68	6.70	6.94	7.18

4.5.4 Batches with $SI_{calcite}$ = 2.0

The dosage of calcium chloride to the batches with an $SI_{calcite}$ of 2.0 was 20.2 mmol/l. Figure 4-14 and 4-14 show the calcium concentrations and the $SI_{calcite}$ values of those batches. All batches showed a significant reduction of the calcium concentrations, with the batch without humic acids clearly approaching an equilibrium state away from the batches without humic acids. The $SI_{calcite}$ of the batch without humic acids is even negative at equilibrium concentration (-0.45). This was very likely due to a wrong dosage of $NaHCO_3$. The equilibrium $SI_{calcite}$ values of the other batches are in the range of 0.12-0.55. The $SI_{calcite}$ and the calcium concentration at equilibrium are higher when the amount of humic acids increases. As opposed to what was observed in the batches with an $SI_{calcite}$ of 1.5, no delay or reduced rate is observed in the batches with relatively high humic acids concentrations.

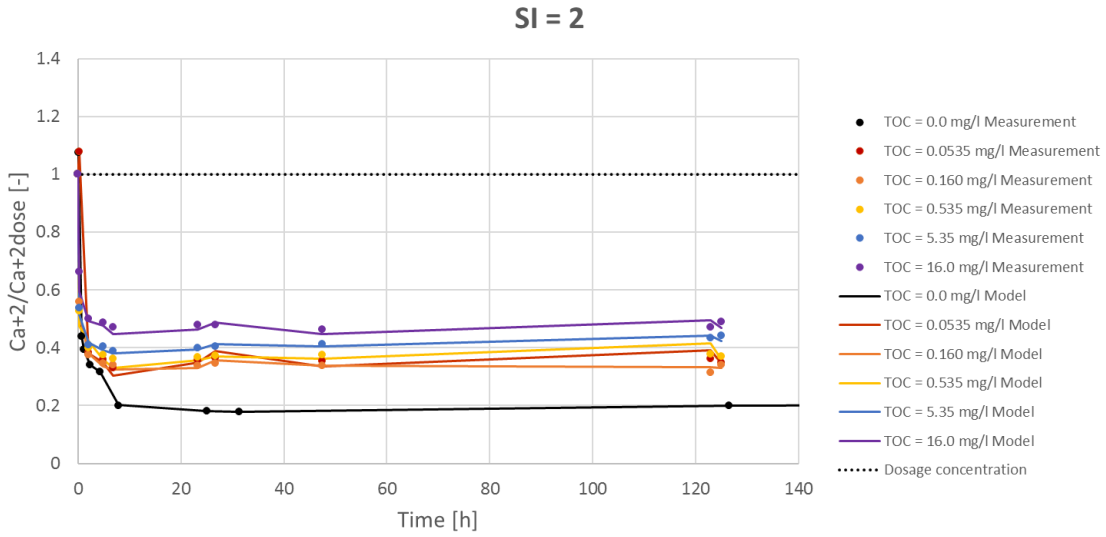

Figure 4-14 The calcium concentrations relative to the amount of calcium dosed (20.2 mmol/l) of the batches with an $SI_{calcite}$ of 2.0. The different amounts of humic acids dosed in mgC/l in each batch are indicated by different colours. The dots represent measured concentrations while the lines represent the modelled concentrations.

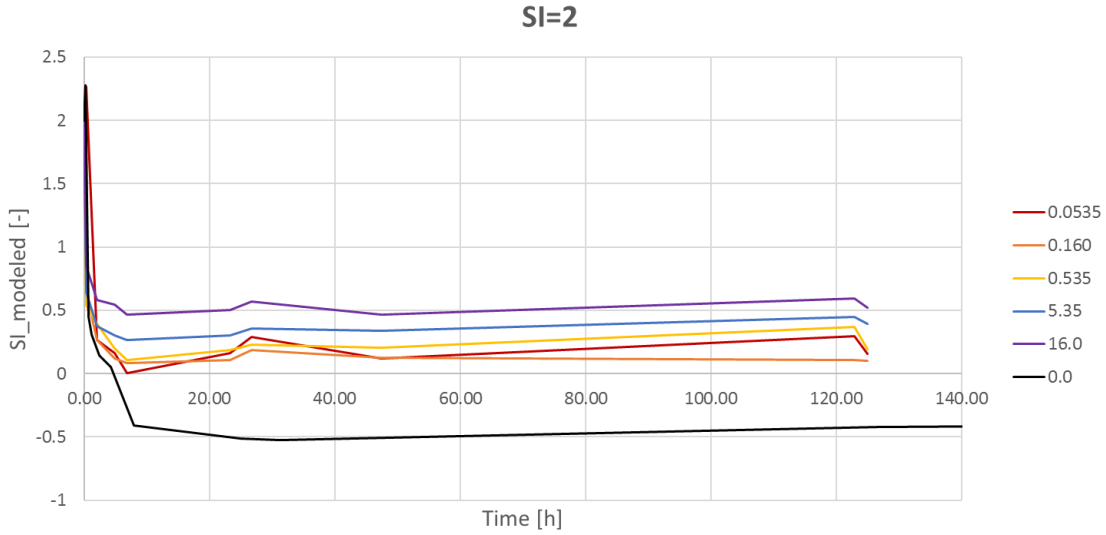

Figure 4-15 The modelled $SI_{calcite}$ values of the batches that at t=0 had an $SI_{calcite}$ of 2.0. The different amounts of humic acids dosed in mgC/l in each batch are indicated by different colours.

The measured and modelled pH's can be found below in table 4-11. No trend can be observed from the modelled pH. Yet, the measured pH values of most batches lay close to the modelled values.

*Table 4-11 The measured and modelled pH's of the steady state situation of the batches with an $SI_{calcite}$ of 2.0. *due to a wrong dosage of $NaHCO_3$, the results of this batch were disregarded.*

	Humic acid concentration (mgC/l)						
SI = 2.0	0.0	0.0535	0.160	0.535	1.60	5.35	16.0
Measured	6.89	6.48	6.49	6.50	-*	6.92	6.64
Modelled	6.41	6.39	6.36	6.41	-*	6.47	6.54

4.6 DISCUSSION OF THE BATCH EXPERIMENTS

The process in the batch experiments was predominantly homogeneous nucleation, since no calcium carbonate precipitated on the sand. However, the sand that was dosed as seed material must have contained a lot of dust particles and other colloidal material on which calcium carbonate would nucleate. Precipitation on colloidal material cannot be avoided in natural waters (Lebron and Suarez 1998). The extend of the effect of colloidal material on the precipitation of calcium carbonate is unknown.

Calcium carbonate precipitated in the batches with an $SI_{calcite}$ of 1.0-2.0 – the batch with an $SI_{calcite}$ of 1.0 and 5.35mgC/l of humic acids did not show any precipitation. No precipitation was observed when the $SI_{calcite}$ was 0.5, regardless of the concentration of humic acids. No clear pattern of inhibition related to increasing concentrations was observed for an $SI_{calcite}$ of 1.0. The batches with an $SI_{calcite}$ of 1.5 and 2.0 showed more inhibition with increasing concentration of humic acids. The inhibition of humic acids resulted in less precipitation for both those $SI_{calcite}$. An initial delay and a lower rate of precipitation was observed only for an $SI_{calcite}$ of 1.5.

Kaandorp (2014) based on the research of Lebron and Suarez (1996) and Reddy (2012) that inhibition by NOM was relevant at concentrations higher than 1.2 mgC/l. Precipitation was completely blocked at 3.6 mgC/l (Lebron and Suarez 1996). This was not observed in these experiments. However, inhibition was observed above the threshold of 3.6 mgC/l for an $SI_{calcite}$ of 1.5 and 2.0. The same concentrations of humic acids were more effective at a lower $SI_{calcite}$ of 1.5 than at 2.0. For their experiments, Lebron and Suarez (1996) used a variety of organic molecules, both humic and fulvic acids. Possibly, inhibition varies for different humic and fulvic acids.

Lebron and Suarez (1996) did not relate the effective amount of humic acids to the $SI_{calcite}$ or calcium and carbonate concentrations, since they said that NOM inhibits precipitation by blocking active surface sites on existing crystals. Observations of a delay of precipitation – when there are no surface areas yet – and a reduction in effectiveness at a higher $SI_{calcite}$ – when there is more Ca^{+2} in the solution – suggest that humic acids do not only block surface sites but also form complexes with Ca^{+2} cations.

The batches eventually reached an equilibrium situation where calcium carbonate did no longer precipitate. The eventual $SI_{calcite}$ at this equilibrium situation depends on the initial $SI_{calcite}$: a higher initial $SI_{calcite}$ results in a lower equilibrium $SI_{calcite}$. Those observations are shown in table 4-12 below.

Table 4-12 The initial and equilibrium $SI_{calcite}$ of all the batch experiments where no inhibition was observed. [1]No precipitation was observed. [2]Only one experiment was conducted without humic acids.

Initial $SI_{calcite}$	0.5	1.0/1.1	1.5	2.0	2.5
$SI_{calcite}$ equilibrium	0.5[1]	1.0-0.5	0.30-0.40	0.12-0.21	0.0[2]

Looking at the calcium concentrations, the concentrations in the batches where precipitation was observed at equilibrium are all about similar. This can be seen below in figure 4-16. Following this trend, the threshold between a metastable solution and an unstable solution lies close below an $SI_{calcite}$ of 1.0.

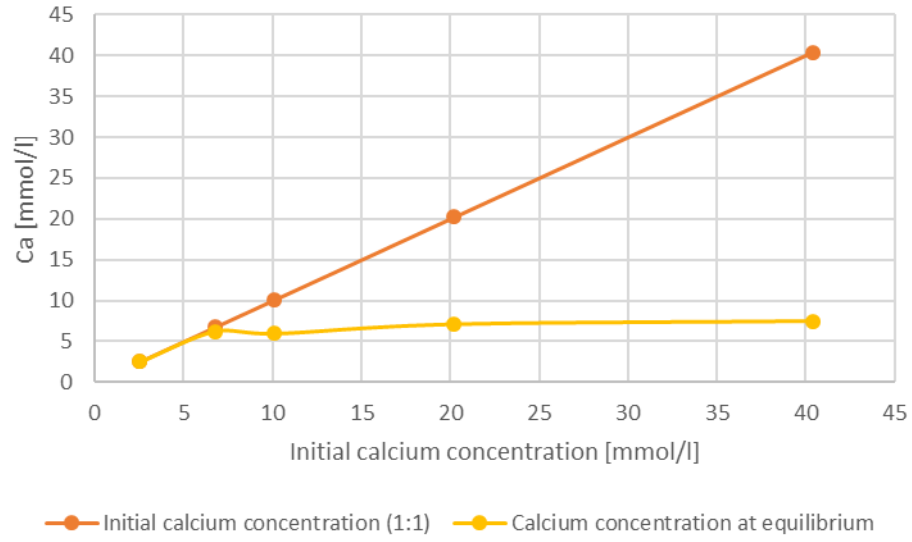

Figure 4-16 The calcium concentrations of the initial situation, the final concentration at equilibrium and the amount of precipitated calcium during the batch experiments without a noticeable effect of inhibitors. The dots from left to right of each line represent the batches with an $SI_{calcite}$ of 0.5, 1.0, 1.5, 2.0 and 2.5.

5 DISCUSSION, CONCLUSION AND RECOMMENDATIONS

Previous chapter showed and discussed the individual results of the column and batch experiments. The discussion in this research continues supported with some Phreeqc modelling. It is followed by the conclusions and some recommendations.

5.1 DISCUSSION

5.1.1 Metastability region

The results of both the column and the batch experiments show the same range of $SI_{calcite}$ in which the solution is metastable: the lower limit lies somewhere between 0.5 and 1.0 and the upper limit somewhere below 1.23 and 1.5. Within this region, the solution is susceptible to precipitation triggered by external factors. In practice, when the $SI_{calcite}$ of the brine from the Freshkeeper in Zevenbergen was reduced with CO_2 to 0.5, it was safe to inject as it did not show any reduction in calcium and carbonate concentrations (Raat and Kooiman, 2012 and Kaandorp, 2014).

5.1.2 The effect of surface area on the distribution of calcium carbonate in the column

Three growth models were discussed in the theory section: the PWP model, the model of Schagen et al. (2008) and the model of Wolthers et al. (2012). In all three models, the growth rate is given in $mmol.cm^{-2}.s^{-1}$. To obtain the rate at which calcium carbonate precipitates from the solution, the growth rate should be multiplied with the surface area of calcium carbonate in that solution. The rate at which calcium carbonate precipitates (in $mmol.s^{-1}$) is therefore linearly dependent on the surface area. Hence, without surface area, the rate of precipitation is zero.

Yet, as was observed at the column experiments that started without calcite seeds, the rate at which calcium carbonate precipitates increases over time, indicating an increase in surface area. Most pre-defined rate equations in the phreeqc.dat database contain a factor that simulates the increase in surface area. For calcite the rate of precipitation is calculated from the rate of growth as (Appelo et al. 1998):

$$r_{precipitation} = r_{growth}\left(\frac{A_{calcite}}{V}\right)\left(\frac{m}{m_0}\right)^{i}_{cal}$$

Where $r_{precipitation}$ is the rate of precipitation from the solution (e.g. in $mmol.s^{-1}$), r_{growth} is the growth rate (e.g. in $mmol.cm^{-2}.s^{-1}$) and $A_{calcite}$ is the surface area of calcite (e.g. in cm^{-2}) in the solution volume V. The factor $(m/m_0)^i$ takes into account the increase in calcium carbonate surface area, with m and m_0 as the current and initial amount of moles of the mineral respectively. In preeqc.dat the exponent i for calcite is set to 0.67.

Figure 5-1 and figure 5-2 below shows the results of various precipitation simulations. The column is modelled using the transport simulation option in Phreeqc. The precipitation of calcium carbonate was simulated with different surface areas and three different precipitation models. The factor $(m/m_0)^i$ was set to 1 for all simulations, so that the surface area didn't vary over time during each run. Instead, the unaerated/closed PWP model was simulated with different surface areas, indicating the effect of the increase in surface area.

As can be seen in figure 5-1, an increasing calcite surface area has a large effect on the precipitation rates over the length of the column. With more surface area in the whole column, the rate at the start of the column is significantly higher and decreases exponentially over the length. Over time, with increasing surface area, precipitation will occur only in the first few centimetres of the column.

Because of the higher rates, the surface area will also be significantly more in the first centimetres, an effect that is not taken into account in this model.

The use of different precipitation models, as is shown in figure 5-2, results in different rates and a different distribution of precipitation. The value used for the variable K in the model of Schagen et al. (2008) is 10^{-3} l.m.s^{-1}.mmol^{-1}. The rates for the models of Schagen et al. (2008) and Wolthers et al. (2012) are generally higher than for the closed PWP model. They simulate a larger precipitation of calcium carbonate in the first centimetres. The influent has a [CO_3^{-2}]/[Ca^{+2}] ratio of $10^{-2.3}$.

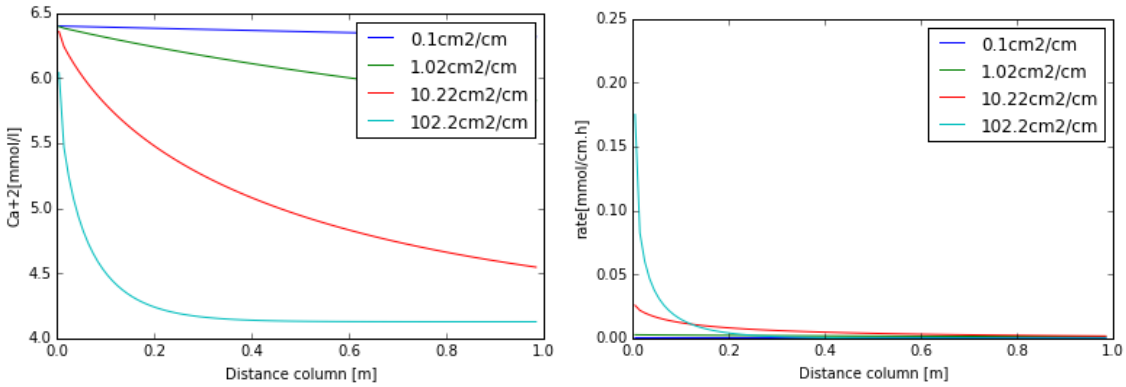

Figure 5-1 Results of the Phreeqc column simulations with the closed (unaerated) PWP-model. The model is run with different calcium carbonate surface areas. The conditions are similar to the first two column experiments: $SI_{influent}$ = 1.14, v=0.3m/h and porosity=0.4.

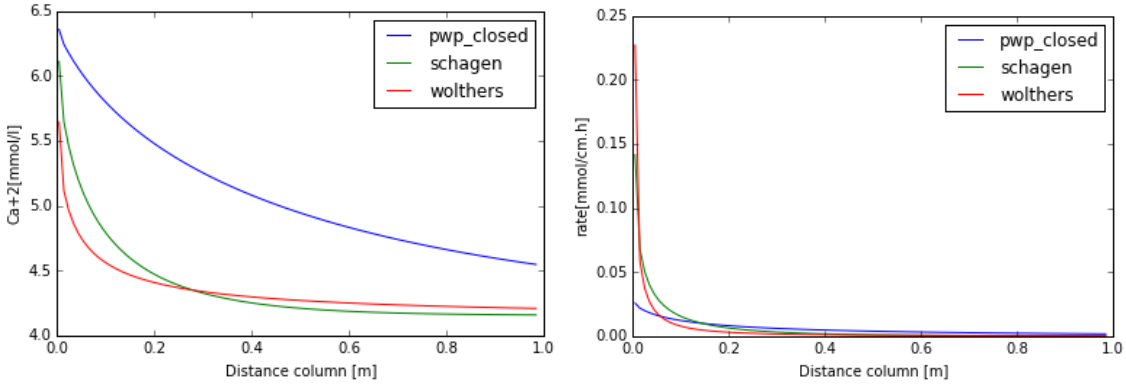

Figure 5-2 Results of the Phreeqc column simulations with various growth models: closed PWP, Schagen et al. (2008) and Wolthers et al (2012). The calcite surface area is set to 10.22cm²/cm. The conditions are similar to the first two column experiments: $SI_{influent}$ = 1.14, v=0.3m/h and porosity=0.4.

The model of Schagen et al. (2008) is the only model that has incorporated the effect of both the velocity and the temperature on the diffusion layer between the bulk liquid and the precipitation surface. The PWP model does take into account the temperature dependency of the diffusion through this diffusion layer.

The PWP model is based on calcium carbonate dissolution in batch experiments that took 7 hours with measurements every 6 seconds (Plummer et al. 1978). In their experiments, Plummer et al. (1978) showed that dissolution rates increased as the stirring rate of the batch was increased – a higher stirring rate increases the flow of water around the crystals which results in a thinner diffusion layer. However, the dependency of the stirring rate was only clearly observed at pH <5. According to Plummer et al (1978), diffusion is limited by the transfer of H^+ through the diffusion layer. Hence, the dependency on the stirring rate became more significant as the pH decreased.

The experiments of Plummer et al. (1978) only looked at the dissolution of calcium carbonate and not the precipitation. The diffusion limitation was based on the transport of H^+ from the bulk liquid through the diffusion layer, where it reacts with the dissoluted CO_3^- to form HCO_3^-. During precipitation, OH^- should be transported through the boundary layer to convert HCO_3^- to CO_3^{-2}. Hence, for precipitation, the dependency on the thickness of the diffusion layer might be larger at higher pH.

The model of Schagen et al. (2008) is used for the precipitation of calcium carbonate in pellet reactors. At the bottom of a pellet reactor, either NaOH or $Ca(OH)_2$ is injected. When NaOH is injected, as in the reactors analysed by Schagen et al. (2008), it immediately lowers the pH and increases the $SI_{calcite}$ at the bottom (Verberk et al. 2011). The higher pH in these reactors might increase the importance of the thickness of the diffusion layer.

Compared to the column experiments, the flow velocities in the pellet reactors are about 200x higher – 60-100m/h (Schagen et al. 2008). Fitting the model of Schagen et al. (2008) using the velocities in the column gave results that were a factor 10^6 smaller than the simulations used above – where a value of 10^{-3} $l.m.s^{-1}.mmol^{-1}$ was used for K. Higher values of $SI_{calcite}$, higher velocities, a higher pH and a lower residence time in the pellet reactors compared to the column experiments could be reasons why the model of Schagen et al. (2008) could not be applied to the column directly. Therefore, the importance of the diffusion layer and the velocity under the circumstances of the column experiments could not be analysed with the model of Schagen et al. (2008).

5.1.3 The effect of small variations in mixing ratios and temperature in the column

Combining the results from the batch experiments, it appeared that the threshold at which a metastable solution becomes unstable lies close below an $SI_{calcite}$ of 1.0. This threshold could vary for a different pH, temperature or ratio of $[Ca^{+2}]/[CO_3^{-2}]$. This threshold laying close to an $SI_{calcite}$ of 1.0 could be a reason for precipitation to occur in column experiment 1 and not in column experiments 2, 4 and 5: small differences in circumstances – for example temperature, surface characteristics, differences in mixing ratios or pH – might be the difference between a metastable and an unstable solution. Figure 5-3 below shows the effect of temperature and different mixing ratios. The variations in temperature or in mixing ratio are not sufficient to change the $SI_{calcite}$ enough, so that the different lines will cross.

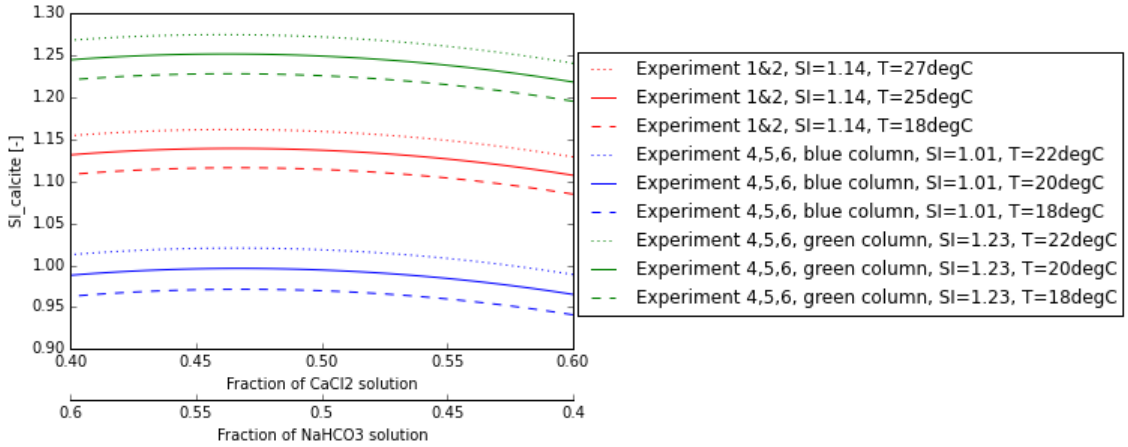

Figure 5-3 The effect of differences in mixing ratio (different from 0.5:0.5) of the two solutions – the $CaCl_2$ solution and the $NaHCO_3$ solution.

As can be seen below in figure 5-4, a deviation in pH of the influent has a strong effect on the pH. A difference in pH of ±0.1 already has a significant effect on the $SI_{calcite}$. Yet, since two columns per

experiment with the same characteristics showed similar results and multiple solutions had to be prepared for a single experiment, it is not very likely that these small errors are the cause of the differences in precipitation and stability of the experiments.

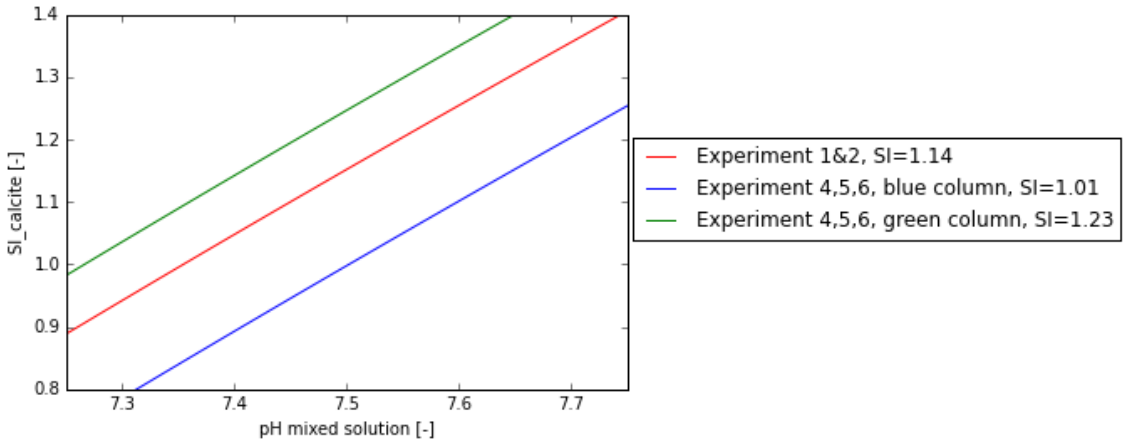

Figure 5-4 The effect of deviations in the pH of the influent on the $SI_{calcite}$.

The only introduced difference between experiment 1 and 2 was the velocity. As discussed in section 2.3.4 Crystal growth, the growth model of Schagen et al. (2008), a higher velocity reduces the thickness of the boundary layer through which the ions have to diffuse before they reach the surface.

To verify experiments 1 and 2, experiments 4 and 5 had two different velocities (with the same two pump settings) and two different values of $SI_{calcite}$: 1.01 and 1.23 – one slightly lower and one slightly higher than the 1.14 of experiment 1 and 2. Neither during experiment 4 nor during experiment 5 did calcium carbonate precipitate. The higher velocity did not trigger precipitation in experiment 5. Why calcium carbonate nucleated during experiment 1 and in the batches where $SI_{calcite}$ was 1.0, and did not precipitate during experiments 2, 4 and 5 cannot be clarified. It does indicate that at an $SI_{calcite}$ between 1.0 and 1.23, the solution is metastable, but can become unstable with the right circumstances. One of those circumstances is the presence of seed material, as pointed out by experiment 6.

5.1.4 The effect of calcium and carbonate ratios on the batch experiments

At equilibrium, those batches starting at an $SI_{calcite}$ of 0.5-2.0 were still supersaturated. Wolthers et al. (2012) showed that there is a relationship between the rate of precipitation and the ratio of the activities of calcium and carbonate ($[Ca^{+2}]/[CO_3^{-2}]$): generally, when the ratio lies further away from 1.0, it slows down precipitation. Figure 5-5 below shows the modelled ratios during complete precipitation of calcium carbonate – up to an $SI_{calcite}$ of 0.0 – from the batches with the five initial values of $SI_{calcite}$. The batches with a higher $SI_{calcite}$ were dosed with more $NaHCO_3$, therewith increasing the buffer capacity. As can be seen in figure 5-5, during precipitation of calcium carbonate, the higher buffering capacity at a higher $SI_{calcite}$ reduces the rate at which the ratio $[Ca^{+2}]/[CO_3^{-2}]$ increases with decreasing Ca/Ca0. However, for a high initial $SI_{calcite}$, the ratio of $[Ca^{+2}]/[CO_3^{-2}]$ is much higher eventually, when $SI_{calcite}$ has become 0. This makes it unlikely that a high ratio of $[Ca^{+2}]/[CO_3^{-2}]$ has stopped precipitation before the $SI_{calcite}$ was 0.

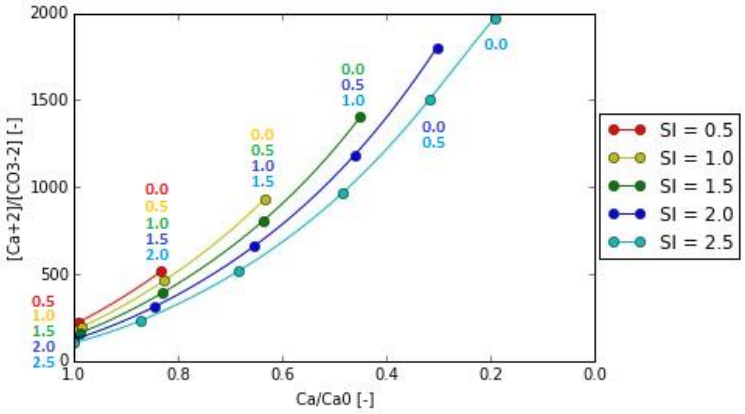

Figure 5-5 The ratio of $[Ca^{+2}]/[CO_3^{-2}]$ during the modelled precipitation of calcium carbonate from the batches with five different starting values of $SI_{calcite}$. The horizontal axis represents the leftover calcium relative to the initial calcium concentration (Ca0). As more calcium carbonate precipitates, Ca/Ca0 and the $SI_{calcite}$ gets lower. The dots represent the concentrations at different values of $SI_{calcite}$ in steps of 0.5 – the values are shown with the dots in the same colour.

Yet, over very long time scales, calcium carbonate might be precipitating until the $SI_{calcite}$ has become 0. However, since for the injection of brine the most relevant time scale is when the supersaturated solution is in the first meters of the bed, it is not very relevant for this research.

5.2 CONCLUSION

Calcium carbonate can precipitate by various processes, depending on the supersaturation of the solution. These processes are, with increasing supersaturations: growth, 2D-nucleation, heterogeneous nucleation and homogeneous nucleation.

Growth and 2D-nucleation rely on the presence of calcium carbonate seeds. Without any calcite seeds present, calcium carbonate has to form nuclei first, either on another surface (heterogeneous nucleation) or freely in the solution (homogeneous nucleation). Hence, with increasing supersaturation, the dependence of precipitation on the surface characteristics of the surrounding soil materials decreases.

Batch experiments show that a solution with an $SI_{calcite}$ of 0.5 is safe to inject. The range of $SI_{calcite}$ at which a metastable solution can become unstable, starts somewhere below 1.0 and ends somewhere below 1.5. In this range, the sustained metastablility is susceptible to precipitation if the characteristics of the surrounding surfaces are favourable. At an $SI_{calcite}$ of 1.5 heterogeneous nucleation and homogeneous nucleation have become more dominant and will result in rapid clogging.

Following the equation of Carman-Kozeny combined with a high precipitation rate and increase in surface area at the start of the bed, the hydraulic resistance increases exponentially over time. The graphs of the effluent concentrations and pH and the recorded pressure confirm this behaviour: the increase in pressure became noticeable only after a period during which reduction of calcium carbonate in the column has been observed. Also, cementation was observed in the first centimetres of the column. Precipitation has taken place only at the start of the bed and not over a longer distance. This will make clogging deceiving: while there is no increase in injection pressure noticeable, calcium carbonate is building up in the pores and eventually the hydraulic conductivity will strongly reduce. Measuring the pressure only is therefore not enough to give an early warning on clogging.

With inhibitors, calcium carbonate precipitation can be reduced or even prevented. Humic acids, as tested in this research, can act as inhibitors for calcium carbonate precipitation. In the models presented by Lebron and Suarez (1996) for growth and nucleation, inhibition solely depends on the humic acid concentration and not on the $SI_{calcite}$. In the batch experiments of this research however, it was observed that at a higher $SI_{calcite}$, more humic acids should be present to have the same inhibiting effect. This relationship between $SI_{calcite}$ and the concentration of humic acids suggests that humic acids not only block surface sites but also form complexes with calcium cations.

The concentration at which humic acids significantly reduced precipitation is higher than 0.1mmol/l of TOC, and concentrations higher than 0.3mmol/l TOC did not completely block precipitation. Hence, humic acids do not seem to be as effective as presented by Lebron and Suarez (1996).

5.3 RECOMMENDATIONS

The presented limits of the metastability region are all found at a pH of 7.5 and a similar ratio of $[Ca^{+2}]/[CO_3^{-2}]$. The different characteristics of other source waters might alter the range of the stability region. This will also help evaluating the what the effects are of a changing pH and $[Ca^{+2}]/[CO_3^{-2}]$ in a solution where calcium carbonate precipitates on. In addition, all experiments were done at room temperature. In practice, the temperature of the groundwater is about 13 °C which alters the chemistry and therewith the precipitation rate and metastability.

More complicated time consuming column experiments are not recommended. It was shown that batch experiments can predict the metastability region of calcium carbonate as well. Further understanding of the metastability region can therefore be achieved best by doing more batch experiments.

No clear relationship between velocity and precipitation or growth could be observed. This could be resolved by conducting more experiments, where supersaturated water flows passed a surface area of calcium carbonate at different velocities.

The different characteristics of the soil are crucial for maintaining metastability. In this research, pure silica sand was used. Garnet sand, which has cations incorporated in its structure, might encourage precipitation more than silica.

6 LITERATURE

Appelo C. A. J., Verweij E. and Schäfer H. (1998) *A hydrogeochemical transport model for an oxidation experiment with pyrite/calcite/exchangers/organic matter containing sand.* Applied geochemistry **13.2**, p257-268.

Astilleros J.M., Fernández-Diaz L. and Putnis A. (2010) *The role of magnesium in the growth of calcite: An AFM study*. Chemical Geology **271**, p52-58

Bang D.P. (2012) *Upflow limestone contactor for soft and desalinated water.* MSc Thesis. Sanitary Engineering Section, Department of Water Management TU Delft.

Bear J. and Verruijt A. (2012) *Modeling groundwater flow and pollution*. Springer Science & Business Media.

Ben Amor M., Zgolli D., Tlili M.M. and Manzola A.S. (2004) *Influence of water hardness, substrate nature and temperature on heterogeneous calcium carbonate nucleation*. Desalination **166**, p79-84

Bracco J.N., Grantham M.C. and Stack A.G. (2012) *Calcite growth rates as a function of aqueous calcium-to-carbonate ratio, saturation index and inhibitor concentration insight into the mechanism of reaction and poisoning by strontium*. Crystal growth & design **12**, p3540-3548

Charlton S.R. and Parkhurst D.L. (2011) *Modules based on the geochemical model Phreeqc for use in scripting and programming languages*. Computers & Geosciences, **37** p1653-1663

Chow N. and James N.P. (1987) *Facies-specific, calcitic and bimineralic ooids from middle and upper Cambrian platform carbonates, Western Newfoundland, Canada.* Journal of Sedimentary petrology, **57-5** p907-921

De Moel P.J., Van der Meer W.G.J. and Van Dijk J.C. (2012) Waterchemie voor drinkwater modeleren met Phreeqc. H2O **3-2012**, p34-36

De Yoreo J.J., Vekilov P.G. (2003) *Principles of crystal nucleation and growth*. Reviews in mineralogy and geochemistry **54.1**, p57-93.

Faure G. (1998) *Principles and applications of Geochemistry*. Prentice Hall, New Jersey.

Flaathen T.K., Oelkers E.H., Gislason S.R. and Aagaard P. (2011) *The effect of dissolved sulphate on calcite precipitation kinetics and consequences for subsurface CO_2 storage.* Energy Procedia **4**, p5037-5043

Gebauer D. and Cölfen H. (2011) *Prenucleation clusters and non-classical nucleation.* Nano Today **6.6**, p564-584

Gebauer D., Völkel A. and Cölfen H. (2008) *Stable Prenucleation Calcium Carbonate Clusters*. Science **322**, p1819-1822

Giroud J.P. (2010) *Development of criteria for geotextile and granular filters*. Proceedings of the 9th International Conference on Geosynthetics, Guarujá, Brazil, p23-27

Grakist G., Maas C., Rosbergen W. and Kappelhof J.W.N.M. (2002) *Keeping our wells fresh.* Proceedings of SWIM–17. Delft University of Technology, Delft, 337-340.

Haidari A.H., Blankert B., Timmer H., Heijman S.G.J. and Van der Meer W.G.J. (2015) *PURO: A unique RO-design for brackish groundwater treatment.* Desalination

Herzog E.R., Qihong S., Patil J.N. and Katz. J.L. (1989) Magnetic Water Treatment: The effect of ion on calcium carbonate nucleation and growth. Langmuir **5**, p861-867

Hu Q., Nielsen M.H., Freeman C.L., Hamm L.M., Tao J., Lee J.R.I., Han T.Y.J., Becker U., Harding J.H., Dove P.M. and De Yoreo J.J. (2013) *The thermodynamics of calcite nucleation at organic interfaces: classical vs. non-classical pathways*. Faraday Discussions **159**, p05-523

Hubbert M. K. (1957) *Darcy's law and the field equations of the flow of underground fluids.* Hydrological Sciences Journal **2.1**, p23-59.

Kaandorp V. (2014) *PURO, subsurface drinking water purification and hydrochemical processes: reactive transport modelling of deep well injection of brackish groundwater reverse osmosis concentrate.* Master Thesis. Hydrology Department, Vrije Universiteit Amsterdam (VU).

Kalikmanov V.I. (2013) *Nucleation Theory*. Springer Science & Business media.

Kawano J., Shimobayashi N., Miyake A. and Kitamura M. (2009) *Precipitation diagram of calcium carbonate polymorphs: its construction and significance.* Journal of Physics: Condensed Matter **21**

Lasaga A.C. (1998) *Kinetic theory in the earth sciences*. New Jersey: Princeton U.P.

Lebron I. and Suarez I.L. (1996) *Calcite nucleation and precipitation kinetics as affected by dissolved organic matter at 25°C and pH > 7.5*. Geochimica et Cosmochimica Acta **60.15**, p2765-2776

Lin Y and Singer P.C. (2006) *Inhibition of calcite precipitation by orthophosphate: speciation and thermodynamic considerations*. Geochimica et Cosmochimica Acta **70.10**, p2530-2539

Liu X.Y., Maiwa K. and Tsukamoto K. (1997) *Heterogeneous two-dimensional nucleation and growth kinetics*. The Journal of chemical physics **106.5**, p1870-1879

Nielsen A.E. (1964) *Kinetics of precipitation.* Oxford: Pergamon Press.

Nielsen L.C., De Yoreo J.J. and DePaolo D.J. (2013) *General model for calcite growth kinetics in the presence of impurity ions*. Geochimica et Cosmochimica Acta **115**, p100-114

Meldrum F.C. and Sear R.P (2008) *Now you see them*. Science **322**, p1802-1803.

Olariu R. (2015) *Treatment of cooling tower blowdown water – The effect of biodispersant on the ultrafiltration membrane.* MSc Thesis. Sanitary Engineering Section, Department of Water Management TU Delft.

Ogino T., Suzuki T. and Sawada K. (1987) *The formation and transformation mechanism of calcium carbonate in water*. Geochimica et Cosmochimica Acta. **51** p2757-2767

Olsthoorn T.N. (1977) *In Nederlandse zandformaties zijn het doorstroomde en het totale porievolume aan elkaar gelijk* (Dutch). H2O **5**, p118-122

Olsthoorn T. N. (2008) *Brackish groundwater as a new resource for drinking water; specific consequences of density dependent flow, and positive environmental consequences.* Program and proceedings of 20th Salt Water Intrusion Meeting (June 23–27 2008 Naples USA), Univ Florida, IFAS Research. 2008.

Raat KJ and Kooiman J.W. (2012) *Brak grondwater: niet mijden, maar gebruiken! Eindrapport BTO onderzoek pilots Noardburgum (Vitens) en Zevenbergen (Brabant Water)* (Dutch). KWR, Watercycle Research Institute

Rankin A.H. and Sutcliffe P.J.C. (1999) *Morphology, chemistry and growth mechanisms of calcite concretions from an industrial water-softening process: implications for the origin of natural ooids in sediments.* Proceedings of the Geologists' Associations, **110** p33-40

Reddy M.M. (2012) *Calcite growth-rate inhibition by fulvic acid and magnesium ion – Possible influence on biogenic calcite formation*. Journal of Crystal Growth **352**, p151-154

Parkhurst D.L. and Appelo C.A.J. (2013) *Description of Input and Examples for Phreeqc Version 3-A Computer Program for Speciation, Batch-Reaction, One-Dimensional Transport, and Invers Geochemical Calculations*. U.S. Geological Survey, Denver, Colorado.

Parsiegla K.I. and Katz. J.L. (1999) *Calcite growth inhibition by copper(II): 1. Effect of supersaturation. Journal of Crystal Growth* **200.1-2**, p213-226

Parsiegla K.I. and Katz. J.L. (2000) *Calcite growth inhibition by copper(II): 1. Effect of solution composition. Journal of Crystal Growth* **213.3-4**, p368-380

Perez M., Dumont M. and Acevedo-Reyes D. (2008) *Implementation of classical nucleation and growth theories for precipitation.* Acta Materialia, **56** p2119-2132.

Plummer L.N. and Busenberg E. (1982) *The solubilities of calcite, aragonite and vaterite in CO_2 and H_2O solutions between 0 and 90°, and evaluation of the aqueous model for the system $CaCO_3$-CO_2-H_2O*. Geochimica et cosmochimica acta, **46** p1011-1040

Plummer L.N., Wigley T.M.L. and Parkhurst D.L. (1978) *The kinetics of calcite dissolution in CO2-water systems at 5 degrees to 60 degrees C and 0.0 to 1.0 atm CO2*. American Journal of Science **278.2**, p179-216.

Schetters M.J.A. (2013) *Grinded Dutch calcite as seeding material in the pellet softening process.* MSc Thesis. Sanitary Engineering Section, Department of Water Management TU Delft.

Spanos N. and Koutsoukos P.G. (1998) *Kinetics of Precipitation of Calcium Carbonate in Alkaline pH at Constant Supersaturation. Spontaneous and Seeded Growth.* Journal of Physical Chemistry B, **102**. P6679-6684

Stack A.G. and Grantham M.C. (2010) *Growth rate of calcite steps as a function of aqueous calcium-to-carbonate ratio: independent attachment and detachment of calcium and carbonate ions*. Crystal Growth & Design **10.3**, p1409-1413

Stumm W. and Morgan J.J. (1996) *Aquatic Chemistry, chemical equilibria and rates in natural waters*. Environmental Science and Technology, Wiley-interscience. New York, Chichester, Brisbane, Toronto and Singapore.

Takasaki S., Parsiegla K.I. and Katz J.L. (1994) Calcite growth and the inhibiting effect of iron(III). Journal of Crystal Growth **143.3**, 2610268

Tegethoff F.W., Rohleder J. and Kroker E. (2001) *Calcium Carbonate, From the Cretaceous Period into the 21st Century.* Birkhäuser Verlag. Basel, Boston, Berlin

Van Weert F., Van der Gun J. and Reckman J. (2009) *Global overview of saline groundwater occurrence and genesis.* International Groundwater Resources Assessment Centre.

Vehkamäki H. (2006) *Classical nucleation theory in multicomponent systems*. Springer Science & Business Media

Verberk J.Q.J.C., Van der Meer W.G.J., Van der Hoek J.P., Heijman S.G.J., De Ridder D. , Grefte A., and Andeweg P. (2011). *Drinking water treatment*. Delft University of Technology, Faculty of Civil engineering and Geosciences, Sanitary Engineering Department.

WHO (2011) *Guidelines for Drinking- water Quality*. Fourth Edition. World Health Organization Press, Geneva.

Wolthers M., Nehrke G., Gustafsson J. P. and Van Cappellen P. (2012) *Calcite growth kinetics: Modeling the effect of solution stoichiometry*. Geochimica et Cosmochimica Acta **77**, p121-134.

Zhang Y. and Dawe R.A. (2000) *Influence of Mg2+ on the kintetics of calcite precipitation and calcite crystal morphology*. Chemical Geology **163.1-4**, p129-138

Zhong S. and Mucci A. (1989) *Calcite and aragonite precipitation from seawater solutions of various salinities: Precipitation rates and overgrowth compositions.* Chemical Geology **78.3**, p283-299.

APPENDIX A – RESULTS OF COLUMN EXPERIMENTS

In total, six column experiments have been done. The results are shown below in figures, all with similar y-axis. The results of the green column are shown in green and the results of the blue column are shown in blue. The position of the pressure sensors can vary per experiment. The height of the pressure sensor is shown in the title of every pressure graph. The saturation indexes are calculated with Phreeqc.

6.1 EXPERIMENT 1

For experiment 1, there was no pressure sensor connected to the influent. The first pressure sensor was placed at about 15cm from the top of both columns. Also, there was no tap in place to take influent samples. The theoretical influent concentration of calcium based on the dosage of calcium chloride is shown instead.

6.1.1 Results green column

Influent stream 1 contains 12.8mmol/l $CaCl_2$. Influent stream 2 contains 27mmol/l $NaHCO_3$ and has a pH of 7.55. As calculated with Phreeqc, after mixing, the SI of the influent is 1.1 and the pH is 7.5. The pump setting was 20rpm, which resulted in an average flow through the column of 39.2cm/h. The porosity is 0.41.

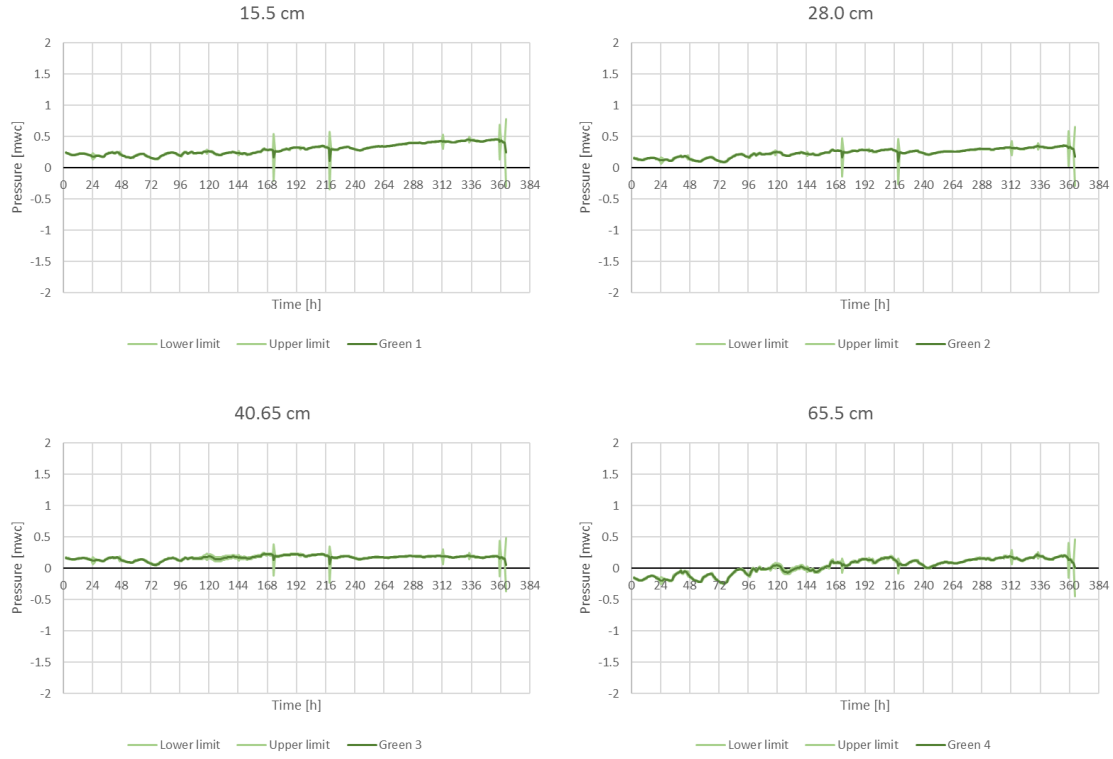

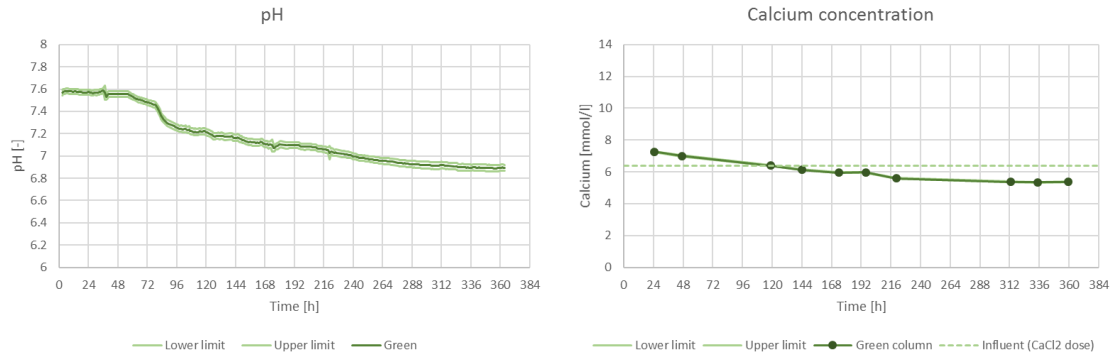

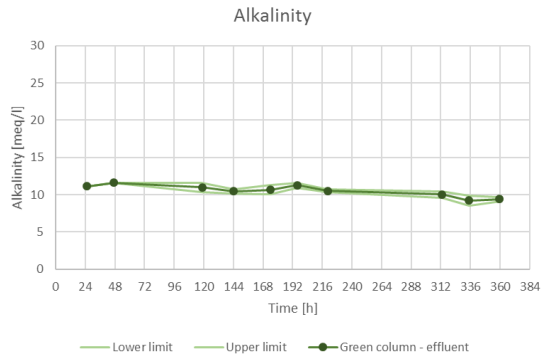

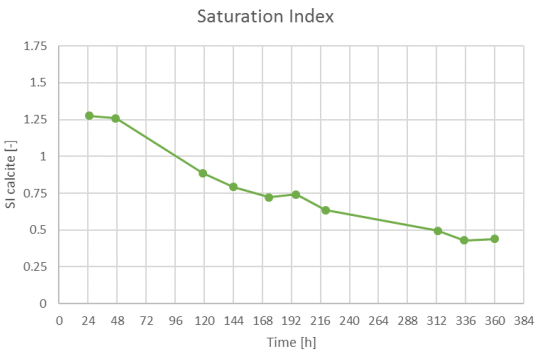

6.1.2 Results blue column

The blue column has the same influent as the green column. Influent stream 1 contains 12.8mmol/l $CaCl_2$. Influent stream 2 contains 27mmol/l $NaHCO_3$ and has a pH of 7.55. As calculated with Phreeqc, after mixing, the SI of the influent is 1.1 and the pH is 7.5. The pump setting was 20rpm, which resulted in an average flow through the column of 36.9cm/h. The porosity is 0.40.

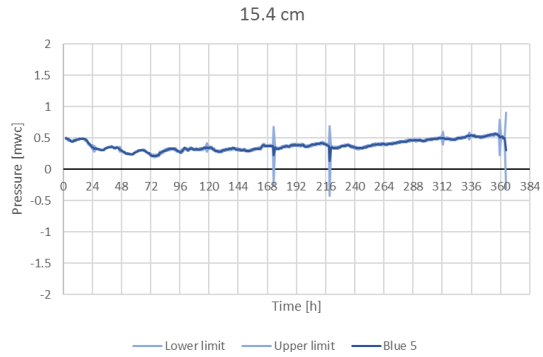

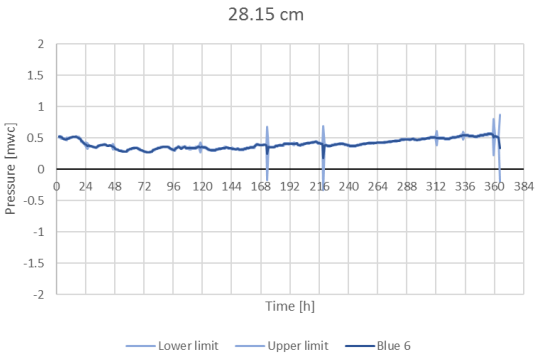

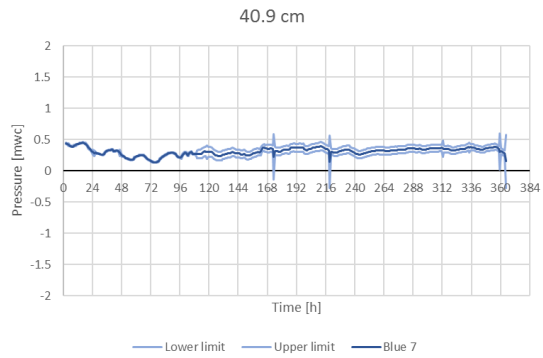

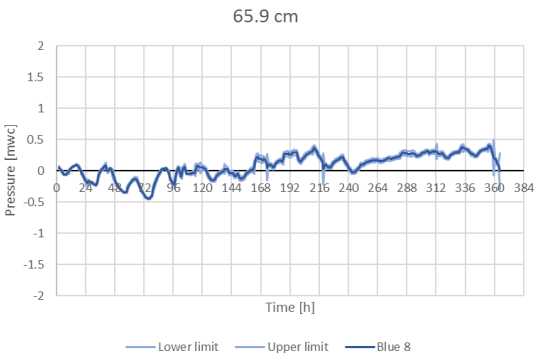

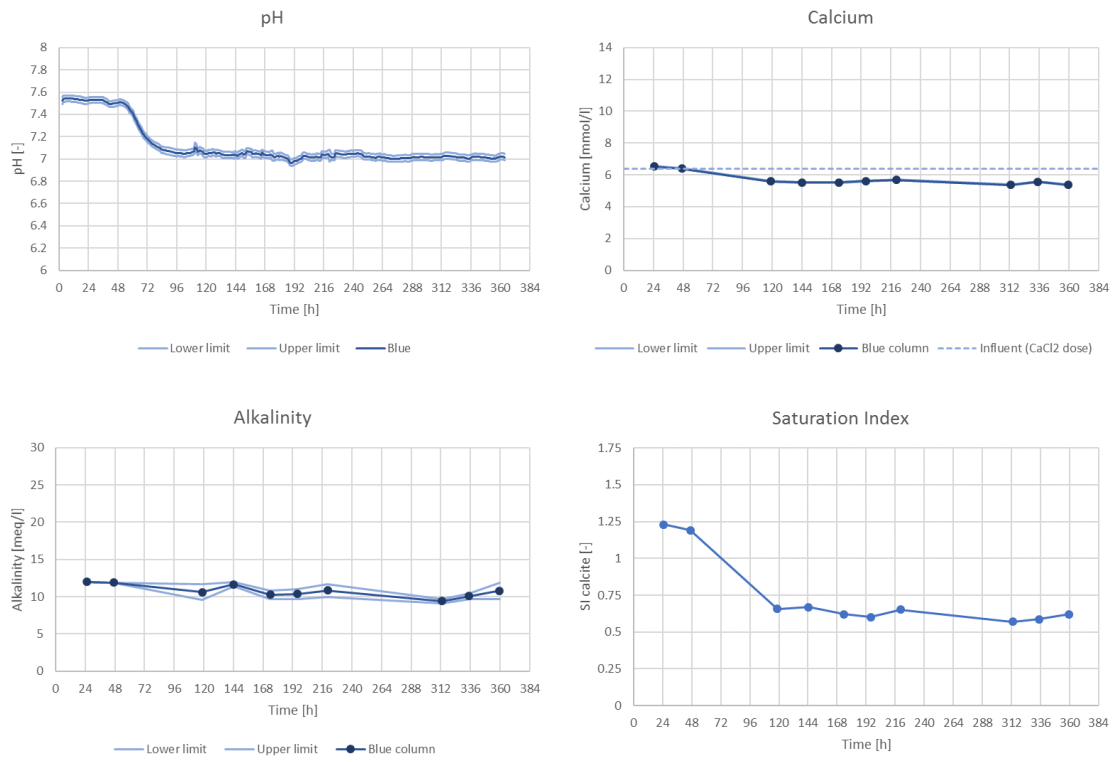

6.1.3 Pictures

Precipitation took place in the first centimetres of both columns. The pictures below show the top of the column with the precipitated calcium carbonate binding the sand. From left to right: the column still filled with sand; the empty column with the cemented sand, the top view of the cemented sand.

The green column:



The blue column:



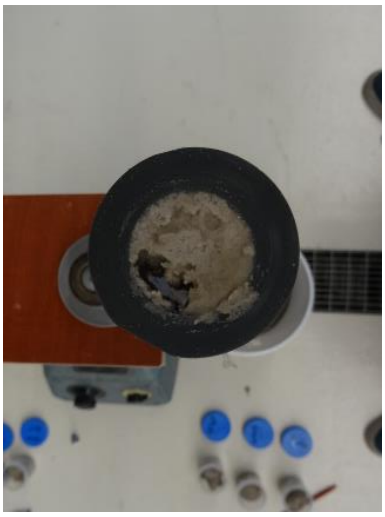

6.2 EXPERIMENT 2

During experiment 1, calcium carbonate had precipitated before the first pressure sensor. Also, the influent was not sampled. This was changed by adding those connections to the influent of the column. A continuous pattern could be observed in every pressure sensor. Therefore, after a few days, a temperature sensor (LM60) was used to measure and continuously monitor the local temperature of the lab.

6.2.1 Green column

The same concentrations are used for experiment 2 as for experiment 2. Influent stream 1 contains 12.8mmol/l $CaCl_2$. Influent stream 2 contains 27mmol/l $NaHCO_3$ and has a pH of 7.55. As calculated with Phreeqc, after mixing, the SI of the influent is 1.1 and the pH is 7.5. The average flow through the column is half the flow during experiment 1 and is 20.4 cm/h – the pump setting was 10rpm. The porosity is 0.42.

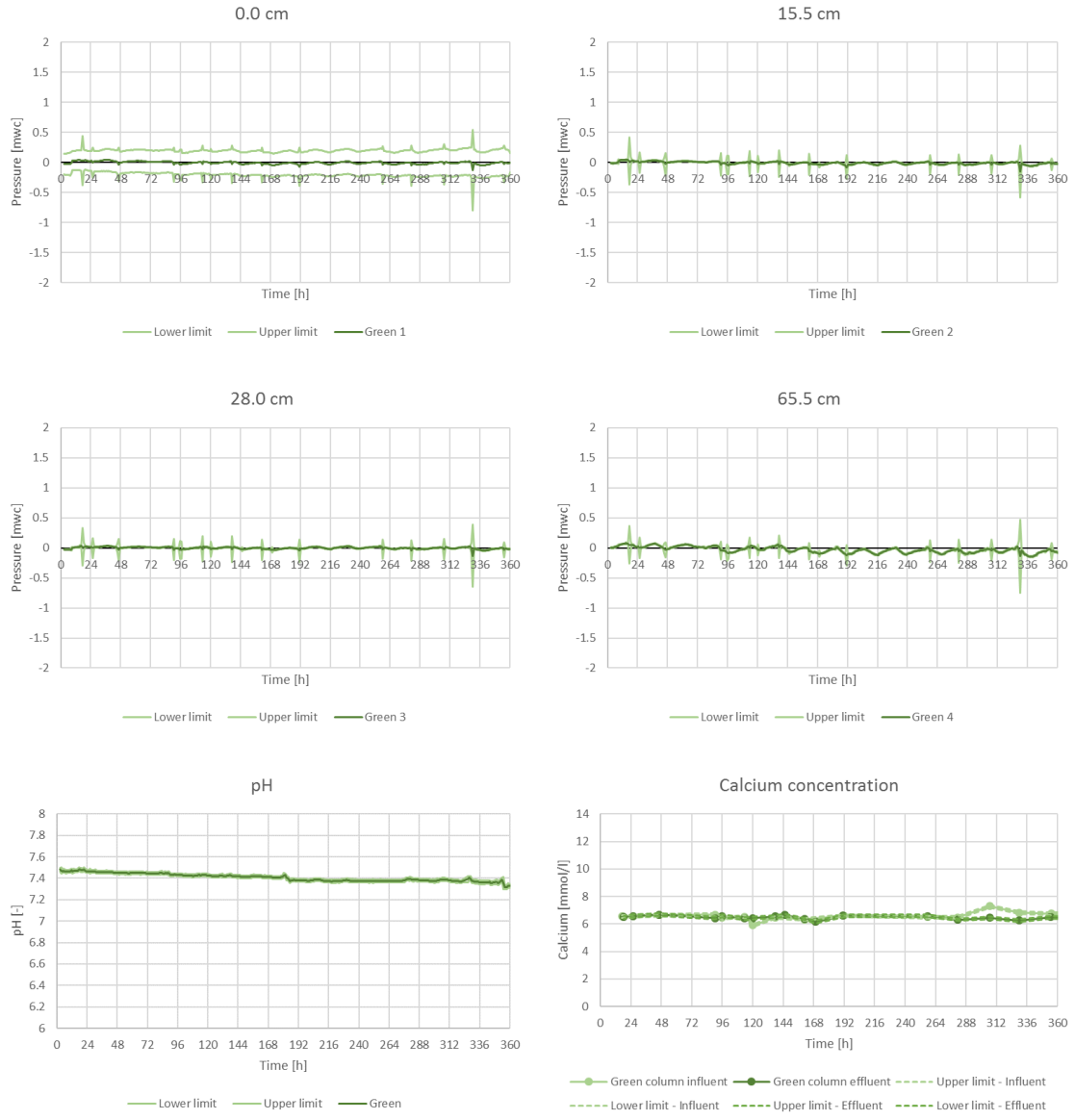

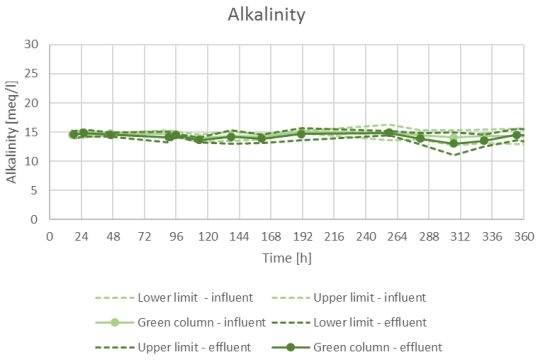
Alkalinity
Alkalinity [meq/l]
Time [h]
Lower limit - influent
Upper limit - influent
Green column - influent
Lower limit - effluent
Upper limit - effluent
Green column - effluent

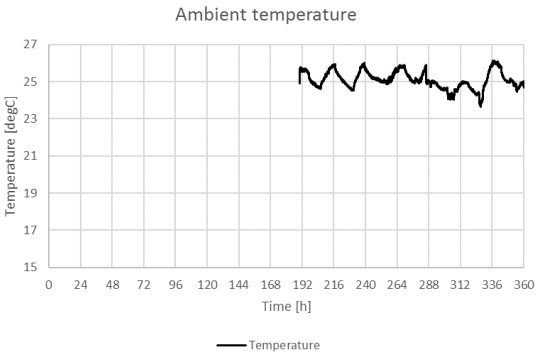
Ambient temperature
Temperature [degC]
Time [h]
Temperature

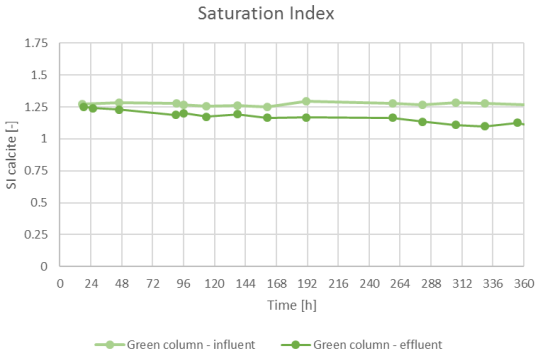
Saturation Index
SI calcite [-]
Time [h]
Green column - influent
Green column - effluent

6.2.2 Blue column

The blue column is similar to the green column and has therefore the same concentrations. Influent stream 1 contains 12.8mmol/l $CaCl_2$. Influent stream 2 contains 27mmol/l $NaHCO_3$ and has a pH of 7.55. As calculated with Phreeqc, after mixing, the SI of the influent is 1.1 and the pH is 7.5. The average flow through the column is half the flow during experiment 1 and is 19.8 cm/h – the pump setting was 10rpm. The porosity is 0.42.

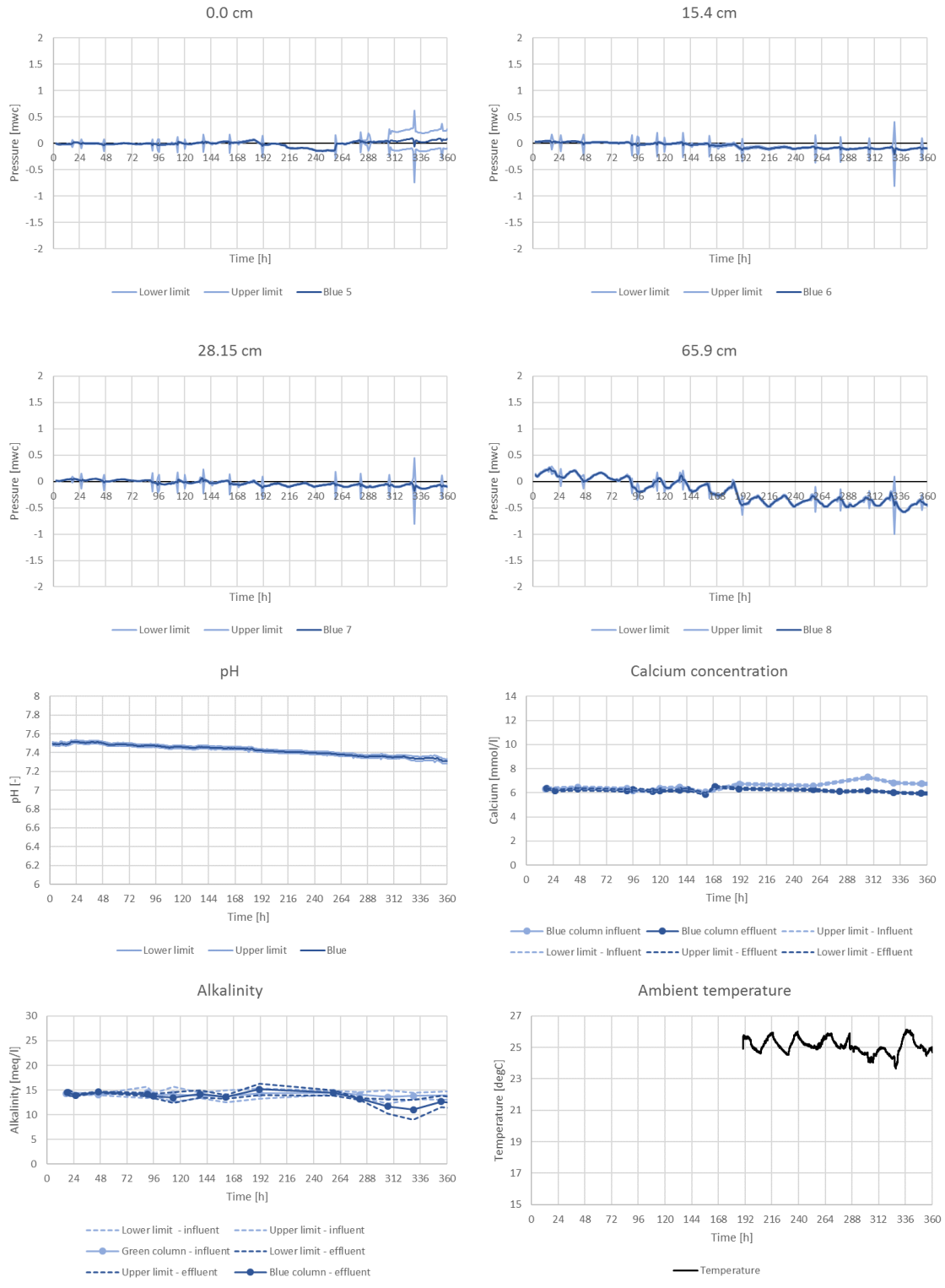

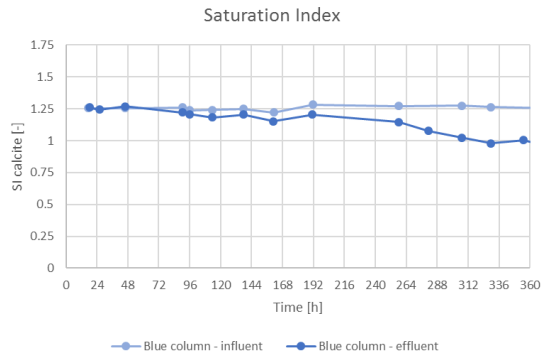

6.2.3 Pictures

No cementation took place between the grains in both columns. However, cementation did occur on the tips of the pressure needles inside the column. This precipitation progressed in the direction of the flow, creating a small stalactite. This happened on the needles at positions II-V in the green column and positions II and III in the blue column.

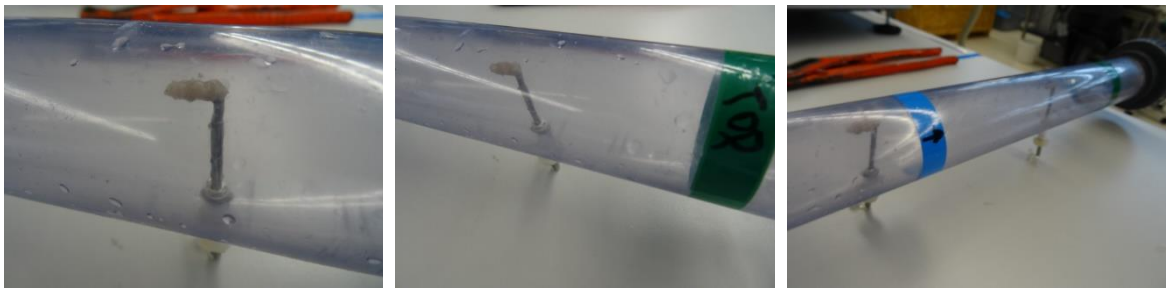

6.3 EXPERIMENT 3

Since no calcium carbonate has clogged the bed during a period of over two weeks, the saturation indexes of experiment 3 has been increased. No changes have been made to the setup.

6.3.1 Green column

Influent stream 1 contains 23.04mmol/l $CaCl_2$. Influent stream 2 contains 48.6mmol/l $NaHCO_3$ and has a pH of 7.58. As calculated with Phreeqc, after mixing, the SI of the influent is 1.55 and the pH is 7.5. The average flow through the column was 13.7 cm/h at a pump setting of 10rpm. The porosity is 0.41.

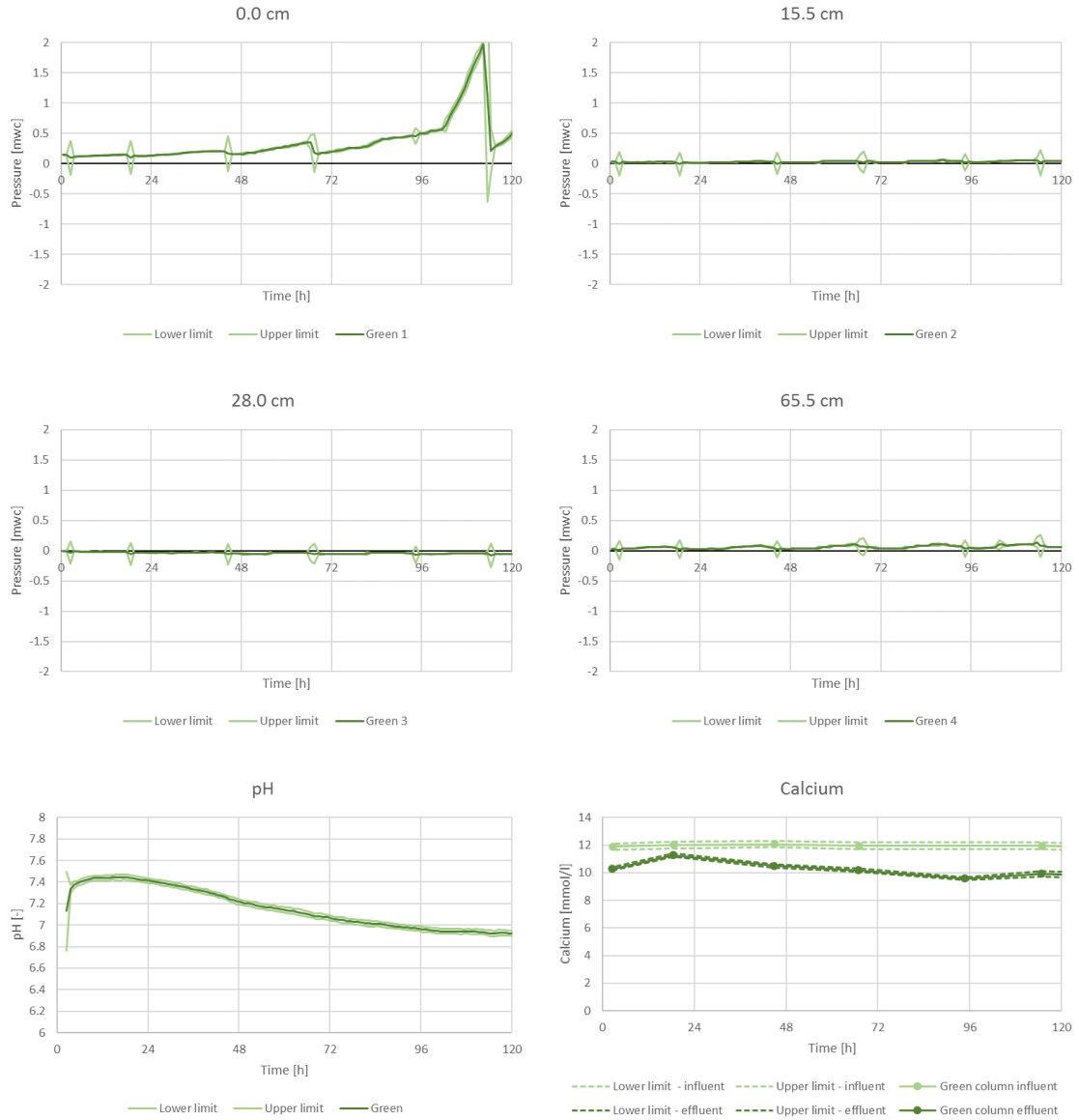

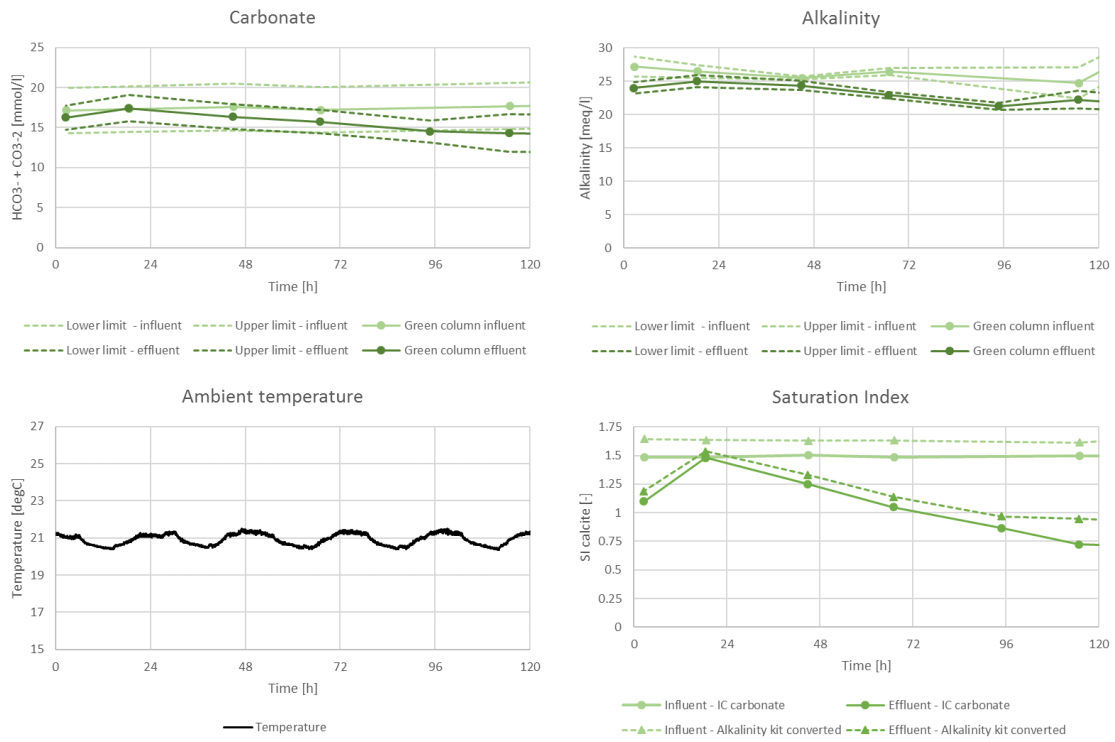

6.3.2 Blue column

Again, the same concentrations are used for the blue column as for the green column. Influent stream 1 contains 23.04mmol/l $CaCl_2$. Influent stream 2 contains 48.6mmol/l $NaHCO_3$ and has a pH of 7.58. As calculated with Phreeqc, after mixing, the SI of the influent is 1.55 and the pH is 7.5. The average flow through the column was 12.3 cm/h at a pump setting of 10rpm. The porosity is 0.40.

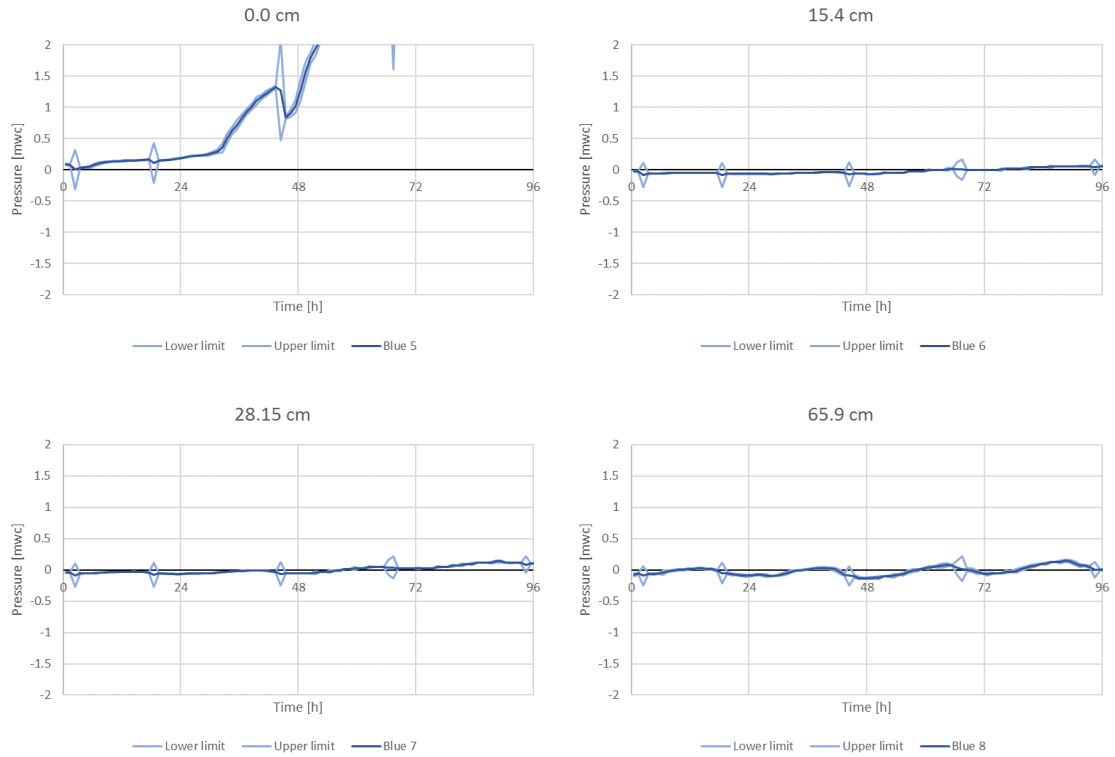

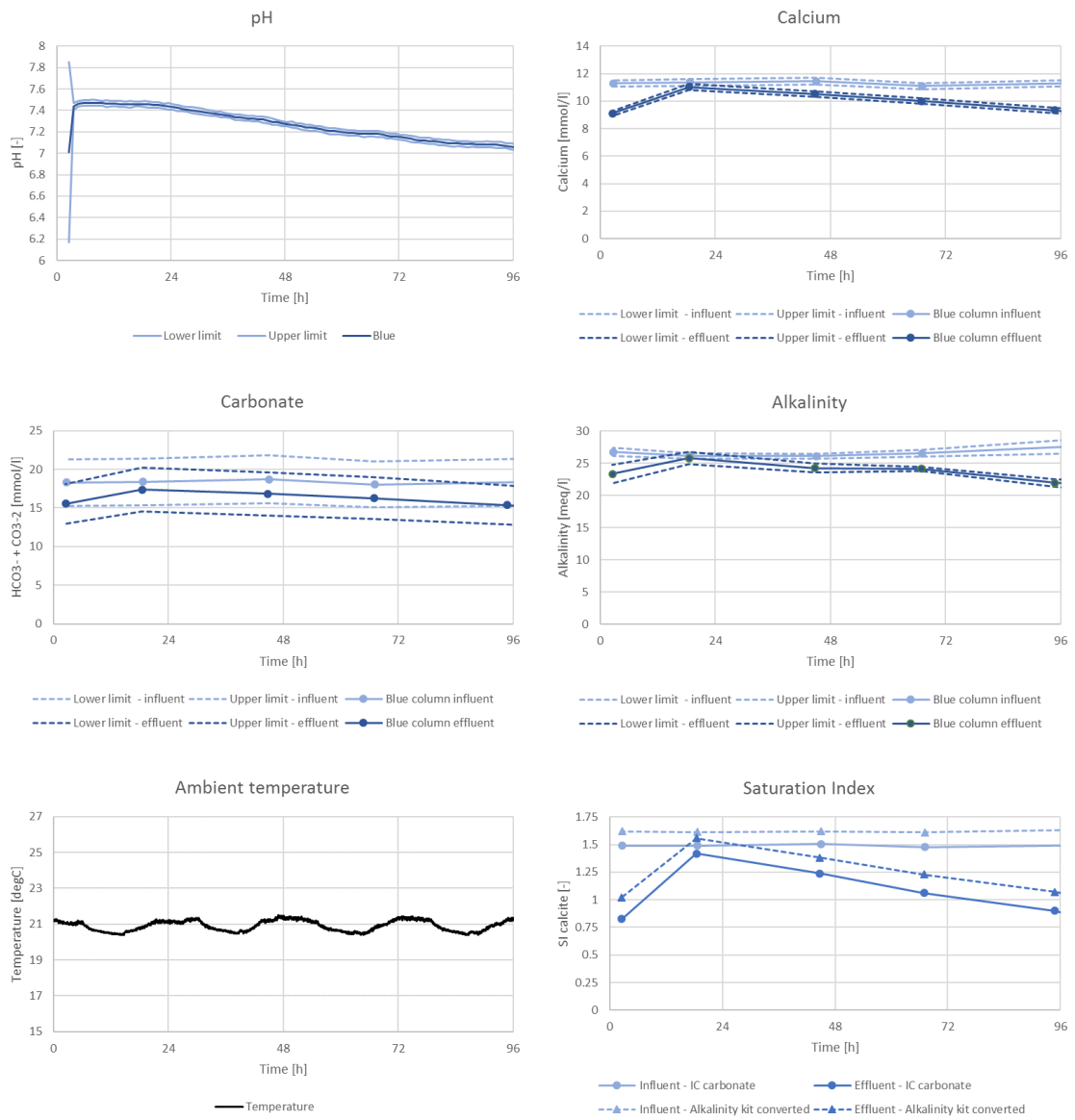

6.3.3 Pictures

Cementation occurred at the top of both columns. The two pictures below show the green column (left) and the blue column (right).

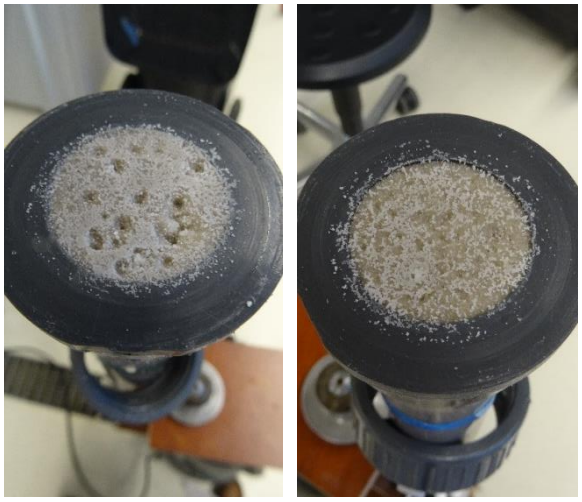

6.4 EXPERIMENT 4

Experiment 4 and 5 were used to validate experiment 1 and 2 and to test the effect of an SI between those of experiments 1 and 2 (SI = 1.1) and experiment 3 (SI = 1.5). Hence, the influent of the blue column and the green column are different for both experiments. Also, half the volume of the influent and effluent samples was filtered and compared to the unfiltered unfiltered half to check for nuclei. Those comparisons are also shown in graphs for both calcium and carbonate.

Also, for the calculations of the influent, Phreeqc was used in combination with python. With python, balancing the ratio of calcium and carbonate and the pH and SI was improved. Since experiment 4, the amount of moles of $CaCl_2$ is exactly half the amount of $NaHCO_3$.

6.4.1 Green column

The influent of the green column was aimed to be between the first two experiments and experiment 3. Influent stream 1 contains 16.45mmol/l $CaCl_2$. Influent stream 2 contains 32.9mmol/l $NaHCO_3$ and has a pH of 7.57. As calculated with Phreeqc, after mixing, the SI of the influent is 1.3 and the pH is 7.5. The average flow through the column is 16.7 cm/h with the pump set at 10rpm. The porosity is 0.40.

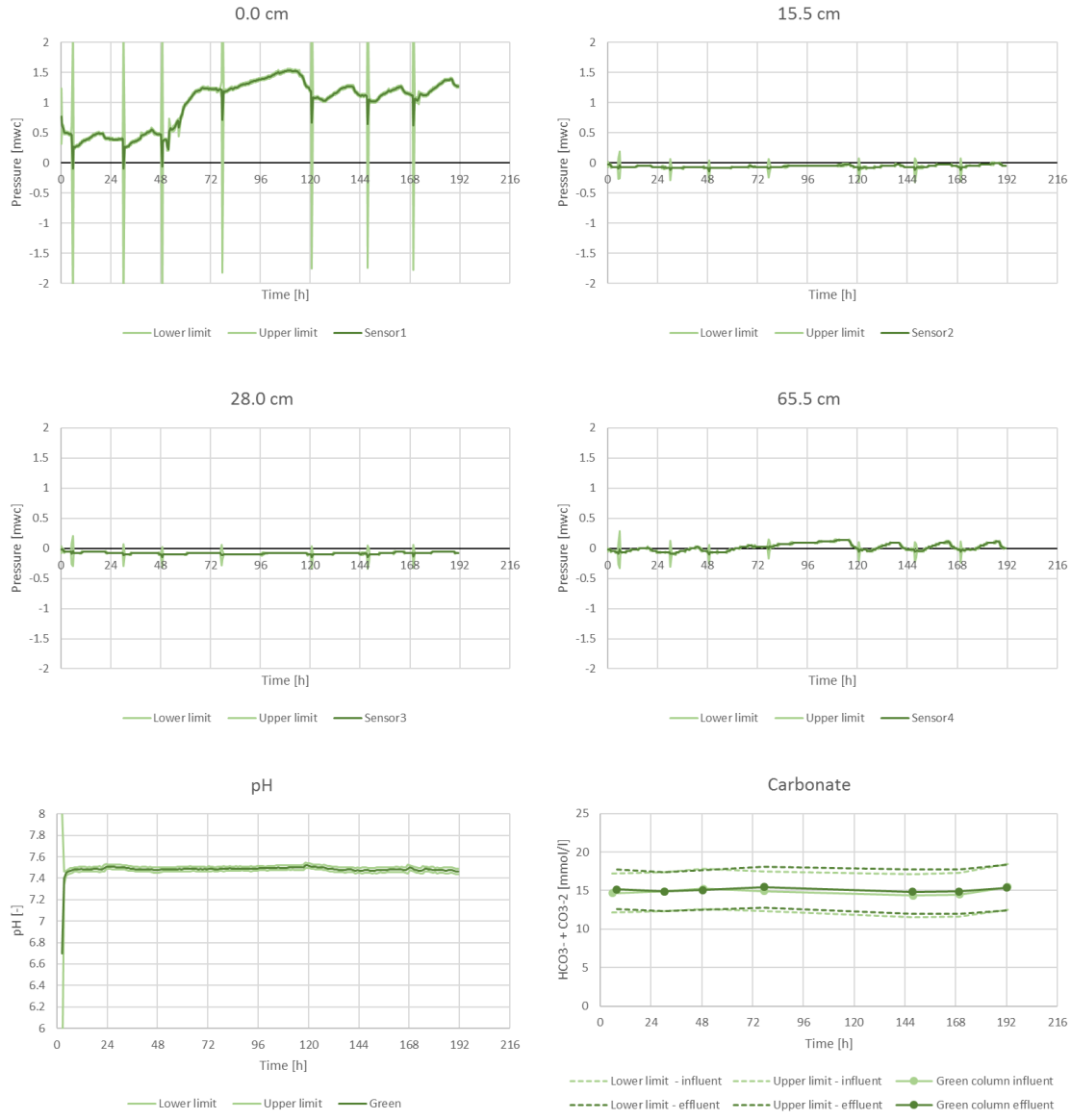

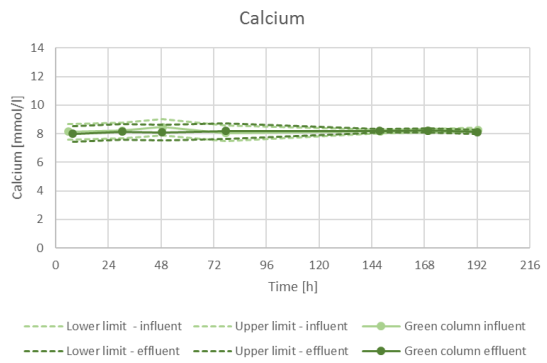

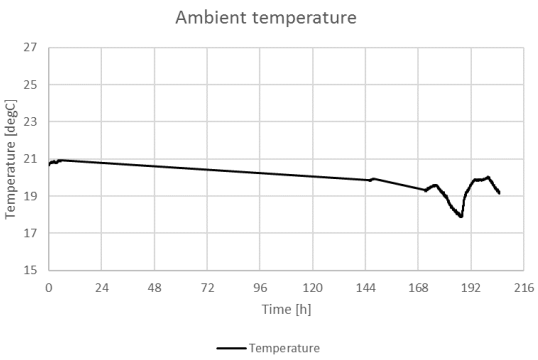

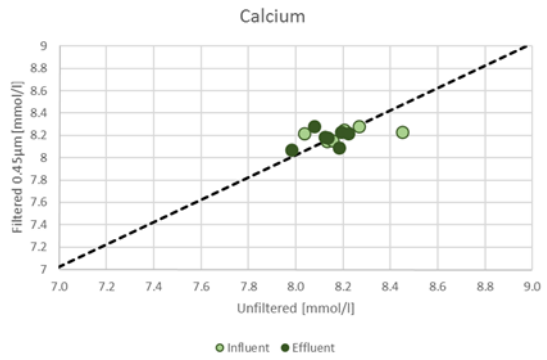

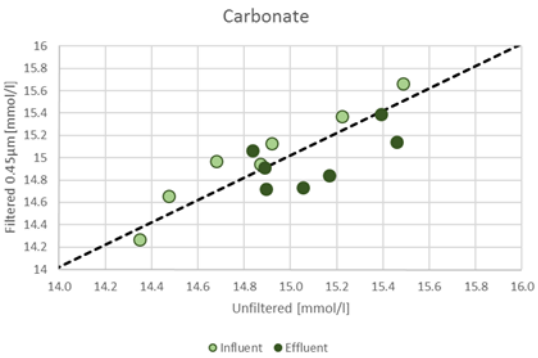

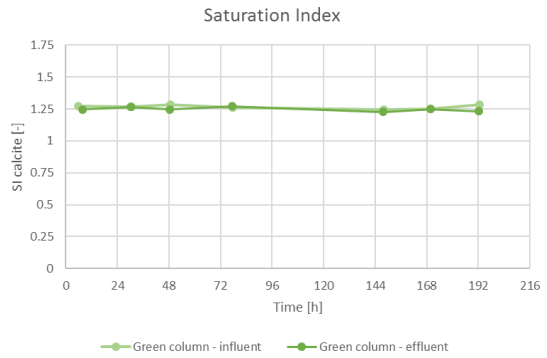

6.4.2 Blue column

The blue column was used to validate experiment 1 and 2, and therefore has the same influent characteristics, other than that it was calculated with Phreeqc and python. Influent stream 1 contains 11.55mmol/l $CaCl_2$. Influent stream 2 contains 23.1mmol/l $NaHCO_3$ and has a pH of 7.55. As calculated with Phreeqc, after mixing, the SI of the influent is 1.1 and the pH is 7.5. The average flow through the column was 14.9 cm/h with the pump set at 10rpm. The porosity is 0.40.

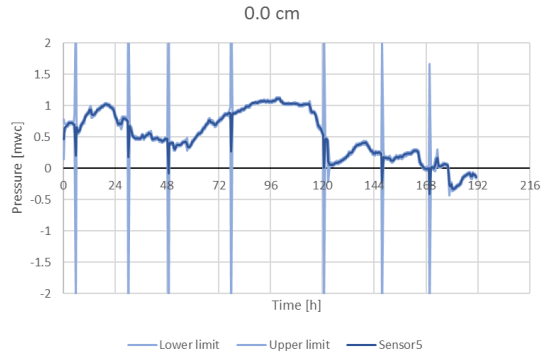

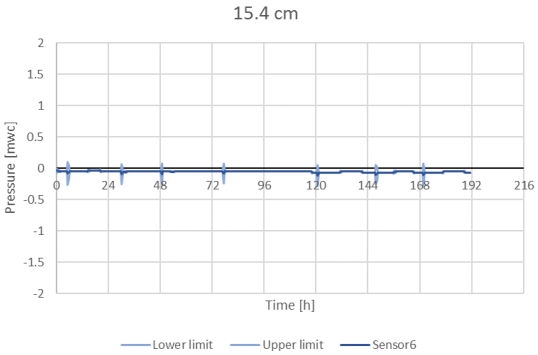

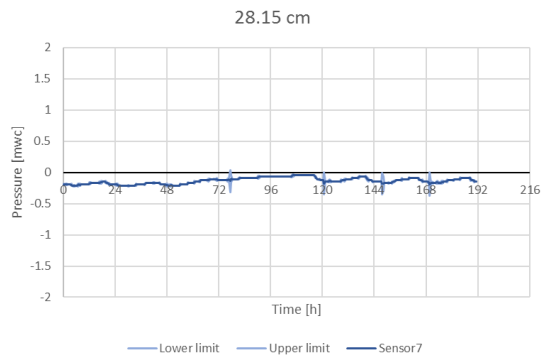
28.15 cm
Pressure [mwc]
Time [h]
Lower limit
Upper limit
Sensor7

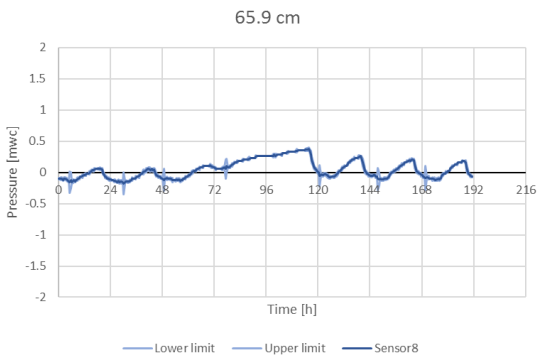
65.9 cm
Pressure [mwc]
Time [h]
Lower limit
Upper limit
Sensor8

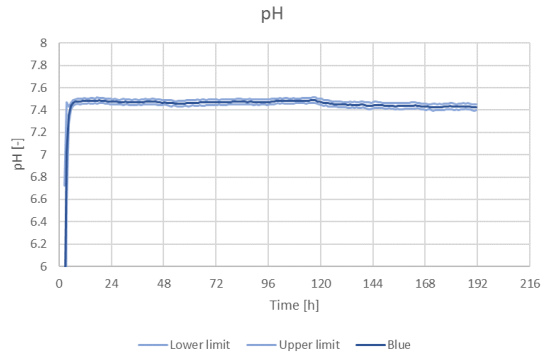
pH
pH [-]
Time [h]
Lower limit
Upper limit
Blue

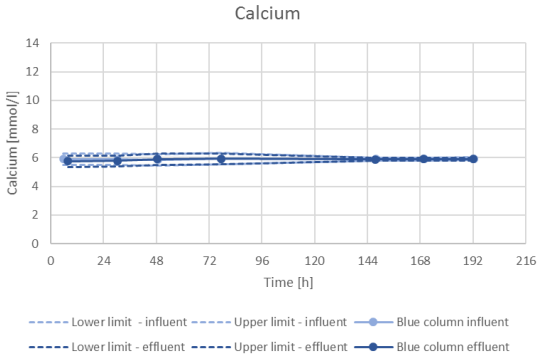
Calcium
Calcium [mmol/l]
Time [h]
Lower limit - influent
Upper limit - influent
Blue column influent
Lower limit - effluent
Upper limit - effluent
Blue column effluent

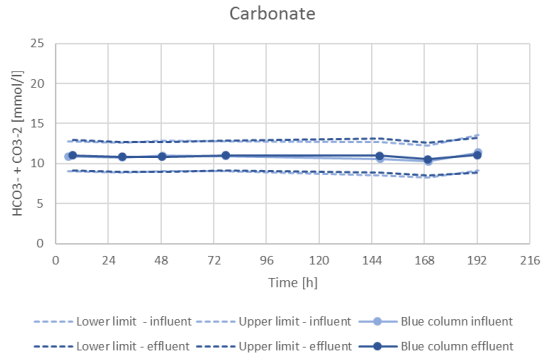
Carbonate
HCO3- + CO3-2 [mmol/l]
Time [h]
Lower limit - influent
Upper limit - influent
Blue column influent
Lower limit - effluent
Upper limit - effluent
Blue column effluent

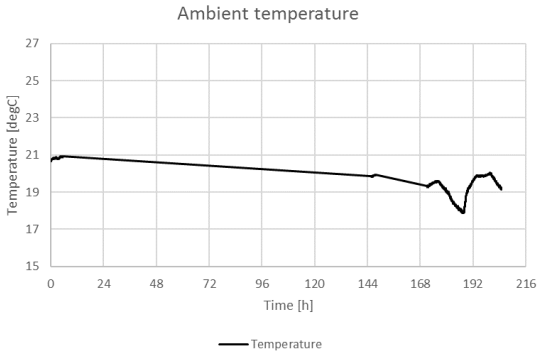
Ambient temperature
Temperature [degC]
Time [h]
Temperature

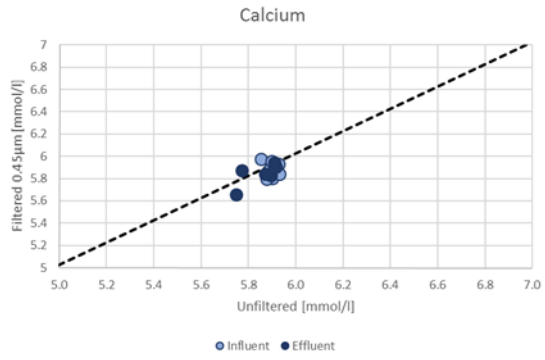
Calcium
Filtered 0.45µm [mmol/l]
Unfiltered [mmol/l]
Influent
Effluent

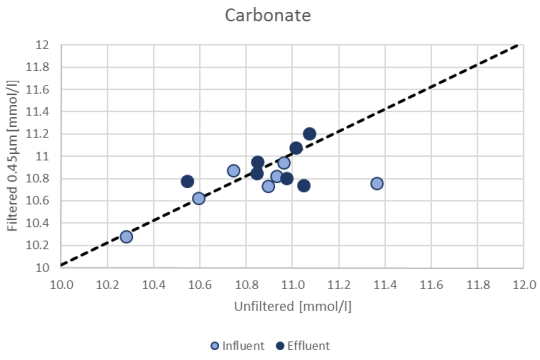
Carbonate
Filtered 0.45µm [mmol/l]
Unfiltered [mmol/l]
Influent
Effluent

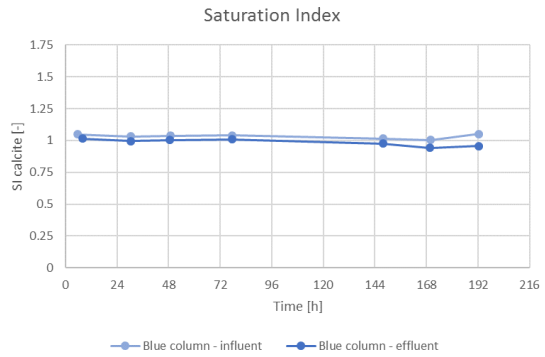

6.4.3 Pictures

The column hasn't been opened after experiment 4. Therefore, no pictures could be taken.

6.5 EXPERIMENT 5

Experiment 5 is used together with experiment 4 to validate experiment 1 and 2 and to test the effect of an intermediate SI. Since there was no direct evidence of precipitation in the column, the sand in the column wasn't replaced. Instead, the columns were flushed with demiwater. The difference between experiment 1 and 2 was the flow. For experiment 5 the flow of experiment 4 was doubled.

6.5.1 Green column

The influent concentrations of the green column are the same as for experiment 5. Influent stream 1 contains 16.45mmol/l $CaCl_2$. Influent stream 2 contains 32.9mmol/l $NaHCO_3$ and has a pH of 7.57. As calculated with Phreeqc, after mixing, the SI of the influent is 1.3 and the pH is 7.5. The average flow through the column was 33.7 cm/h with the pump set at 20rpm. The porosity is 0.40.

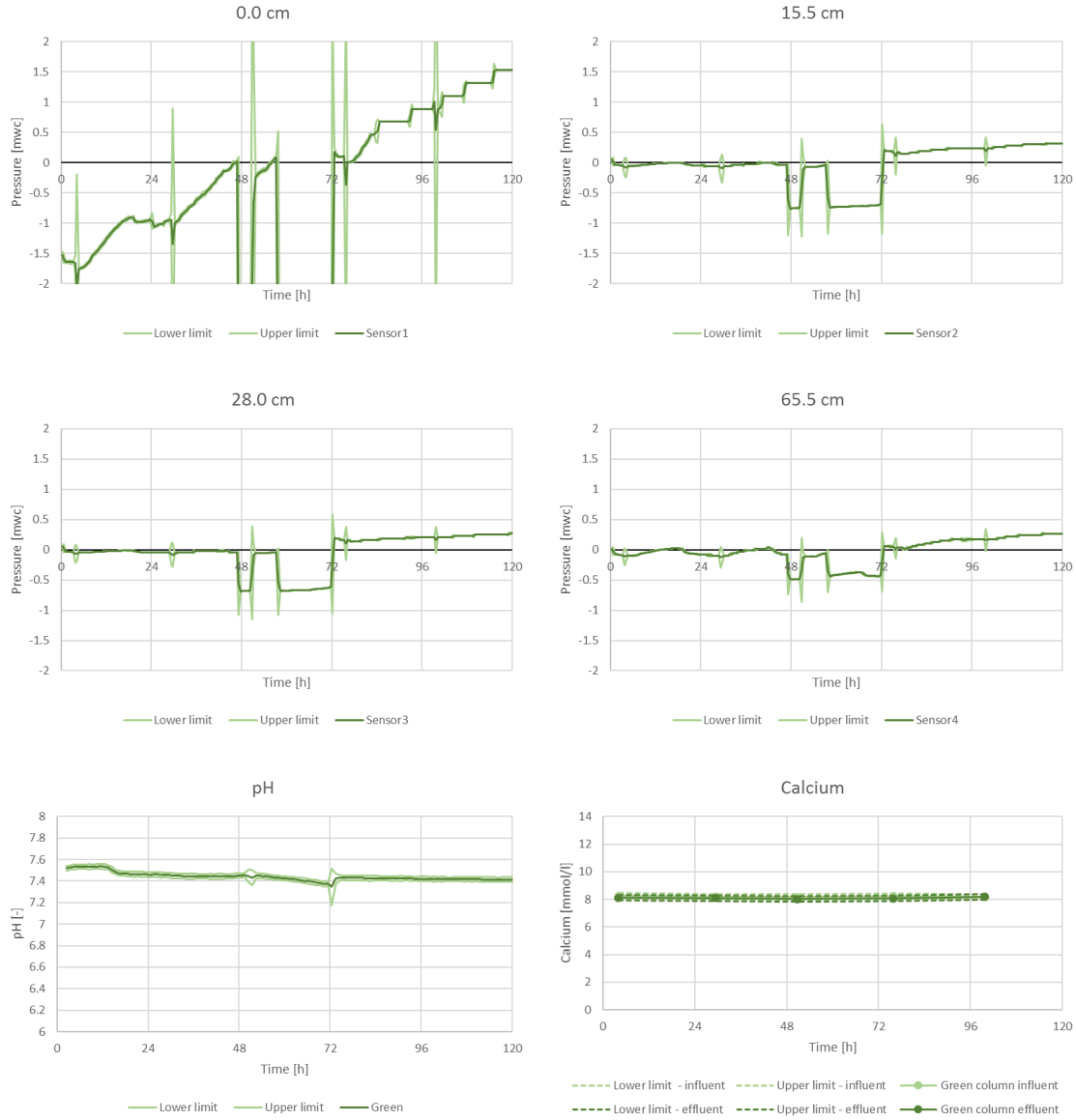

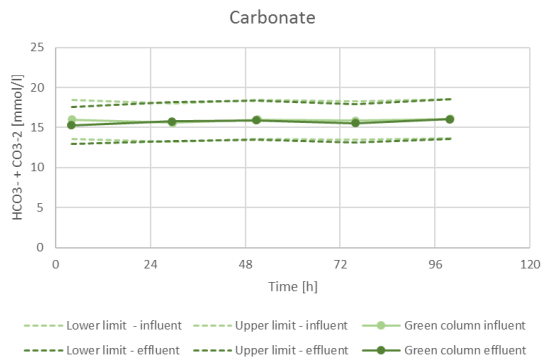

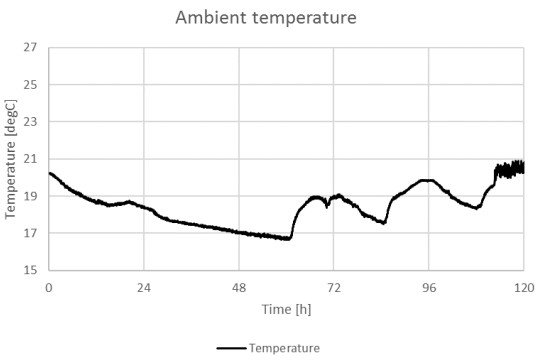

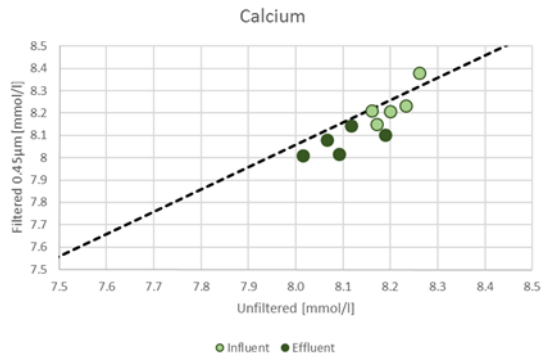

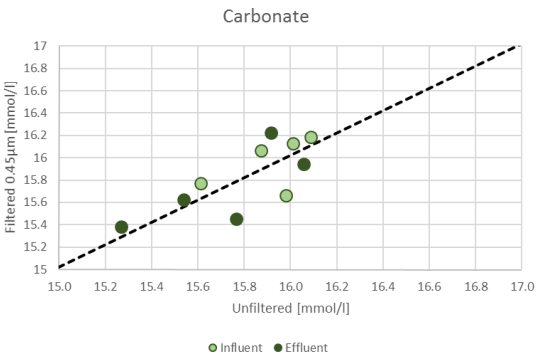

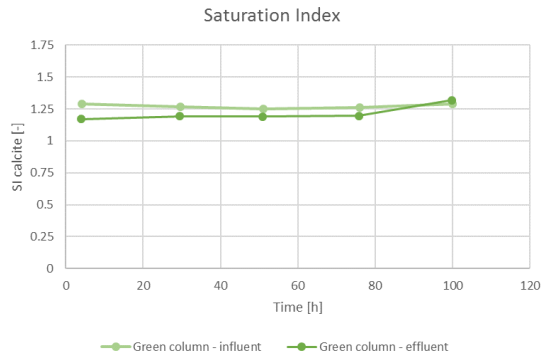

6.5.2 Blue column

Influent stream 1 contains 11.55mmol/l $CaCl_2$. Influent stream 2 contains 23.1mmol/l $NaHCO_3$ and has a pH of 7.57. As calculated with Phreeqc, after mixing, the SI of the influent is 1.1 and the pH is 7.5. The average flow through the column is 31.8 cm/h with the pump set at 20rpm. The porosity is 0.40.

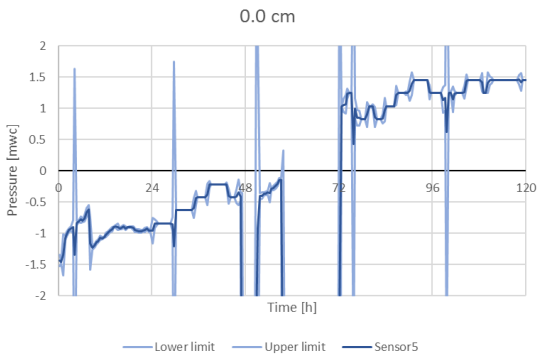

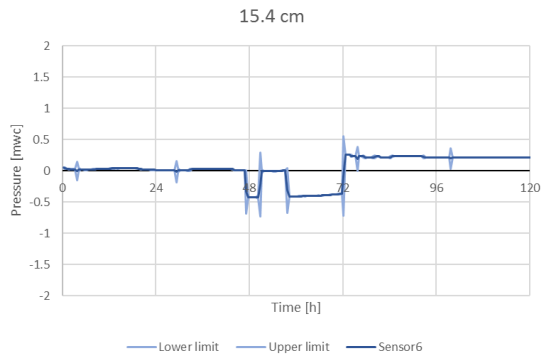

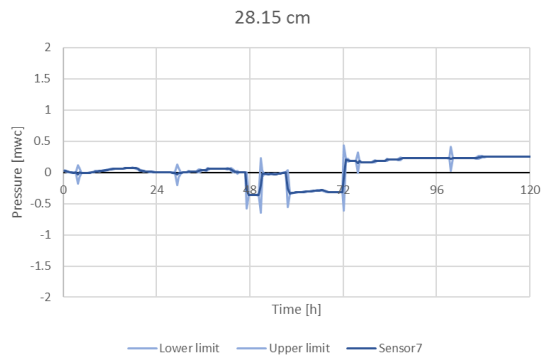
28.15 cm
Pressure [mwc]
Time [h]
Lower limit
Upper limit
Sensor7

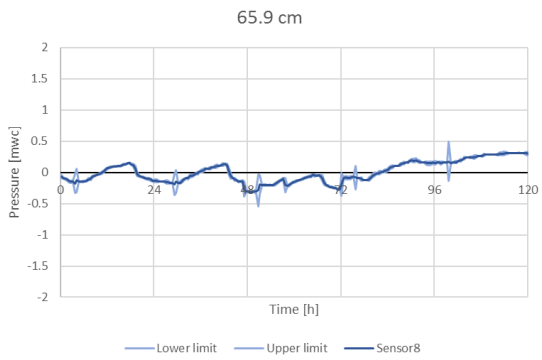
65.9 cm
Pressure [mwc]
Time [h]
Lower limit
Upper limit
Sensor8

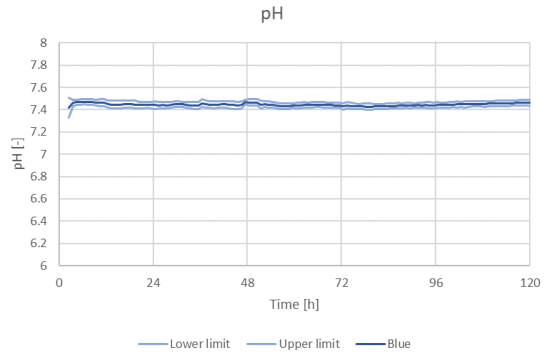
pH
pH [-]
Time [h]
Lower limit
Upper limit
Blue

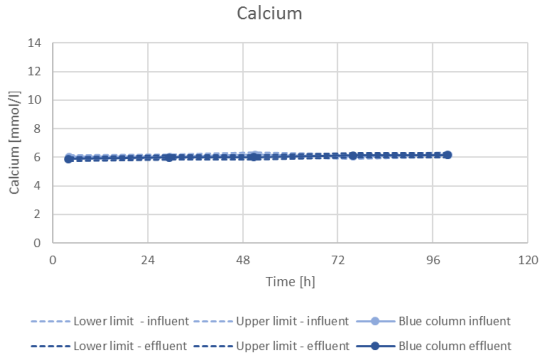
Calcium
Calcium [mmol/l]
Time [h]
Lower limit - influent
Upper limit - influent
Blue column influent
Lower limit - effluent
Upper limit - effluent
Blue column effluent

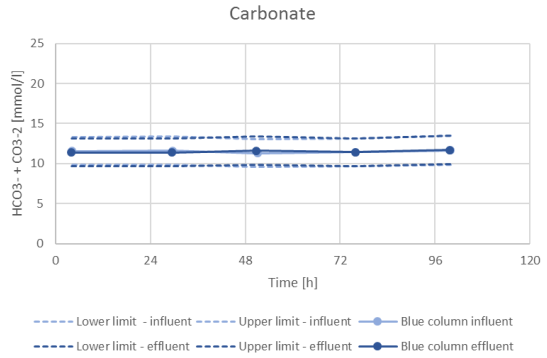
Carbonate
HCO3- + CO3-2 [mmol/l]
Time [h]
Lower limit - influent
Upper limit - influent
Blue column influent
Lower limit - effluent
Upper limit - effluent
Blue column effluent

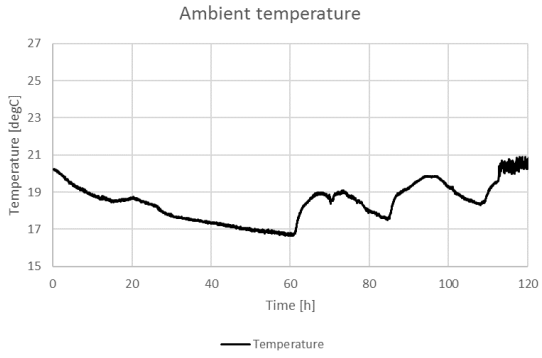
Ambient temperature
Temperature [degC]
Time [h]
Temperature

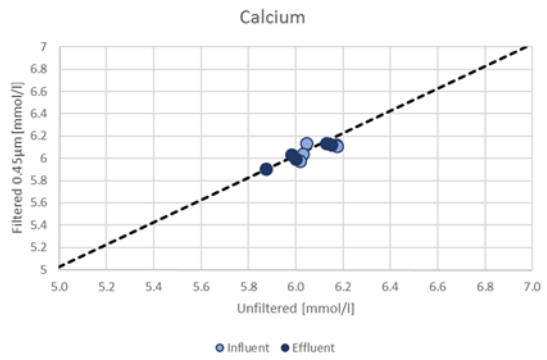
Calcium
Filtered 0.45µm [mmol/l]
Unfiltered [mmol/l]
Influent
Effluent

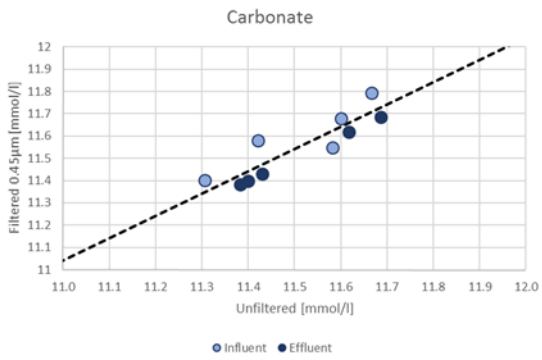
Carbonate
Filtered 0.45µm [mmol/l]
Unfiltered [mmol/l]
Influent
Effluent

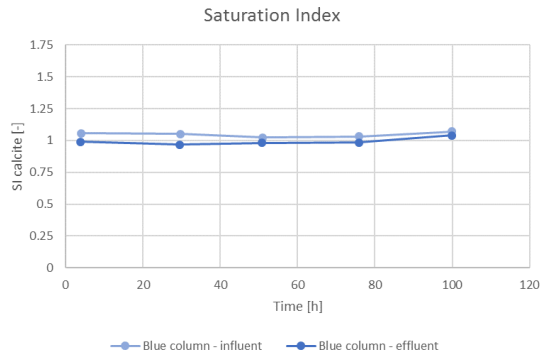

6.5.3 Pictures

No cementation has occurred during experiment 4 and 5. The picture shows a small amount of solid calcium carbonate that has precipitated on the tip of the needle of the blue column (location II).

6.6 EXPERIMENT 6

Experiment 6 was used to test the effect of the presence of limestone on the precipitation of calcium carbonate. One gram of calcium carbonate grains was added per kg of sand.

6.6.1 Green column

The influent of the green column was similar to experiment 4 and 5. Influent stream 1 contains 16.45mmol/l $CaCl_2$. Influent stream 2 contains 32.9mmol/l $NaHCO_3$ and has a pH of 7.57. As calculated with Phreeqc, after mixing, the SI of the influent is 1.3 and the pH is 7.5. The average flow through the column was 18.6 cm/h with the pump set at 10rpm. The porosity is 0.39.

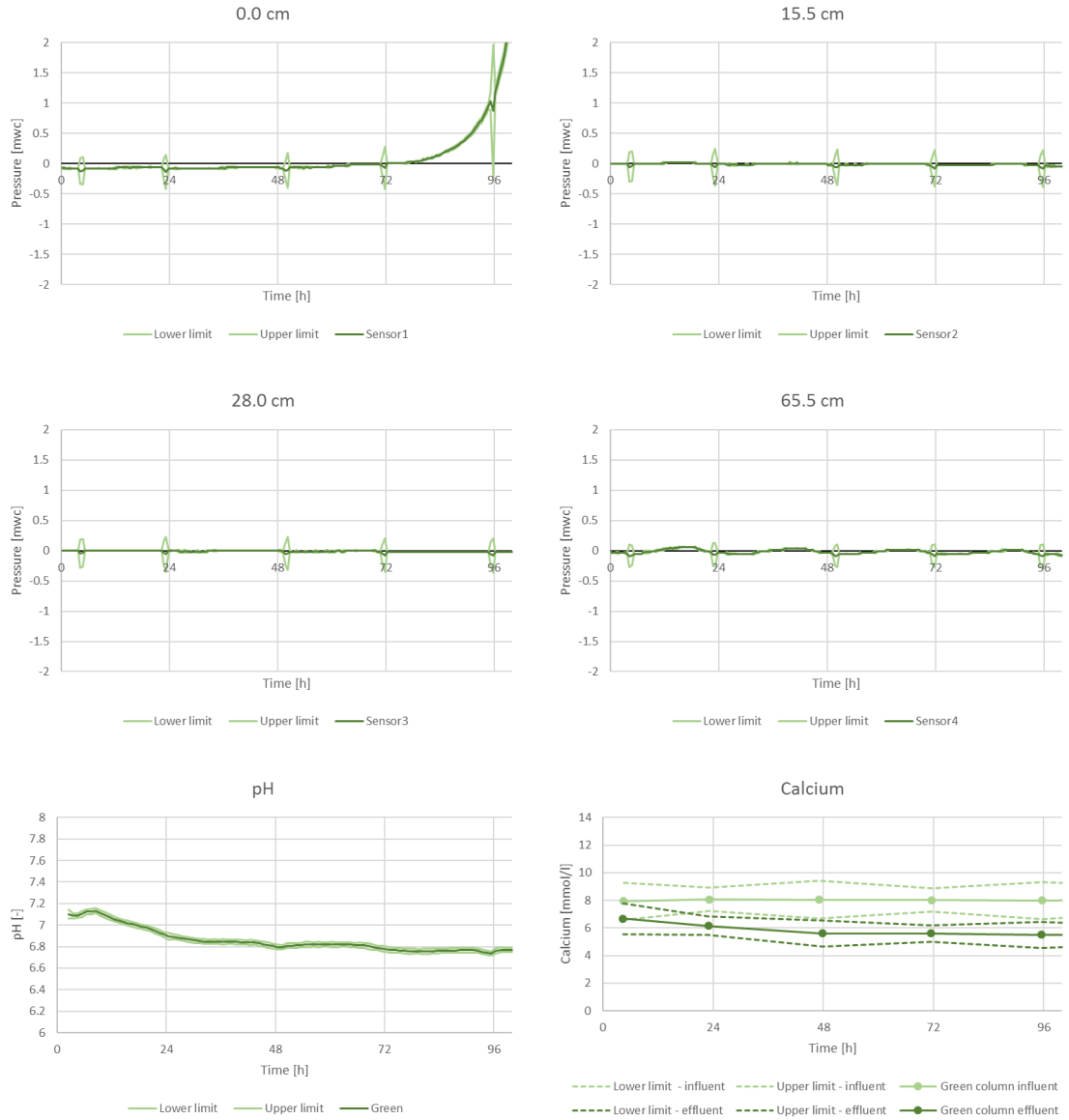

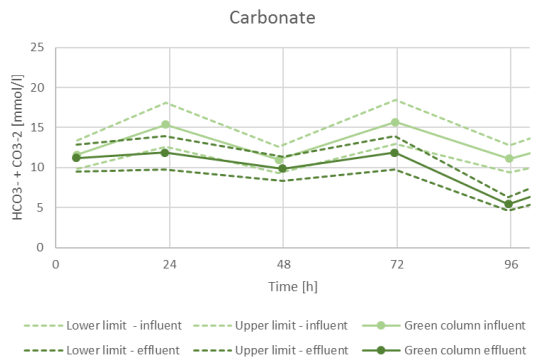

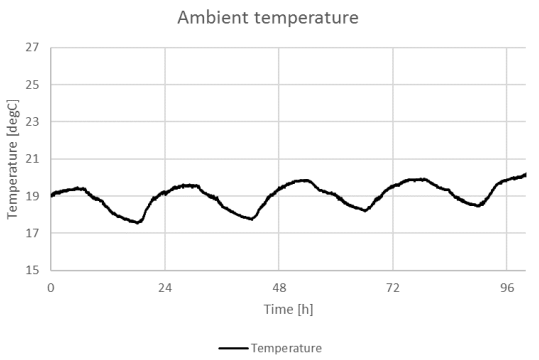

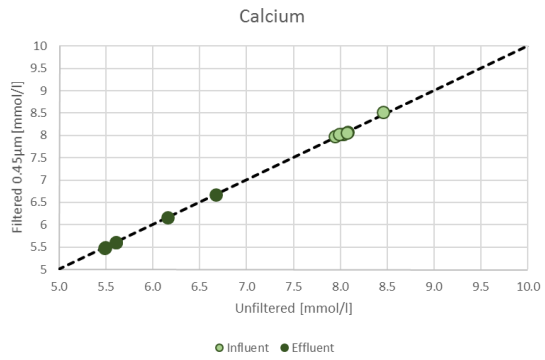

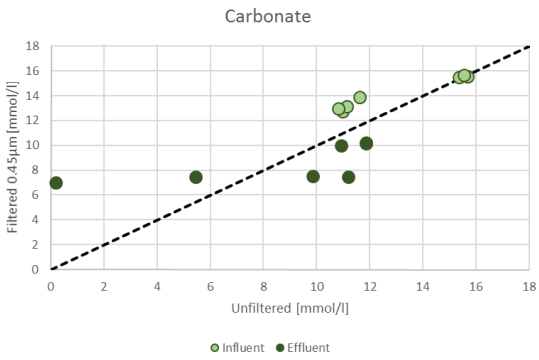

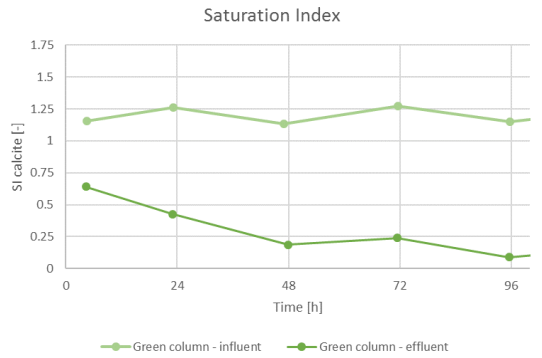

6.6.2 Blue column

Influent stream 1 contains 11.55mmol/l $CaCl_2$. Influent stream 2 contains 23.1mmol/l $NaHCO_3$ and has a pH of 7.57. As calculated with Phreeqc, after mixing, the SI of the influent is 1.1 and the pH is 7.5. The average flow through the column was 20.2 cm/h with the pump set at 10rpm. The porosity is 0.38.

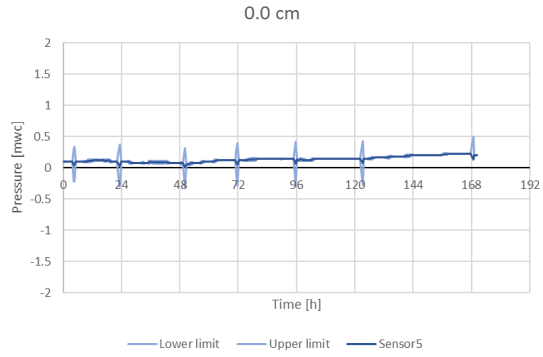

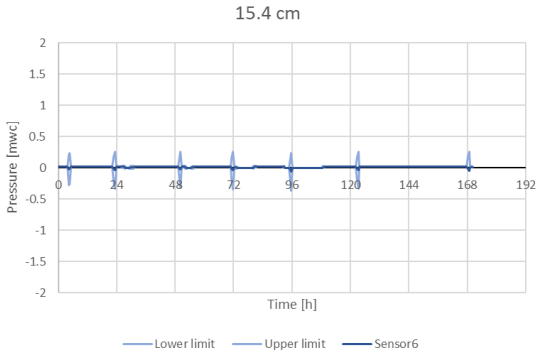

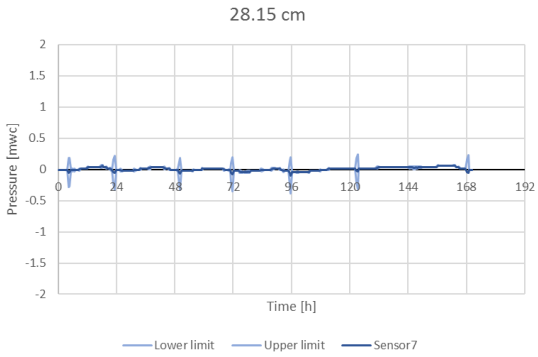
28.15 cm
Pressure [mwc]
Time [h]
Lower limit
Upper limit
Sensor7

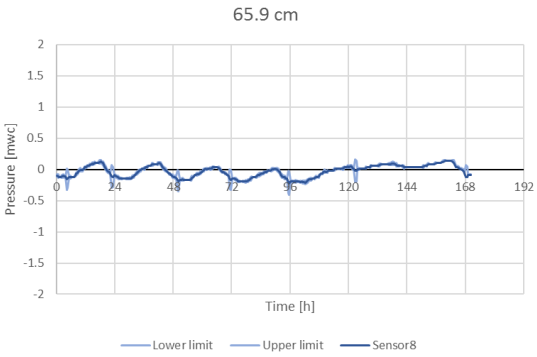
65.9 cm
Pressure [mwc]
Time [h]
Lower limit
Upper limit
Sensor8

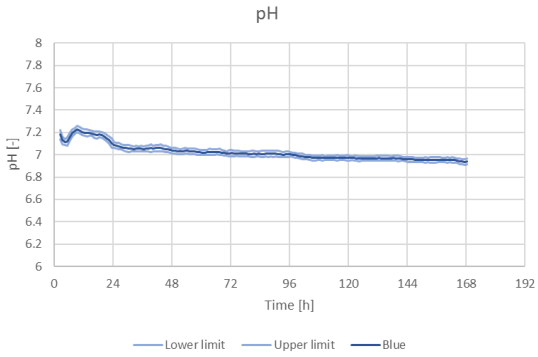
pH
pH [-]
Time [h]
Lower limit
Upper limit
Blue

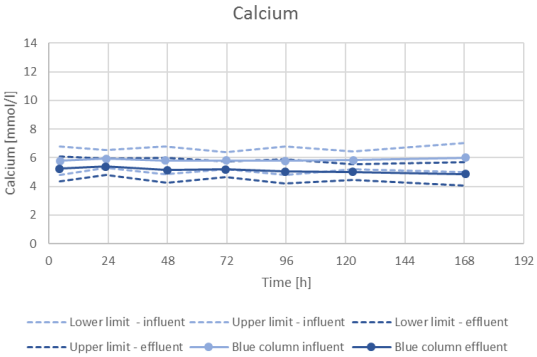
Calcium
Calcium [mmol/l]
Time [h]
Lower limit - influent
Upper limit - influent
Lower limit - effluent
Upper limit - effluent
Blue column influent
Blue column effluent

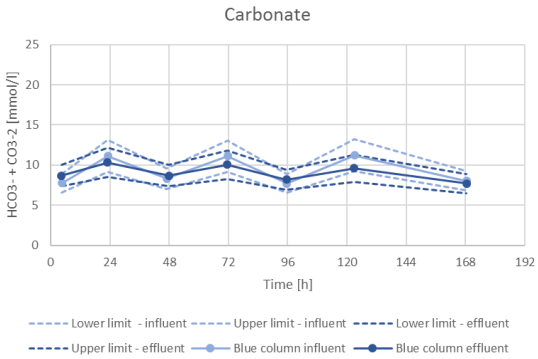
Carbonate
HCO3- + CO3-2 [mmol/l]
Time [h]
Lower limit - influent
Upper limit - influent
Lower limit - effluent
Upper limit - effluent
Blue column influent
Blue column effluent

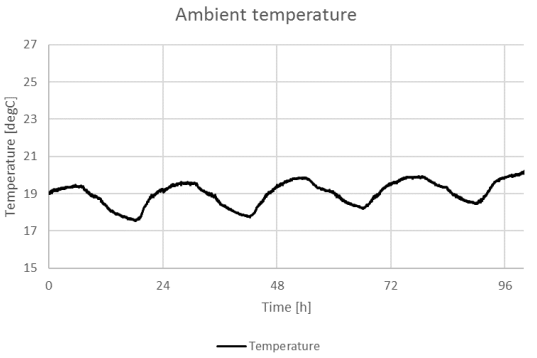
Ambient temperature
Temperature [degC]
Time [h]
Temperature

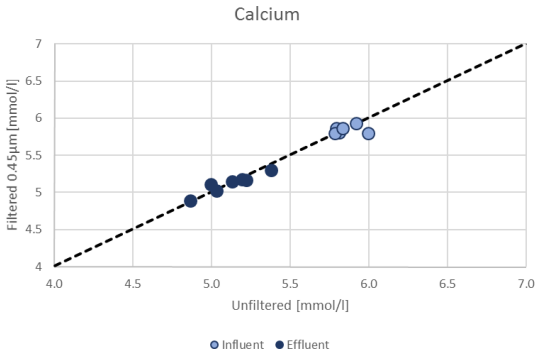
Calcium
Filtered 0.45µm [mmol/l]
Unfiltered [mmol/l]
Influent
Effluent

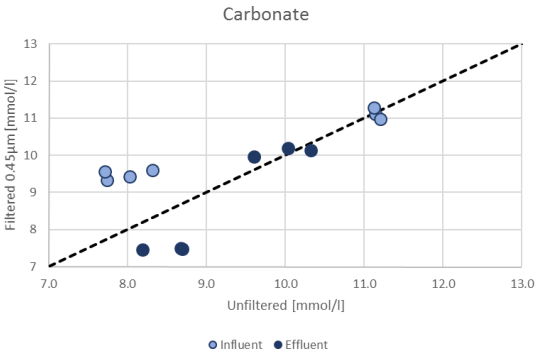
Carbonate
Filtered 0.45µm [mmol/l]
Unfiltered [mmol/l]
Influent
Effluent

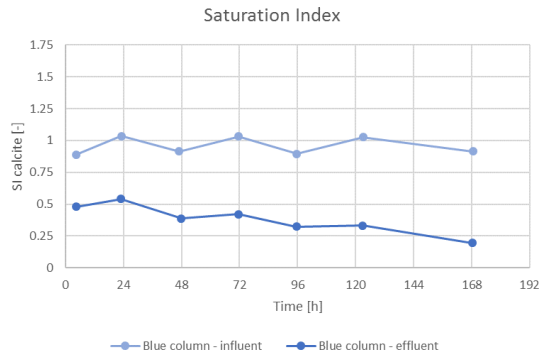

6.6.3 Pictures

Cementation only occurred at the top of the green filter, and did not occur in the blue column. The pictures below show the top of the green and the blue column.

Green column:

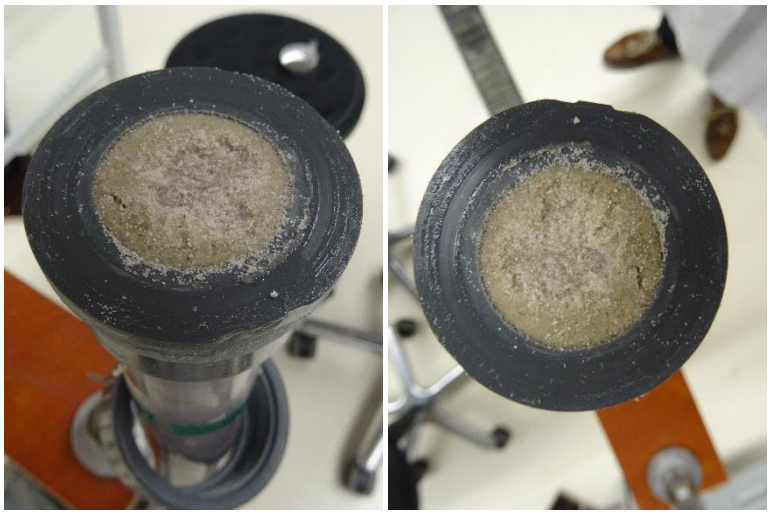

Blue column:

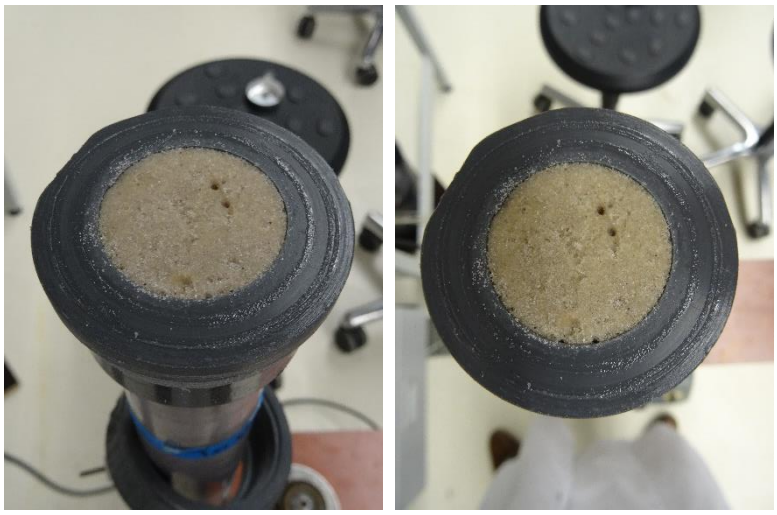

APPENDIX B – RESULTS OF BATCH EXPERIMENTS

Thirty batches were prepared to analyse the kinetics an inhibition by humic acids of calcium carbonate precipitation. Table XXX below gives an overview of all the batch experiments. This attachment is split in five parts: the batches without humic acids, and four parts with $SI_{calcite}$ values of 0.5, 1.0, 1.5 and 2.0. In each part, the measured concentrations of calcium and (bi)carbonate are presented along with their modelled concentration, pH and $SI_{calcite}$.

*Table 0-1 Overview of batch tests, ordered per $SI_{calcite}$ and the dosage of humic acids. Each batch is indicated by an X. *The batches with humic acid received too much $CaCl_2$: 6.74mmol/l instead of the planned 5.06mmol/l.*

$SI_{calcite}$	CaCl2 dose [mmol/l]	NaHCO3 dose [mmol/l]	pH	Humic acid concentration [mgC/l]						
				0.0	0.0535	0.160	0.535	1.60	5.35	16.0
-99	10.1	0.0	7.5	X						
0.5	2.53	6.0	7.5	X	X	X	X	X	X	X
1.0	5.06/6.74*	12.0	7.5	X	X*	X*	X*	X*	X*	X*
1.5	10.1	24.0	7.5	X	X	X	X	X	X	X
2.0	20.2	48.0	7.5	X	X	X	X	X	X	X
2.5	40.4	96.0	7.5	X						

6.7 BATCH TESTS WITHOUT HUMIC ACIDS

Modeling of the $SI_{calcite}$ and pH for the batches without humic acids was done by using the calcium concentrations only. The carbonate concentrations measured in the first 50 hours deviated too much from what would be expected. This has most likely been a measurement error of the IC spectrometer. The carbonate concentrations measured after 50 hours were more in line with what could be expected.

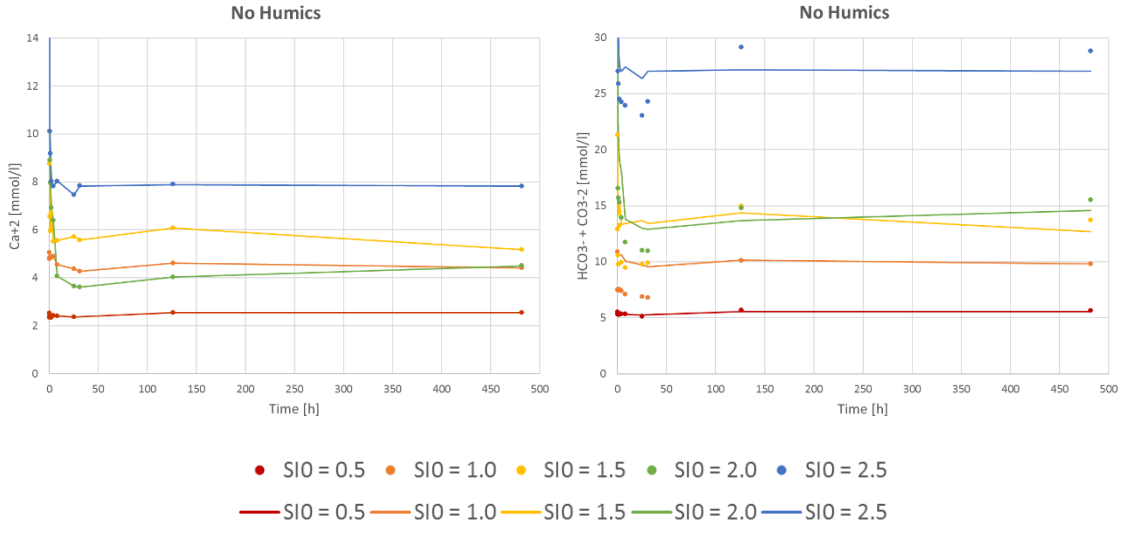

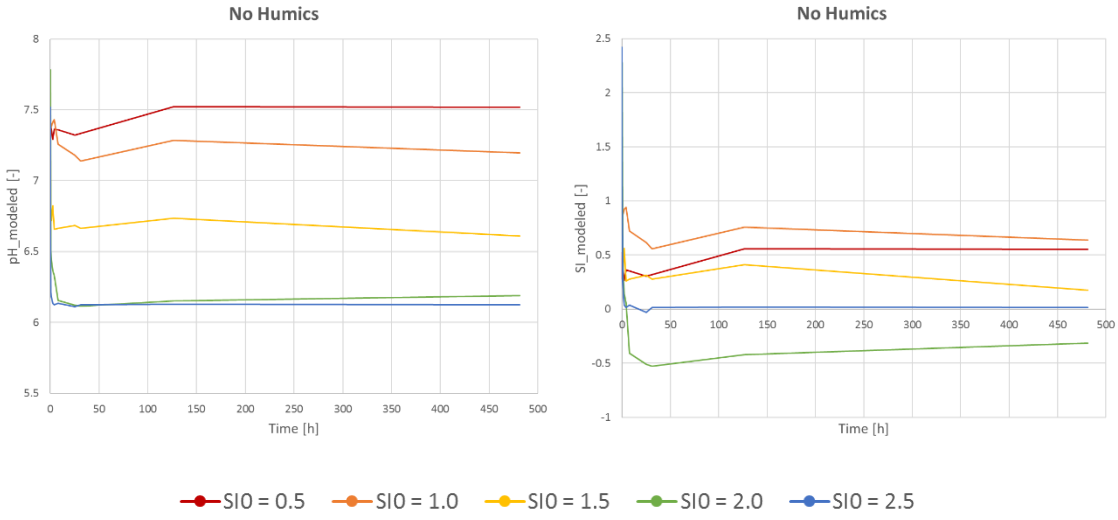
No Humics
pH_modeled [-]
Time [h]
No Humics
SI_modeled [-]
Time [h]
SI0 = 0.5
SI0 = 1.0
SI0 = 1.5
SI0 = 2.0
SI0 = 2.5

6.8 SI = 0.5

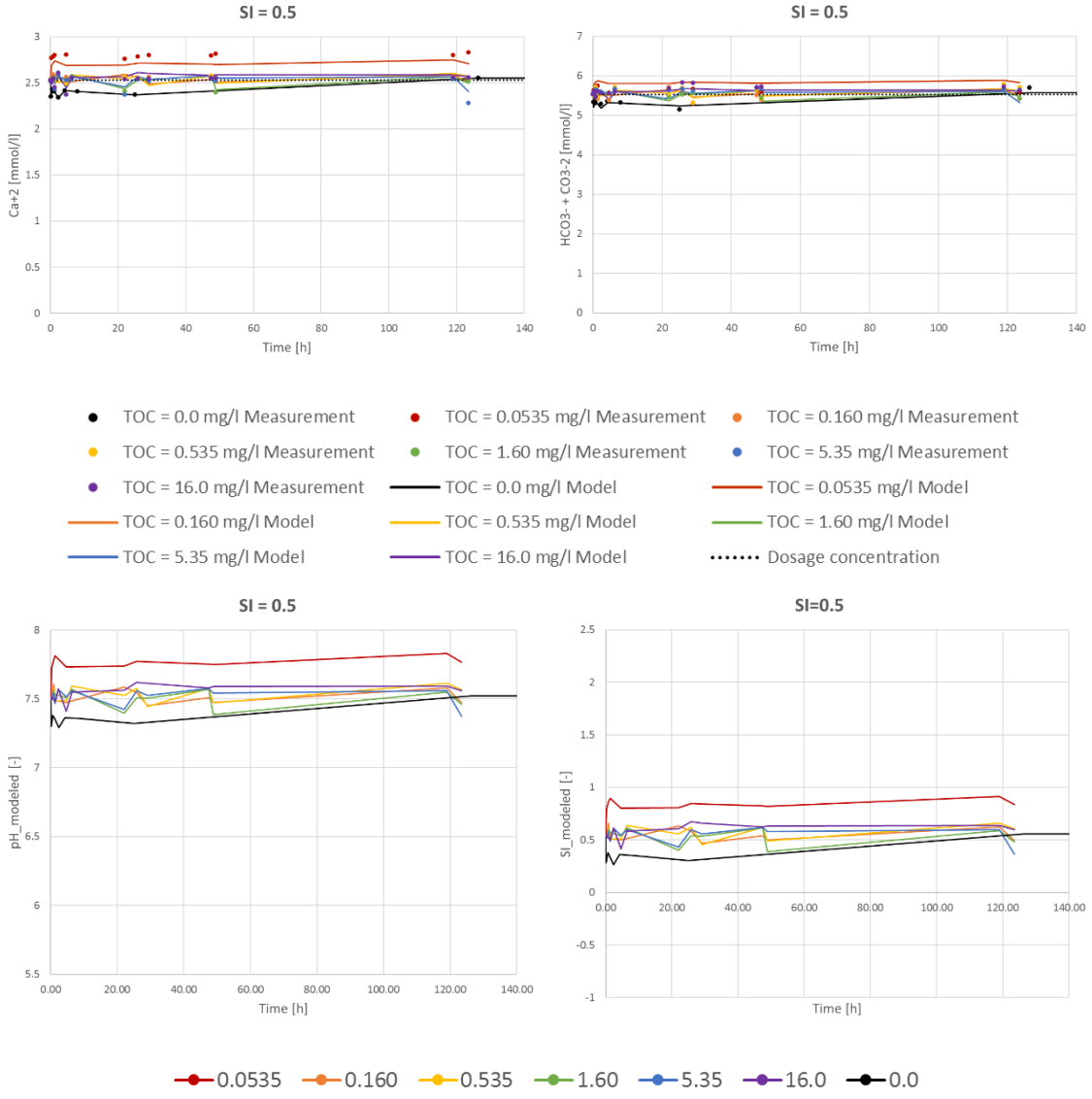
SI = 0.5
Ca+2 [mmol/l]
Time [h]
SI = 0.5
HCO3- + CO3-2 [mmol/l]
Time [h]
TOC = 0.0 mg/l Measurement
TOC = 0.0535 mg/l Measurement
TOC = 0.160 mg/l Measurement
TOC = 0.535 mg/l Measurement
TOC = 1.60 mg/l Measurement
TOC = 5.35 mg/l Measurement
TOC = 16.0 mg/l Measurement
TOC = 0.0 mg/l Model
TOC = 0.0535 mg/l Model
TOC = 0.160 mg/l Model
TOC = 0.535 mg/l Model
TOC = 1.60 mg/l Model
TOC = 5.35 mg/l Model
TOC = 16.0 mg/l Model
Dosage concentration
SI = 0.5
pH_modeled [-]
Time [h]
SI=0.5
SI_modeled [-]
Time [h]
0.0535
0.160
0.535
1.60
5.35
16.0
0.0

6.9 SI = 1.0

As mentioned in the table above, the batch without humic acids – the black solid line in the graphs below – received the planned amount of 5.06mmol/l $CaCl_2$, while the batches with humic acids received 6.74mmol/l $CaCl_2$. Note: the datapoints of the graph with (bi)carbonate before 50 hours are too low.

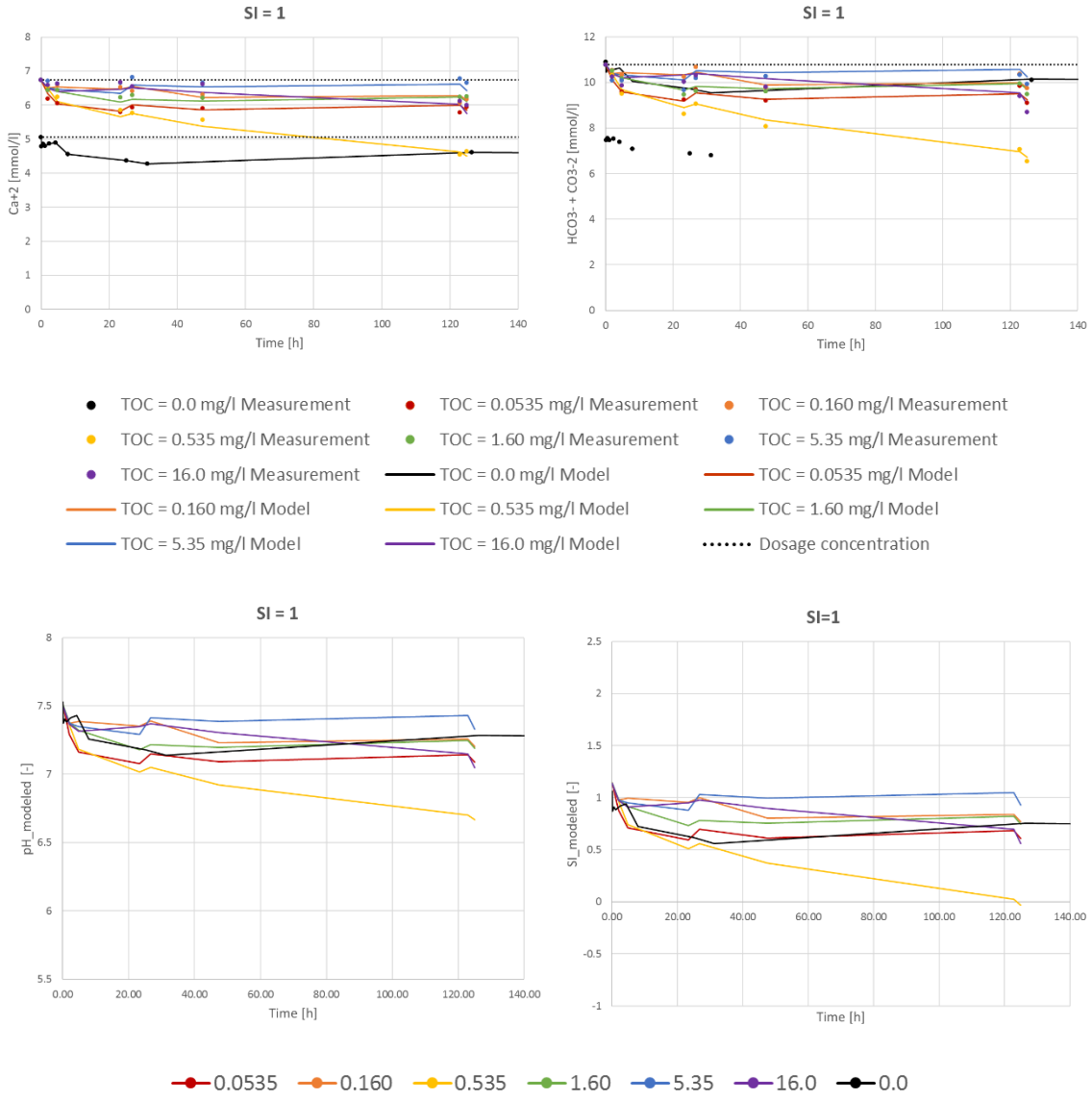

6.10 SI = 1.5

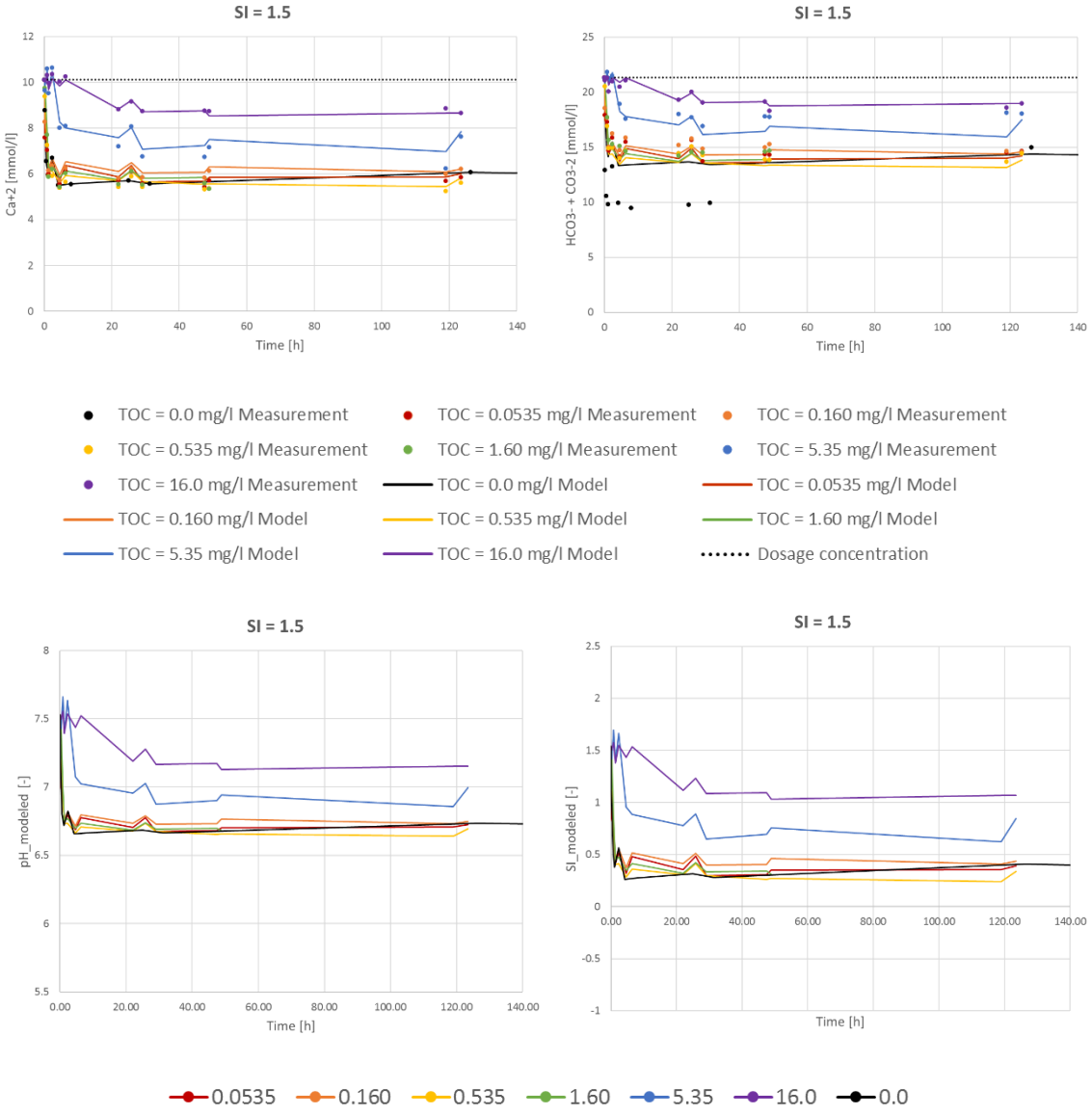
SI = 1.5
Ca+2 [mmol/l]
Time [h]
SI = 1.5
HCO3- + CO3-2 [mmol/l]
Time [h]
TOC = 0.0 mg/l Measurement
TOC = 0.0535 mg/l Measurement
TOC = 0.160 mg/l Measurement
TOC = 0.535 mg/l Measurement
TOC = 1.60 mg/l Measurement
TOC = 5.35 mg/l Measurement
TOC = 16.0 mg/l Measurement
TOC = 0.0 mg/l Model
TOC = 0.0535 mg/l Model
TOC = 0.160 mg/l Model
TOC = 0.535 mg/l Model
TOC = 1.60 mg/l Model
TOC = 5.35 mg/l Model
TOC = 16.0 mg/l Model
Dosage concentration
SI = 1.5
pH_modeled [-]
Time [h]
SI = 1.5
SI_modeled [-]
Time [h]
0.0535
0.160
0.535
1.60
5.35
16.0
0.0

6.11 SI = 2.0

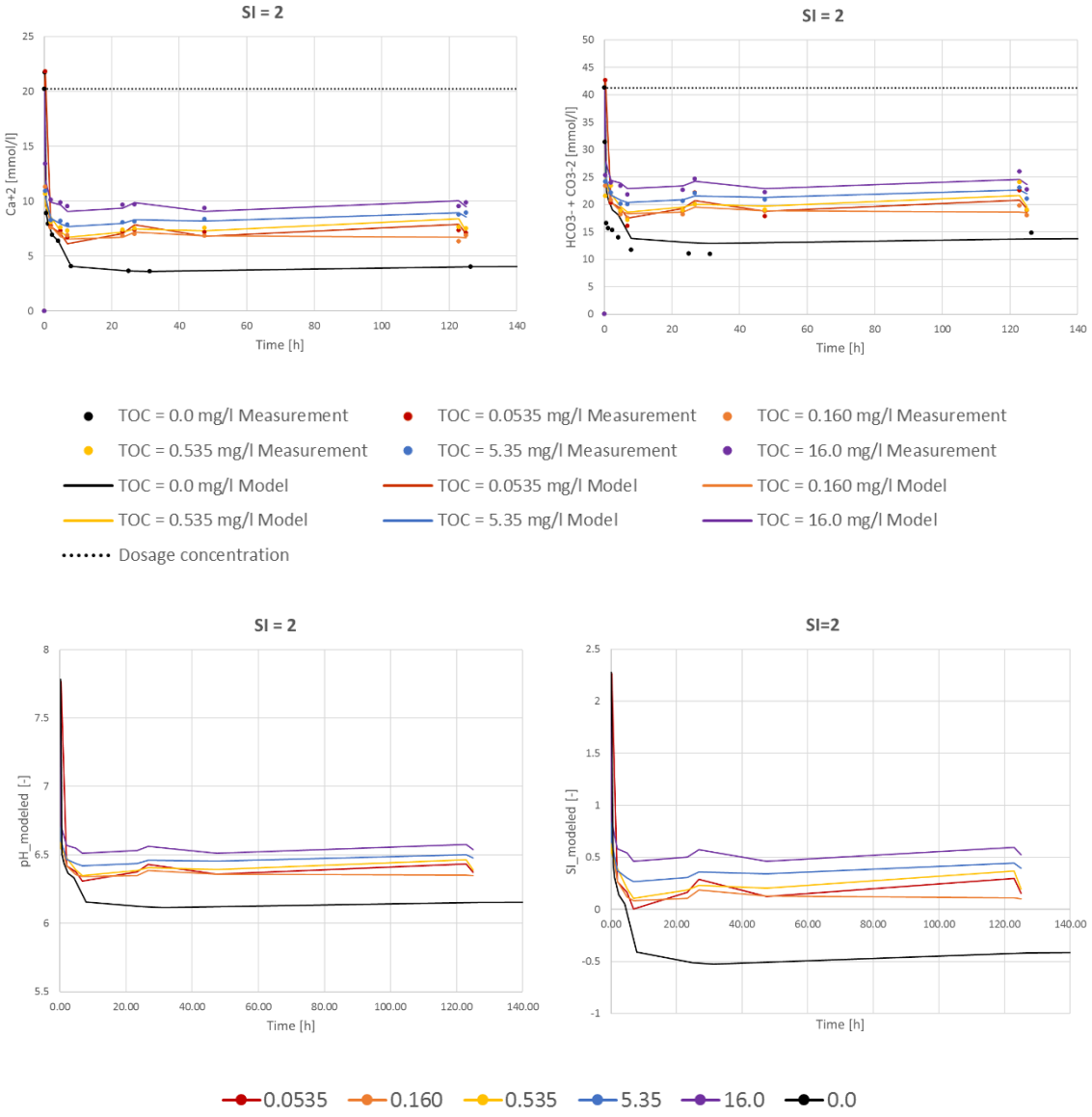
SI = 2
Ca+2 [mmol/l]
Time [h]
SI = 2
HCO3- + CO3-2 [mmol/l]
Time [h]
TOC = 0.0 mg/l Measurement
TOC = 0.0535 mg/l Measurement
TOC = 0.160 mg/l Measurement
TOC = 0.535 mg/l Measurement
TOC = 5.35 mg/l Measurement
TOC = 16.0 mg/l Measurement
TOC = 0.0 mg/l Model
TOC = 0.0535 mg/l Model
TOC = 0.160 mg/l Model
TOC = 0.535 mg/l Model
TOC = 5.35 mg/l Model
TOC = 16.0 mg/l Model
Dosage concentration
SI = 2
pH_modeled [-]
Time [h]
SI=2
SI_modeled [-]
Time [h]
0.0535
0.160
0.535
5.35
16.0
0.0

APPENDIX C – CALIBRATION OF THE PRESSURE SENSORS

The graphs below show the graphs of the calibration of the pressure sensors. Sensors 1-4 are used for the green column – connected in the order from top to bottom. Sensors 5-8 are used for the blue column.

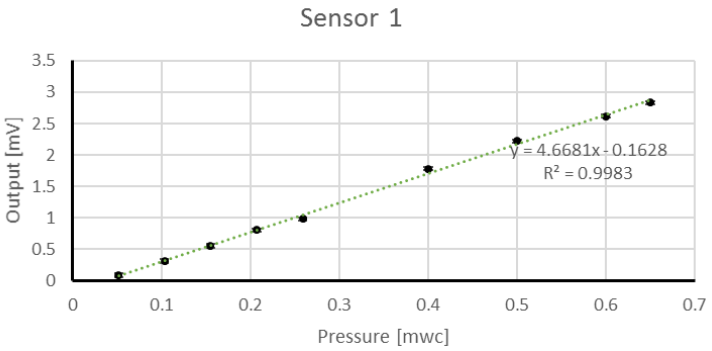

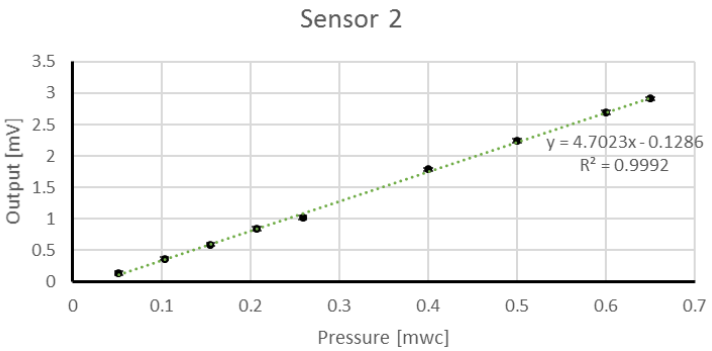

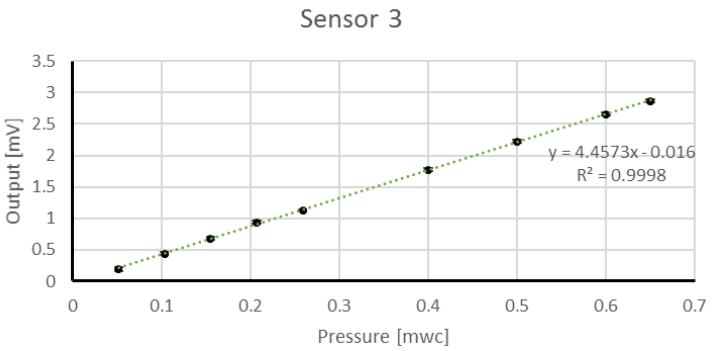

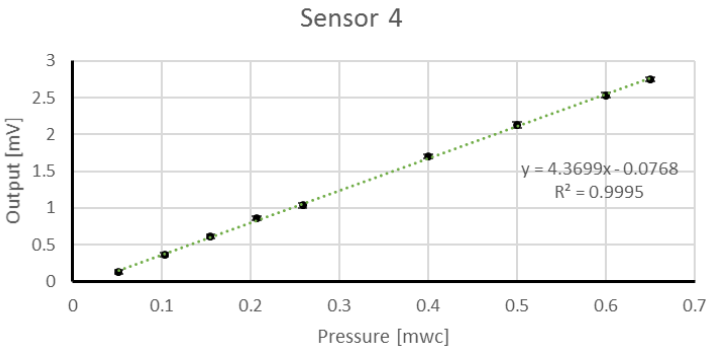

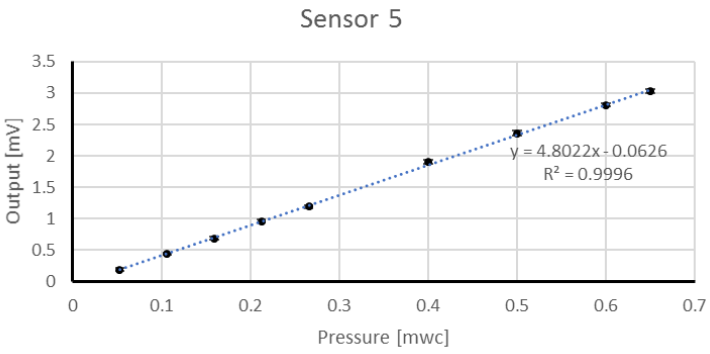
Sensor 5
Output [mV]
Pressure [mwc]
y = 4.8022x - 0.0626
R² = 0.9996

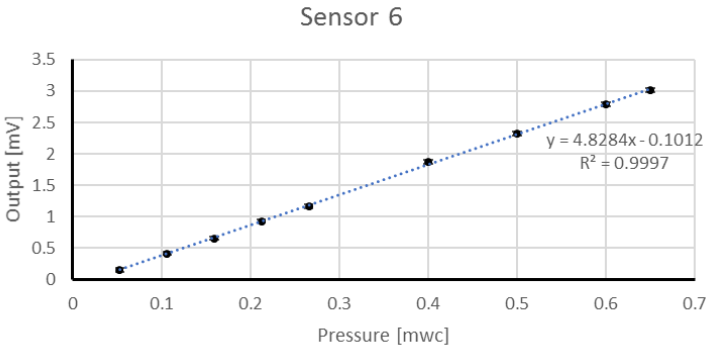
Sensor 6
Output [mV]
Pressure [mwc]
y = 4.8284x - 0.1012
R² = 0.9997

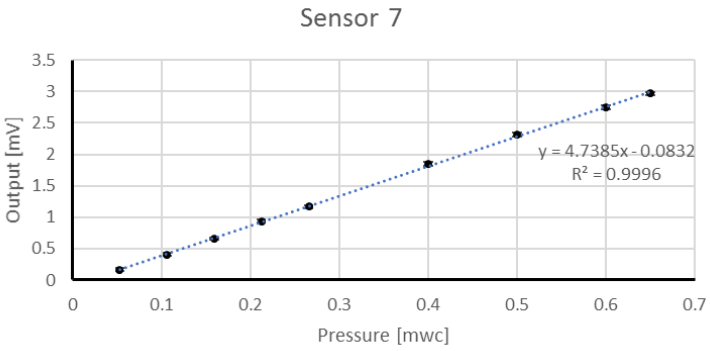
Sensor 7
Output [mV]
Pressure [mwc]
y = 4.7385x - 0.0832
R² = 0.9996

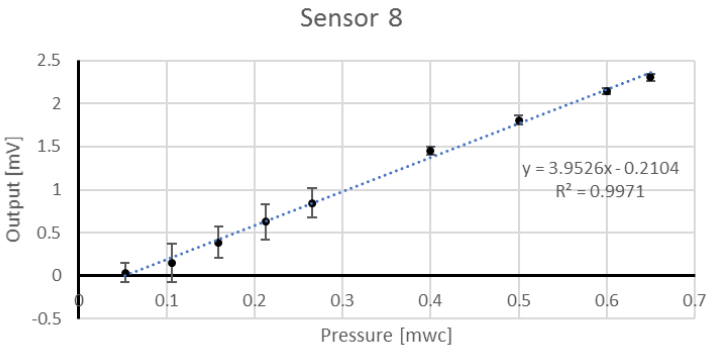
Sensor 8
Output [mV]
Pressure [mwc]
y = 3.9526x - 0.2104
R² = 0.9971